Barker, P.F., Camerlenghi, A., Acton, G.D., et al., 1999
*Proceedings of the Ocean Drilling Program, Initial Reports* Volume 178

# 1. Leg 178 Summary[1]

Shipboard Scientific Party[2]

## ABSTRACT

The Antarctic Ice Sheet is both a major component of the global climate system (involved in global deep- and bottom-water formation and sea-level change) and a source of ambiguity in the oxygen isotopic record that limits the value of this record to other studies of Cenozoic paleoclimate. The proposal on which this leg was based is one of five linked proposals intended to extract the Cenozoic glacial history of Antarctica from the sediments of its continental margin. On Ocean Drilling Program (ODP) Leg 178, nine sites were drilled on the Pacific continental margin of the Antarctic Peninsula. These included a transect of the outer continental shelf and sites on two hemipelagic drifts on the continental rise, extending back 6–10 m.y., as well as shallow holes at two sites on the inner continental shelf that provide an ultrahigh-resolution Holocene record.

## INTRODUCTION

At present, the history of the Antarctic Ice Sheet is unknown. It has been inferred from low-latitude proxy data, such as oxygen isotopic measurements on deep-ocean benthic foraminifers and the record of eustatic sea-level change adduced from sediments on low-latitude margins (Miller et al., 1987; Haq et al., 1987). However, these inferences are ambiguous and in disagreement (Sahagian and Watts, 1991; Barker, 1992), which leaves the history unresolved and limits the credibility and usefulness of both proxy data sets. For example, there is a dispute over whether the principal increases in Antarctic ice volume, which affect the benthic isotopic record, occurred at about 35 Ma, at 16–13 Ma, or only after 3 Ma. Similarly, changes in grounded ice volume pro-

[1]Examples of how to reference the whole or part of this volume.
[2]Shipboard Scientific Party addresses.

Ms 178IR-101

vide the only generally accepted repeatable, rapid-acting cause of global, eustatic sea-level change, yet the timing and amplitudes of sea-level change adduced from low-latitude margin sediments are disputed. Changes also occur at times when there is no independent evidence for substantial volumes of grounded ice on Antarctica or elsewhere. Further, the isotopic and sea-level estimates of grounded ice volume disagree substantially at both long and short periods through most of the Cenozoic. Onshore Antarctic evidence of glacial history is sparse and at present controversial at present: the argument continues as to how stable the early Pliocene Antarctic Ice Sheet has been (Webb and Harwood, 1991; Denton et al., 1993).

Deep and intermediate Southern Ocean waters generally corrode the carbonate tests used in isotopic analysis. Therefore, despite the production of high-resolution data sets (e.g., Tiedemann et al., 1994; Shackleton et al., 1995), the problems of using distal proxy data will persist. Antarctic margin sediments hold a direct record of ice-sheet fluctuation that can determine ice-volume change and clear the way for a more useful interpretation of high-latitude isotopic and sea-level data in the future.

The five linked Antarctic Offshore Acoustic Stratigraphy initiative (ANTOSTRAT) drilling proposals are intended to estimate size variations of the Antarctic Ice Sheet through the Cenozoic. This will include warmer periods when the ice sheet was much smaller, reaching the margin in only a few places, with fluvial sediment transport and deposition elsewhere. The proposals aim to sample both the East and West Antarctic margins and to distinguish an interior ice sheet, barely reaching the margin, from an ice sheet with a large coastal ice budget. Leg 178, the first of these proposals funded, succeeded in sampling the Pacific margin of the Antarctic Peninsula at nine sites (Figs. **F1, F2, F3**). Selection of these site locations and those in the other proposals was aided by numerical models that indicate patterns of past glaciation. For example, Figure **F4** (from Huybrechts, 1993) shows a glaciological model of ice sheets that cover only parts of the continent during warmer conditions. Some regions are clearly more sensitive to particular stages of ice-sheet volume change than others, and no single region will provide a complete history. The models allow data from different regions of the Antarctic margin to be combined in a complete history of ice-sheet development.

## Glacial Sediment Transport

The collaborative interpretation of Antarctic margin seismic data through ANTOSTRAT (Cooper et al., 1994, 1995; Barker and Cooper, 1997) and the simplicity of the modern Antarctic glacial regime have led to rapid emergence and application of a unifying model of glacial-sediment transport and deposition (Alley et al., 1989; Larter and Barker, 1989; Bartek et al., 1991; Cooper et al., 1991; Kuvaas and Kristoffersen, 1991). Briefly, almost all ice transport to the ice-sheet margins takes place within broad, rapidly moving ice streams. Rapid flow is enabled by low basal friction, whose main source is an overpressured and undercompacted, unsorted, shearing basal till. The shear ensures that ice transport is accompanied by till transport, and virtually all of the transported till is melted out/dropped/deposited close to the grounding line, where the ice sheet becomes an ice shelf before calving into icebergs. The ice stream erodes and transports inshore of the grounding line and

F1. General map of Leg 178 with ship track, **p. 28.**

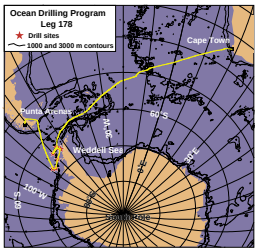


F2. Bathymetric chart of the Antarctic Peninsula Pacific margin, **p. 29.**

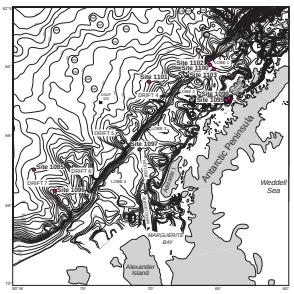


F3. Schematic figure of tectonic and glacial elements of Antarctic Peninsula margin, **p. 30.**

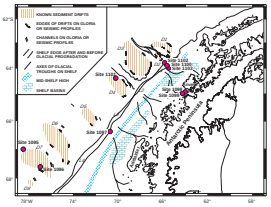

F4. Graph and maps of ice-sheet size and location at mean sea-level temperatures, **p. 31.**

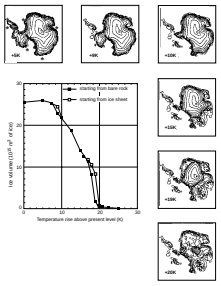

deposits offshore, in a high-latitude analogue of the low-latitude subaerial erosion/shoreline/marine deposition system. Further, the grounding line advances and retreats under the influence of upstream ice provision and basal sediment supply (and sea-level change), all climate related. The very large prograded sediment wedges beneath the Antarctic margin were developed during glacial maxima, when the ice sheet was grounded to the continental shelf edge (Fig. **F5**).

The glacial sedimentary regime has other characteristics. Progradation is usually focused into broad "trough-mouth fans" opposite the main ice streams, and the shelf is overdeepened (generally to between 300 and 600 m, but in places much deeper) and inward sloping. Continental slopes are often steep, and in places turbidity-current transport of the unstable component of slope deposition (with downcurrent deposition of suspended fines) has produced large hemipelagic sediment drifts on the continental rise (e.g., Kuvaas and Leitchenkov, 1992; Tomlinson et al., 1992; McGinnis and Hayes, 1995; Rebesco et al., 1996, 1997; Fig. **F6**). Sediment supply to the slope is highly cyclic, with large quantities of unsorted diamict deposited during glacial maxima and very little deposited during interglacial periods.

Three depositional environments are recognized: shelf topsets and slope foresets of the prograded wedge, and proximal hemipelagic drifts on the continental rise. Of these, the shelf record is potentially the least continuous. There, sediment is preserved mainly by slow subsidence, from cooling and from flexural response to the topset and foreset load, and the sediment is prone to re-erosion during the next glacial advance (e.g., Larter and Barker, 1989; Vanneste and Larter, 1995). Topsets tend to mark only the major changes in glacial history, so the more continuous foreset record is complementary. Before Leg 178, the drifts proximal to the rise were sparsely sampled (see Camerlenghi et al., 1997) but potentially contained an excellent record, closely related to that of the upper-slope foresets from which they are derived. Existing seismic data and drill sites from around Antarctica had demonstrated the coarse- (but not yet the fine-) scale climate record in continental rise sediments and the likely climate sensitivity of margin-wedge geometry (Barker, 1995). They had also revealed the partial nature of the shelf topset record (Hayes, Frakes, et al., 1975; Barron, Larsen, et al., 1989). During Leg 178, the glacial shelf prograded wedge was sampled at Site 1097 and the linked transect Sites 1100, 1102, and 1103; the rise drifts were sampled at Sites 1095, 1096, and 1101.

The continental shelf is an area of high biogenic productivity during interglacials. Although long-term sediment preservation on the shelf is limited because grounded ice sheets erode during subsequent glacials, biogenic interbeds will be preserved within sequence groups composed mainly of thick glacial diamict topsets and foresets. In addition, glacially eroded deeps can preserve expanded Holocene sections that may be continuous and essentially biogenic, if the ice-sheet grounding line is remote enough that ice-rafted debris is minor or absent and the section is sufficiently protected from bottom currents. Such sections can provide a record of decadal and millennial variability that can be compared with records from low latitudes and the ice sheet itself. This environment is available on the inner shelf of the Antarctic Peninsula (Domack and McClennen, 1996; Leventer et al., 1996) and was sampled during Leg 178 in Palmer Deep at Sites 1098 and 1099.

F5. Sequence model of deposition on shelf and slope through a glacial cycle, **p. 32.**

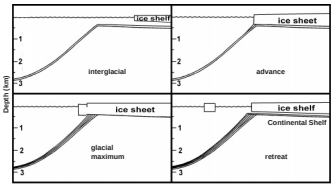


F6. Schematic drawing of the processes active during glacial half-cycles, **p. 33.**

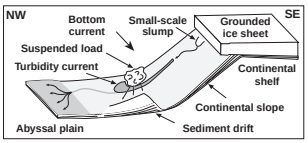

## The Antarctic Peninsula

Each ANTOSTRAT proposal is focused on the particular contributions its region might make toward understanding Antarctic glacial history. A single region does not offer the best opportunities for drilling in all respects. The particular value of drilling on the Antarctic Peninsula is the simplicity of its environment, together with the existing level of baseline understanding.

### Tectonics and Subsidence

All Antarctic margins are extensional (or effectively so) in a thermal and flexural sense, but most are old. Age governs thermal subsidence and rigidity, which controls response to erosion and deposition and to cyclic ice loading. The Antarctic Peninsula behaves as a young passive margin, having subducted a ridge crest (at 50 Ma in the southwest to only 6–3 Ma in the northeast [Barker, 1982; Larter and Barker, 1991a]). The margin undergoes steady thermal subsidence, which means better preservation of topset beds of the prograded wedge than at an older, colder margin and a more local isostatic response to sediment load.

### Tectonics and Age Constraint

Ridge subduction occurred well before the onset of glaciation in the southwest but not in the northeast. In the northeast, this provides a useful constraint on the maximum age of glacial sediments (which overlie young ocean floor of known age) but also threatens interference between tectonic and glacial events. For the older glacial history, it is prudent to avoid the northeast area of the margin.

### Geological Simplicity

Sub-ice geology (resistance to erosion) is a significant variable, to the extent that a till base facilitates ice streaming. The peninsular interior is 2000 m high and is composed largely of Andean-type plutonic and volcanic rocks. Before ridge subduction, the Pacific margin was a well-developed forearc terrain, on which the glacial regime has superposed an extensive prograded wedge (Larter and Barker, 1989, 1991b; Anderson et al., 1990; Larter and Cunningham, 1993; Bart and Anderson, 1995; Larter et al., 1997). The topography and geology of the peninsula vary little along strike, which simplifies the models of erosional and depositional response to climate change. Short cores on the outer shelf show diamict beneath a thin cover of Holocene hemipelagic mud (Pope and Anderson, 1992; Pudsey et al., 1994).

### Climate

Snow accumulation varies with temperature and is greatest around the continental edge, particularly along the Antarctic Peninsula, which is warmer than East Antarctica (Drewry and Morris, 1992). Snow accumulation governs the required rates of ice transport, hence basal sediment transport. Greater accumulation means an expanded sediment record. Warmer ice means (probably) faster ice flow, which also contributes to a rapid response to climate and an expanded sediment record.

### Ice Catchment

The extent of the ice drainage basin affects the speed of response to climate change and adds the complexity of a distal to a proximal signal (which allows the possibility of seeing the effects of a small, purely inland ice sheet at the coast during less-glaciated periods). The Antarctic Peninsula is a narrow strip of interior upland, dissected by fjords and bordered by a broad continental shelf. It therefore has a low-reservoir, high-throughput glacial regime with only a proximal source and so is both simple and highly responsive to climate change.

Onshore evidence of Eocene and Oligocene glaciation on the South Shetland Islands (northern Antarctic Peninsula) has been published (see Birkenmajer, 1992), but this conflicts with other evidence of regional climate. The Antarctic Peninsula is able to provide a high-resolution record of glaciation back to at least 10 Ma. To go back farther could involve entanglement with the tectonics of ridge-crest collision, making this a problem instead of an asset. However, because of the Antarctic Peninsula's more northerly position, its glacial history may be shorter than East Antarctica's. The record before 10 Ma may be largely nonglacial, or it may reveal a stage of valley glaciation lacking regular ice-sheet extension to the continental shelf edge.

## Scientific Objectives

The principal drilling objectives of Leg 178 were (1) to extract and compare high-resolution records of the past 10 m.y. of continental glaciation contained in topset beds (paleoshelf) of the glacial prograded wedge at the Antarctic Peninsula Pacific margin, in foreset beds (paleoslope) of the same sequence groups, and in a hemipelagic sediment drift on the continental rise; (2) to compile an optimal high-resolution history of grounded ice-volume fluctuation and compare it with low-latitude records of sea-level change and isotopic estimates of ice-volume change over the past 10 m.y.; (3) to assess the main controls on sediment transport and deposition during glacial intervals and use the insights gained to optimize investigation of the longer, more complicated East Antarctic record of glaciation and glacioeustatic sea-level change; and (4) to extract an ultrahigh-resolution Holocene record from a protected basin on the inner continental shelf for comparison with similar records from the ice sheets and lower latitude sites to investigate decadal- and millennial-scale climatic variation.

Leg 178 was drilled at nine sites: three (1095, 1096, and 1101) on continental rise drifts; four (1097, 1100, 1102, and 1103) on the outer continental shelf prograded wedge; and two (1098 and 1099) on an inner-shelf basin, Palmer Deep. For a brief summary of drilling at these sites, see Table **T1.**

T1. Leg 178 coring summary, p. 54.

# SCIENTIFIC RESULTS

## Continental Rise Drift Sites (1095, 1096, and 1101)

### Site 1095

Site 1095 is the more distal of two sites on a hemipelagic sediment drift on the continental rise off the northwestern, Pacific margin of the Antarctic Peninsula. Site 1095 lies in 3840 m of water on the northwestern, lower flank of the drift (Fig. **F2**) and was drilled to obtain the

deeper part of the stratigraphic section, where the overlying sediments are thinner than at the drift crest (Site 1096). The location was chosen on the upper part of a gentle slope bordering to the southwest a deep-sea channel system that separates adjacent drifts (Fig. F7). Drilling at Site 1095 was intended to examine the earlier stages of drift development and glacial evolution and (together with Site 1096) to answer specific questions related to the state of glaciation of the continent:

1. Is the present depositional system a plausible analogue for the older depositional environment reflected within the cored section?
2. Was deposition cyclic within the lower part of the drift section? What are the cycle frequencies, and what does any such cyclicity represent?
3. Is there a relationship between drift development and continental glacial history? Can the onset of the present stage of continental glaciation (involving regular ice-sheet excursions to the shelf edge) be recognized in the drift sediments?
4. Can the terrigenous fraction be used to examine the uplift history of the Antarctic Peninsula?

These are ambitious objectives, and not all can be addressed immediately.

About 7 days were spent recovering (effectively) a double advanced hydraulic piston corer (APC) record to about 85 meters below seafloor (mbsf), with one hole deepened by APC and extended core barrel (XCB) to 561 mbsf and logged. Drilling in the deep hole was ended after clogged jets had dramatically reduced recovery, when ship heave became excessive. One APC hole was lost to iceberg approach, and part of the logging was impeded by ship heave. Recovery was complete in the double APC section and was 89% down to 484 mbsf in the deep hole. Provisionally, the multiple records from the upper section have been spliced, using primarily magnetic susceptibility, and a common depth provided.

The sedimentary section extends from the Holocene to the early late Miocene at 480 m (Fig. F8). It comprises alternations of predominantly fine-grained terrigenous and hemipelagic deposits, containing only trace amounts of inorganic and organic carbon (<0.1 wt%). The uppermost 50 m consists of laminated and massive, often extensively bioturbated, diatom-bearing silty clays. Diatoms, radiolarians, and benthic and planktonic foraminifers all indicate a Quaternary age, and sedimentation rates are low (2.5 cm/k.y.) (Fig. F8). These deposits show a marked cyclic pattern of alternating gray, terrigenous, and brown biogenic-rich silty clays, the stratigraphic expression of successive glacial and interglacial cycles. Weak bottom (contour) currents influenced depositional patterns, with the bulk of fine-grained sediment probably introduced from dilute muddy turbidity currents. The base of the unit is marked by an increased frequency of parallel-laminated silty clay turbidites and beds of silty clay containing abundant ice-rafted debris.

Lithostratigraphic Unit II, the thickest lithostratigraphic unit at Site 1095, extends from 50 down to 435 mbsf and consists mainly of green laminated silts and muds of Pliocene and late Miocene age. Sedimentation rates are higher (5 to 7 cm/k.y.) than in Unit I. Some intervals appear barren, based on limited shipboard sampling, but biostratigraphic control is usually good. Reworked late Miocene diatoms occur throughout. Cycles in which structureless, intensely bioturbated sec-

F7. Part of MCS reflection profile I95-137 across Site 1095, p. 34.

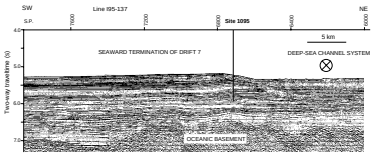


F8. Depth-age profile determined from geomagnetic reversals and diatom and radiolarian datums, p. 35.

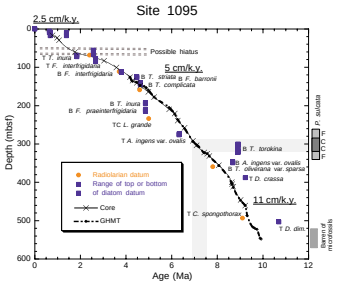

tions up to 1 m thick (with marked color changes and the appearance of higher concentrations of ice-rafted debris), alternating with sections of abundant thin, graded silt laminae (distal turbidites), are interpreted as glacial cycles that controlled sediment supply. Longer period variations in construction of the continental shelf may be reflected in coarsening- and fining-upward trends. At the top of this unit lies a possible debris flow (seen in only one of two core sections) and, from paleomagnetic and seismic reflection evidence, a possible brief hiatus. Below 285 mbsf, in upper Miocene sediments, the neritic diatom *Paralia sulcata* is observed in greater abundance, suggesting the existence of a shallow continental shelf at that time.

Sediments below 435 mbsf at Site 1095 consist of nonbioturbated parallel-laminated siltstone-claystones with sporadic occurrences of late Miocene diatoms. This facies (thin-bedded turbidites) does not show the second-order cyclic pattern observed in overlying sediments, which may be significant for understanding glacial history. Core recovery is very poor below 480 mbsf and the lowermost sediments appear barren, so the age of the deepest sediment cored is uncertain. Core-based magnetostratigraphic control is excellent to this point, and geological high-sensitivity magnetic tool (GHMT) log data show signs of being able to extend control to the base of the hole. Sedimentation rates are higher still, reaching 12 cm/k.y. (Figs. **F8, F9**).

The characteristics of cores retrieved at Site 1095 are consistent with a distal deep-water setting accessible (until the Quaternary) to small-scale turbidity currents. The pronounced cyclicity of the depositional record is evident in visual core descriptions and is recorded to date in color scanner, magnetic susceptibility, gamma-ray attenuation porosity evaluator (GRAPE), and downhole magnetic (GHMT) logging records, as well as (probably) in clay content. Preliminary shipboard analysis has shown this record to contain Milankovic orbital frequencies, which will allow comparison with the low-latitude record of orbitally induced climate change. The downhole variation of occurrence of biogenic components is in general inversely related to sedimentation rate, owing either to variation in surface primary production or to dilution by terrigenous components. The most abundant biogenic component is diatoms, which normally account for 10%–30% but occasionally reach 60% of the sediment.

Ice-rafted debris is ubiquitous in Site 1095 cores, a significant part of the total flux of terrigenous sediment to the site. Ice-rafted debris is readily identified because of the fine-grained nature of the host sediment. It appears as scattered sand grains and granules, isolated pebbles (lonestones), and lenses of granules and sand. In the absence of core X-radiographs, estimates of ice-rafted debris abundance are qualitative. A more detailed study of ice-rafted debris flux through time is potentially valuable but has to take into account changes in rates of background sedimentation. This is demonstrated by lower ice-rafted debris content in sediments interpreted as turbidite sequences and higher content in bioturbated intervals that may record slower sedimentation.

Site 1095 sediments generally contain only trace amounts of inorganic (<0.5 wt%) and organic (<0.1 wt%) carbon. Interstitial water chemistry shows evidence of organic matter decay and other diagenetic reactions, however, including carbonate and silica dissolution, cation exchange, and perhaps apatite and dolomite precipitation.

The deep hole was logged with the triple combination (TC) and GHMT tool strings, and a vertical seismic profile (VSP) with 12 stations was obtained. Hole and core correlation with seismic reflection profiles

F9. Lithostratigraphic, magnetostratigraphic, and biostratigraphic findings at sediment drift sites, **p. 36.**

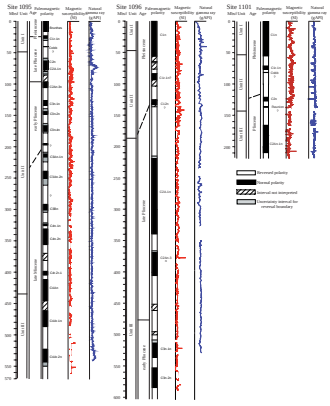

crossing Site 1095 is well constrained using VSP seismic traces and velocities, multisensor track (MST) and discrete sample velocities, and log and core densities. VSP data also correlate with strong reflectors on seismic profiles between 500 ms and oceanic basement at 1200 ms.

## Site 1096

Site 1096 is the more proximal and the more elevated of two sites on a hemipelagic sediment drift on the continental rise off the northwestern Pacific margin of the Antarctic Peninsula (Fig. F2). This site lies in 3152 m of water close to the crest of the drift and was drilled to obtain the shallower part of the stratigraphic section, where it is most expanded (Fig. F10). With the more distal site (1095), Site 1096 was intended to answer specific questions about the state of glaciation of the continent, as listed above for Site 1095. Not all of those questions can be answered immediately, but shipboard work provides the basic information needed.

In almost 9 days on site, we recovered a complete double APC section to 120 mbsf, extended the cored section to 607.7 mbsf by XCB drilling, and then logged the hole. Operations were not straightforward: clogged jets required a round trip, logging was achieved in two halves (upper and lower) because of a bridge, and the Formation MicroScanner (FMS)–sonic and well-seismic tools were not run because the hole had become too wide.

The sedimentary section extends in age from the Holocene to the early Pliocene (~ 4.7 Ma) at 607 m (Fig. F8). Sediments are predominantly fine grained and terrigenous and are divided into three depositional units. Unit I (0 to 33 mbsf) consists of laminated and massive, often intensely bioturbated, diatom-bearing silty clays of Pleistocene age. These have a well-defined alternation of biogenic-rich and biogenic-poor horizons, which are the stratigraphic expression of glacial–interglacial cycles. Sedimentation rates averaged 7 cm/k.y. (Fig. F11). The top of Unit II is placed at the first appearance downcore of common parallel-laminated silt and mud turbidites. Unit II is a late Pliocene to Pleistocene partly turbiditic succession some 140 m thick (33 to 173 mbsf) with a calcareous biogenic component, generally low. Sedimentation rates average 9 cm/k.y. Although the turbidite silts are thin and subordinate to muds, two coarsening-upward sequences may be discerned in the upper part of Unit II. A massive, well-sorted sand bed occurs at 112 mbsf. Unit III, Pliocene in age, extends from 173 mbsf to the bottom of the hole at 607.7 mbsf. It is composed of alternations, up to tens of meters thick, of (1) very thinly laminated and generally nonbioturbated clays perhaps derived from muddy turbidity currents and (2) intensely bioturbated homogenous silty clays with a higher biogenic component. Overall, Unit III has a sedimentation rate of 18 cm/k.y., although fluctuations in deposition rate may be recorded by intervals of intense bioturbation with more abundant ice-rafted debris. The biogenic component of Unit III is siliceous.

In Units II and III, the alternation of laminated sediments (interpreted as turbidite facies) and bioturbated hemipelagic facies records cyclic fluctuations in sediment supply and transport processes. Some of these fluctuations may be related to glacial–interglacial cycles along the Antarctic Peninsula margin similar to those identified within Unit I, but longer period cycles also exist. Likely proxies for glacial–interglacial variation include magnetic susceptibility, color reflectance, and clay-mineral composition.

F10. Part of MCS reflection profile I95-130A across Site 1096, p. 37.

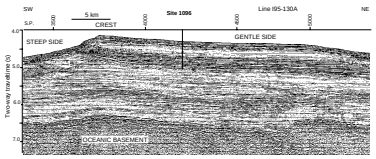


F11. Depth-age relationship for Site 1096 based on geomagnetic reversals and diatom and radiolarian datums, p. 38.

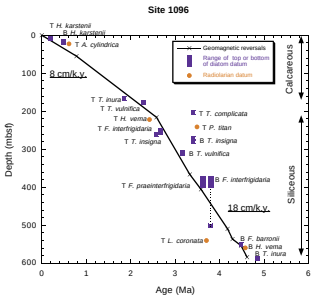

Above 170 mbsf (Units I and II), the sediments contain calcareous nannofossils and foraminifers, which occur rarely to abundantly only in this upper interval of Site 1096. *Neogloboquadrina pachyderma* sinistral dominates the planktonic foraminiferal assemblage. Benthic foraminifers are rare and consist mostly of shallow-water species presumed to be reworked from the continental shelf. Calcareous nannofossils provide the datums in this upper interval. Reworking is evident in all fossil groups in the upper 170 m, with some samples containing an entire reworked assemblage. Radiolarians are present in several intervals, but the marker species for the two zones below Psi (Chi and Phi) were not found. In the upper 110 m, the diatom zonal boundary markers are not seen, and samples studied from 110 to 165 m are barren of diatoms. From 170 to 608 mbsf (Unit III) siliceous microfossils dominate, but the planktonic foraminifer *N. pachyderma* sinistral is seen to the base of the hole. The record of radiolarians is relatively complete for Unit III, and most of the marker species are present through the entire Upsilon Zone. The diatom record for the lower part of this site is also virtually complete, with zonal datums being available for nearly all the zones.

Magnetostratigraphic data from Site 1096 show promise. The Brunhes/Matuyama boundary is very well defined at 55 m. The Jaramillo and Olduvai Subchrons are not ideal for magnetostratigraphy because part of the interval shows a low remanent intensity resulting in a noisy inclination record. Below this, reversals are well defined, the oldest reversal observed being the onset of Chron C3n.2n (4.62 Ma) at 585 mbsf.

Physical properties and chemical data are interesting: below 170 mbsf grain density is reduced, and porosity increases steadily downhole within Unit III. Heat-flow measurements suggest that the base of the methane hydrate stability zone lies at ~300 m, but a gas hydrate bottom-simulating reflector (BSR) is not seen. The diffuse BSR at ~700 ms in the seismic section, not reached by coring, is assumed to be from silica diagenesis. A total of 172 bulk sediment and 35 interstitial water samples from Site 1096 have been analyzed. The sediment generally contains only minor amounts of inorganic (<0.1 wt%) and organic (<0.6 wt%) carbon, yet the interstitial water chemistry shows clear evidence of organic matter decay, with the sulfate reduction zone extending to 50 mbsf. Other diagenetic reactions occurring include carbonate precipitation, silica dissolution, cation exchange, and perhaps disseminated apatite precipitation. Methane concentrations were high and caused expansion in most cores, but methane/ethane ratios stayed above 200 to the base of the hole.

The deep hole was logged under unstable hole conditions, which both limited and complicated the operation. In total, the porosity-density–natural-gamma tool string was deployed through almost the entire hole (from 556 mbsf) and the GHMT (magnetic) tool between 510 and 356 mbsf. Natural-gamma activity was logged to the seafloor, and clay content can be estimated after correction for the gamma attenuation of the pipe.

Seismic unit boundaries defined at Site 1095 were traced across multichannel seismic (MCS) profiles to Site 1096. Only the uppermost (I and IIa–c) were penetrated at Site 1096 because of more rapid sedimentation.

## Site 1101

Site 1101 is located at a water depth of 3509 m on the continental rise of the Pacific margin of the Antarctic Peninsula, centrally within a

sediment drift ~500 km northeast of Sites 1095 and 1096 (Figs. F2, F12). Because the sediment drift (Drift 4) is much smaller than that drilled at Sites 1095 and 1096 (Drift 7), the site is no farther from the continental margin than Site 1096.

Site 1101 was chosen to answer questions raised by drilling at Sites 1095 and 1096:

1. Is the sedimentary record obtained at Sites 1095 and 1096 representative of the entire Pacific margin of the Antarctic Peninsula?
2. Does the regional correlation between seismic units observed in MCS profiles reflect actual lithologic and stratigraphic correlation?
3. Can we test the hypothesis that sedimentary evidence of the late Pliocene Eltanin meteorite impact is to be found at Site 1096 by finding a synchronous event, similarly anomalous within the cored sequence, on a different drift?

The opportunity to drill Site 1101 came from the persistently unfavorable sea conditions encountered on the continental shelf (exceeding a 2-m limit on vessel heave during shallow-water drilling). In less than 2 days, a single hole was APC cored to 142.7 mbsf and extended by XCB drilling to 217.7 mbsf with 99.1% recovery. Having recovered the shallow section at Site 1101, and with improving sea conditions, the ship returned to shelf Hole 1100D.

Recovered sediments consist of 217.7 m of predominantly hemipelagic clayey silt that contains a nearly continuous distal glacial record of the past 3.1 to 3.4 m.y. (late Pliocene to present) (Fig. F13). Unit I (0–53.3 mbsf) and Unit II (53.3–142.7 mbsf) are composed of alternating biogenic-bearing massive clayey silts and laminated clayey silts that we interpret as the sedimentary expression of interglacial and glacial periods, respectively. Sedimentation rates are fairly steady at ~7 cm/k.y. in the top 120 m, but a period of slow sedimentation may occur toward the base of Unit II (Fig. F13). Within Unit I, warm oxygen isotope stages are identified by diatom-bearing layers. Unit II has at least 19 discrete foraminifer-bearing layers in which carbonate concentration can be as high as 28 wt%, which alternate cyclically with barren laminated or massive intervals. Extremely well-developed cyclicity in magnetic susceptibility matches variation in color reflectance and the alternation of biogenic and terrigenous intervals in Units I and II. Unit III (142.7–217.7 mbsf) lacks the regular variation in carbonate content of the overlying units. Its upper part (above 198 mbsf) contains massive, barren clayey silt that could have originated in turbid plumes or sediment gravity flows from glaciers near the continental shelf edge, as well as thin diamicts (deposited by ice rafting). The lower part of Unit III may represent a warmer interval with deposition of diatom-bearing massive and laminated facies. Sedimentation rates in Unit III are less well defined but may reach 10 cm/k.y.

Calcareous microfossils were found in the uppermost core as well as in the biocalcareous intervals between 50 and 134 mbsf. Siliceous microfossils were found throughout the core and become more abundant in the lowest three cores. Several planktonic foraminiferal oozes were identified, mostly in Unit II. The only ooze in Unit I occurs in marine isotopic Stage 5. More than 90% of these assemblages are *N. pachyderma* sinistral with rare *N. pachyderma* dextral and *Globigerina bulloides*, plus benthic foraminifers. The biocalcareous interval appears coeval at Sites 1101 and 1096. Calcareous nannofossils were recovered

F12. Part of MCS reflection profile IT92-114 across Site 1101; seismic stratigraphic record at proposed sites APRIS-05A and 06A, p. 39.

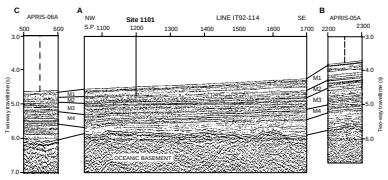


F13. Depth-age profile determined from geomagnetic reversals and diatom and calcareous nannofossil datums, Site 1101, p. 40.

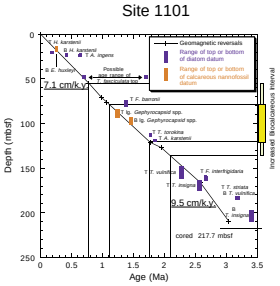

in the upper 120 m. The first and last occurrence of the large form of *Gephyrocapsa* spp. was observed, making the nannofossil record at Site 1101 more complete than at Site 1096. Diatoms were present throughout the hole, with alternating well-preserved and barren intervals. The lowest six cores contain more diverse, abundant assemblages of diatoms than found above. Radiolarians were generally abundant and moderately preserved, with only two barren intervals. The Psi through Upsilon Zones (Pleistocene–Pliocene) were recovered. Reworked late Pliocene assemblages (thick shelled) occurred in the Pleistocene part of the section, which contained thin-shelled in situ specimens.

The Brunhes/Matuyama boundary occurs at ~55 mbsf, the same depth as at Site 1096 (Fig. F14). Site 1101 has the most complete, well-defined Matuyama epoch reversals of all of the drift sites. Coring disturbance in Core 178-1101A-16H appears to affect the record of the Reunion event. The termination of Chron C2A (2.58 Ma) was observed at ~170 mbsf, and the onset of C2An.1n (3.04 Ma) was found at 210 mbsf.

The interstitial water chemistry profiles at Site 1101 closely resemble those of the upper 250 mbsf at Sites 1095 and 1096, reflecting the strong similarity in moderate sedimentation rates (5–10 cm/k.y.) and low organic carbon contents (<0.4 wt%) among the three rise sites. Sulfate decreases to zero, and manganese reaches a minimum concentration at 130 mbsf, where measurable concentrations of methane and ethane first occur. Other indicators of organic-matter decay, such as alkalinity and ammonium, increase with depth and reach maximum values at the bottom of the hole. They probably continue to increase at greater depths, based on comparison with Sites 1095 and 1096. Dissolved silica concentrations remain high throughout the hole and reach the solubility limit of opal-A at 150 mbsf near the top of Unit III. This suggests that biogenic opal dissolves principally between 0 and 150 mbsf and that the interstitial water becomes saturated with respect to silica in Unit III. Dissolved calcium increases significantly downhole in the upper 50 mbsf, then decreases to a minimum at 130 mbsf near the base of the sulfate reduction zone. It increases again at the bottom of the hole. The low content of calcareous microfossils in Units I and III could therefore be traceable to dissolution of carbonates.

Porosity initially decreases downhole, as might be expected under normal consolidation conditions. However, porosity rises again below 140 mbsf. At Site 1101, we found a weak positive correlation between siliceous biogenic content and porosity, which was seen previously at Sites 1096, 1098, and 1099. This suggests that the presence of significant amounts of rigid, siliceous biogenic material in the sediment, associated with a relatively fast sedimentation rate, renders the lower part of the drift sedimentary column underconsolidated.

F14. Biostratigraphic findings in continental rise sites, p. 41.

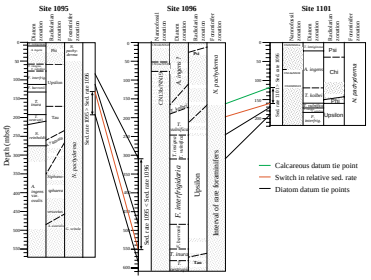


## Continental Shelf Sites (1097, 1100, 1102, and 1103)

### Site 1097

Site 1097 is located on the outer continental shelf of the Antarctic Peninsula at a water depth of 552 m, some 14 km from the continental shelf edge (Fig. F2). It lies in a topographic low between two of the lobate depocenters where the uppermost, fully glacial progradational sediment Sequence Groups S1 and S2, recognized in seismic data on the continental shelf, are best developed (Fig. F15). It was selected to examine the underlying Sequence S3 where that sequence would be more

F15. Location of Site 1097 on single-channel seismic reflection profile PD88-04, p. 42.

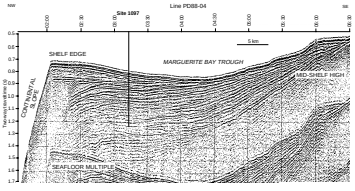

easily accessible, being less deeply buried. The nature of S3 was unknown, and the site was intended to examine Antarctic Peninsula paleoclimate before the fully glacial sediment sequence groups were deposited.

Drilling at Site 1097 was slow and difficult for three main reasons. First, the nature of the sediments (unsorted, including large clasts) confined us to rotary core barrel (RCB) drilling, not the best way of recovering the soft till matrix, and dictated a slow start. Second, icebergs interrupted drilling on two occasions; and third, limitations on ship heave in water depths <650 m also halted drilling twice. In rather more than 5 days, Hole 1097A was drilled to a depth of 436.6 mbsf. The sediment shows glacial influence in all of the recovered intervals, including S3. Recovery varied from ~2.3% in the uppermost 80 m of Sequence Group S1 to 18% in Sequence Group S2 down to 150 m, and to 16% in Sequence Group S3.

Recovery was too poor for S1 to be described or dated. Material recovered from the underlying S2 is massive diamict, defined as poorly sorted sediment, with clasts supported by a muddy matrix. It appears to reflect subglacial deposition, in keeping with seismic reflection interpretations of the nature of S2. The age of S2 at this site is constrained mainly by diatoms (*Fragilariopsis barronii* and the upper part of *Thalassiosira inura* Zones), supported by a radiolarian assemblage (Upsilon Zone) with a broader age range (younger than 4.6 Ma and older than ~3.8 Ma). The boundary between S2 and the underlying S3 (seen as conformable in presite seismic survey) lies within the upper *T. inura* and Upsilon Zones, at ~4.5 to 4.6 Ma.

Sequence S3 sediments are more variable but include similar massive diamicts, clast-rich, with sizes ranging up to boulders (a 0.5-m granite boulder was drilled within S3), and containing reworked diatoms and foraminifers (as do S2 diamicts). Diamicts are interpreted as deformation tills formed by subglacial reworking and transport of marine muds beneath a grounded ice sheet that periodically occupied the continental shelf (Fig. **F16**). Stratified diamicts in one core, with erosive bases that grade upward to clayey silt with dropstones, are interpreted as debris flows that occurred near the ice-sheet grounding line. Laminated and massive bioturbated muds contain variable amounts of iceberg-rafted debris and are considered glaciomarine. They show evidence of soft-sediment deformation that could be the result of iceberg turbation.

Biofacies variation throws light on the changing depositional environments sampled within S3. Three biofacies were distinguished—based on the degree of reworking of benthic foraminifers and other biogenic matter—that reflect subglacial deposition, ice-proximal deposition, and open, shallow marine shelf conditions (Fig. **F16**). On this basis, the topmost sediments of S3 are subglacial, as is S2. However, they are marine from 180 to 210 mbsf and subglacial from 220 to 290 mbsf; deeper sediments vary between more marine and ice proximal beneath. This variation reflects periodic migration of the ice-grounding line across the continental shelf.

Preliminary biostratigraphic age determination of Sequence S3 was difficult because of reworked forms, but two possible diatom age constraints are (1) younger than 4.85 Ma below 218 mbsf and (2) younger than 5.6 Ma above 289 mbsf. Radiolarians suggest an age older than 4.6 Ma below 294 mbsf. Regional similarities in benthic foraminifers suggest an early Pliocene age for much of S3 at this site. Paleomagnetic measurements show some stable, high-inclination directions; others are stable but low inclination (possible debris flows); and still others (diam-

F16. Summary of facies recovered at Site 1097, **p. 43.**

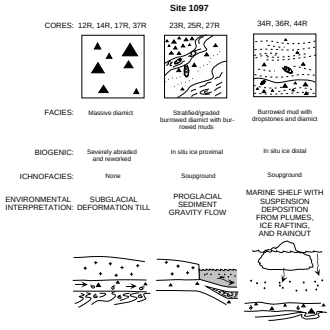

icts) are unstable. At this time, in the absence of clear biostratigraphic age constraints, a magnetostratigraphic interpretation is unjustified.

Downhole logs were not run because of hole instability, and many shipboard measurements on Site 1097 cores were of limited value because of poor recovery. The physical properties data are sparse, but porosity in Unit II as low as 30% may be attributed to subglacial shear consolidation. Also, natural gamma activity drops toward the base of the hole, matching a general decrease in clay content. Limited velocity and density measurements prevent an accurate correlation between hole and seismic profiles but serve to clearly distinguish the seismic sequences.

Drilling at the site was sufficient to confirm the nature of S1 and S2 and to establish the upper part of S3 as glacial (although perhaps less fully glacial than S1 and S2). The age and nature of the S3/S2 boundary were established.

## Shelf Transect Sites (1100, 1102, and 1103)

A central objective of Leg 178 was to sample, date, and understand the glacially transported, unsorted sediments deposited in a generally progradational wedge on the outer continental shelf and continental slope. On the Antarctic Peninsula continental margin these sediments are focused into four lobes, in which both shelf topsets and progradational shelf foresets are maximal. The entire West Antarctic margin, however, to at least 105°W, shows the same seismic sequence groups. The main approach to this problem by Leg 178 was to drill a suite of sites along a transect through a well-developed progradational lobe off Anvers Island. Four sites were planned to describe the main changes in depositional geometry within the lobe (Fig. **F17**). An additional site (Site 1097) had already been drilled in an interlobe area to the southwest, where the deeper section, beneath the main glacial sequence groups, was more accessible.

F17. Continental shelf transect (Sites 1100, 1102, and 1103), **p. 44.**

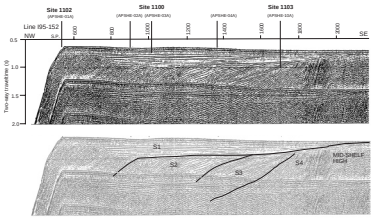


We attempted three sites (1100, 1102, and 1103) along the shelf transect, with mixed success. One problem was the difficulty of recovering the sediment, which is unconsolidated in the upper section: it is ice transported, so essentially unsorted, with hard clasts (some very large) within a soft, fine-grained matrix. Another, crucial problem was the 2-m limitation on vessel heave during shallow-water drilling, which severely slowed progress at all shelf sites but particularly at Sites 1100 and 1102. Site 1100 was chosen to sample and date the boundary between the two main glacial seismic sequence groups (S1 and S2), where S1 topsets overlie truncated S2 foresets at ~350 mbsf. The site lies at the edge of an area of hummocky, ice-scoured topography that has been interpreted as the top of a subglacial till, produced by the last ice-sheet advance. Four holes were drilled with very poor recovery in ~4 days. The deepest hole, 1100D, reached 110.5 mbsf but with only 4.8% recovery. By then, repeated pipe trips had so degraded the hole condition that the deep target (~400 mbsf) was judged impracticable.

The only core of Hole 1100C recovered 4.05 m of massive diamict, clast-rich in places and with a diatom-bearing silty clay matrix. In Hole 1100D, only the top three core catchers contained any trace of diatoms, with Section 178-1100D-3R-CC offering the most diverse assemblage. Traces of recrystallized and reworked radiolarians occurred in most core-catcher samples. Foraminifers were rare, and no age inferences can be drawn from the material examined because of the poor nature of preservation. In essence, faunas are open shelf and marine but abraded.

The sediments, poorly consolidated diamicts throughout, have been interpreted at the top of the section as tills and glaciomarine muds, reworked by iceberg grounding. They are useful analogues for deeper sediments at other shelf sites.

Site 1102, at the edge of the continental shelf at a water depth of 442 m, was selected to examine S1 foresets on the uppermost slope. Four holes were attempted in 1.5 days on site, but excessive heave limited penetration to 7 m at the first two. A seabed camera survey of 50-m radius around the site, undertaken while waiting on heave, showed massive rock boulders grading to a fine sediment cover, allowing Hole 1102C to be better located (see Movie **M1,** a QuickTime video). Further heave curtailed 1102C at 6.5 m, but when this receded, very difficult conditions in Hole 1102D persuaded us that the rock carapace evident on the television images was thicker than anticipated and would prevent establishment of a stable hole. The rock field at the shelf edge may be the result of the sorting of tills by repeated iceberg scour, with bottom-current removal of suspended fines. Such a carapace may survive at paleoshelf breaks or may have been removed during a subsequent glacial advance.

M1. **QuickTime video** (shelf seabed).

Site 1103 was our final chance, at the inshore end of the shelf transect at a water depth of 494 m. The drilling strategy was to sample the young S1 glacial topsets, here as much as 250 m thick, and the underlying S3 glacial sediments, which we considered likely to be slightly older here than at our other successful shelf hole at Site 1097. The long swell went away, and we were able to drill to 362.7 mbsf in about 3 days until drilling time expired. Recovery from the upper 247 m was only 2.3% but improved to 34% in the lower 115 m where the matrix became hard. We logged to 240 mbsf.

In the absence of a continuous sedimentary record, stratigraphic subdivision was not attempted. Three lithofacies, however, could be distinguished within the lower 115 m: (1) diamictites, (2) poorly sorted sandstones, and (3) muddy siltstones, interpreted as reflecting deposition on a glacially influenced slope (Fig. **F18**). Massive diamictites lack internal structure, but there are composite successions where thinner, massive diamictites are interbedded with thin zones of crudely stratified facies defined by deformed mudstone stringers. Mud stringers may demarcate bed contacts if muds were deposited on bed tops between gravity flow events, and are subsequently reworked. Textural grading in deformed mudstones might indicate they were emplaced as thin turbidites. Consequently, composite diamictite successions can be interpreted as the result of alternating debrite and turbidite deposition. The scale of downslope movement is uncertain, and therefore so is the environment of deposition. Protracted downslope motion results in the generation of mature, well-sorted, graded sandstones, but sandstones here are compositionally immature and poorly sorted. Diatoms are very rare and poorly preserved, and siltstone clasts are a source of reworked diatoms. A setting is indicated on a glacial continental shelf or slope, close to a source of poorly sorted debris. Biofacies are insufficient to constrain age, water depths, or position relative to the shelf break, but the open-marine influence is less evident than at Site 1097.

F18. Simplified lithostratigraphy at Site 1103, **p. 45.**

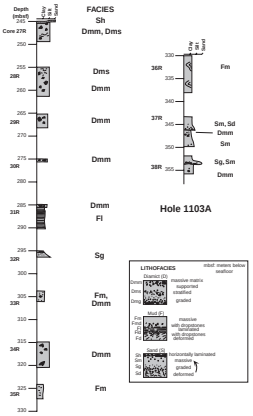


Age-diagnostic biostratigraphic material is sparse in the poorly recovered upper part and is partly reworked in the lower part. Diatom valves were often fragmented beyond identification, yet these fragments could be abundant in the material recovered. From the top of the hole down to 210 m, several biostratigraphically important species (*Actinocyclus ingens, F. barronii, T. insigna, T. inura, T. oestrupii,* and *T. torokina*) were

periodically present, allowing dates younger than their first appearances to be established. Below 210 mbsf, identifiable diatoms were more sparse. Samples from ~290 m had some diatoms of low abundance and diversity (*Denticulopsis* spp., *Nitzschia januaria,* and *Rouxia californica*), possibly of late Miocene age. (Because of the preservation state of the assemblage, however, the sediment may not be of this age.) Radiolarians were sparse in core-catcher samples, precluding any biostratigraphic determination. Reworked Cretaceous radiolarians were present in four out of five of these. Sample 178-1103A-24R-CC (228.0 mbsf) contained radiolarians from the Upsilon Zone, but marker species were not encountered in any other sample.

The foraminiferal fauna in core-catcher samples down to 218 mbsf contain rare, well-preserved, and white-colored *N. pachyderma* sinistral and older, reworked, darker colored benthic and planktonic foraminifers, together with *Inoceramus* prisms and sponge spicules. Below 250 mbsf, foraminifers are rarer with more evidence of reworking, but Samples 178-1103A-31R-CC and 33R-CC include a well-preserved assemblage of the shelf species *Cassidulinoides parkerianus*. The lowest three samples, 178-1103A-35R-CC to 37R-CC (338.77 to 355.34 mbsf), are barren. Several of the upper cores (178-1103A-13R, 14R, 15R, 17R, and 18R) contain partly dissolved calcareous nannofossils. No identifications were possible, but coccolith production is indicated.

At Site 1103 we measured the magnetization of cores spanning 250–350 mbsf. As with previous shelf sites, diamicts yielded unstable directions, and finer grained lithologies were stable. The low recovery and sparse occurrence of these lithologies make construction of a magnetostratigraphy difficult at this time. It may be possible to combine GHMT and split-core paleomagnetic data.

Hole 1103A was logged with the TC, GHMT, and FMS-sonic tool strings over an upper 150-m interval where there was no significant core recovery, but a blockage at 242 mbsf prevented penetration lower into the hole. The narrow hole diameter allowed good-quality logs. Porosity varied between 30% and 50% (lower than at the rise sites), showing a change to higher porosity only at the base of the log below 225 mbsf, close to the lithified diamictite seen below 250 mbsf in the core. Resistivity and susceptibility display broad peaks and troughs, and individual clasts can be seen in FMS images, which are all of high quality. Distinct zones of spikes in the GHMT magnetic field log probably indicate clast-rich intervals. The magnetic induction of the sediment causes most of the remaining field anomaly, and it remains to be seen whether magnetic polarities can be determined for the clast-free intervals. Log sonic velocities, combined with Hamilton Frame *P*-wave velocities from the lower hole, should allow the seismic record to be tied to drilling results. Poor core recovery from Site 1103 also means that there is no continuous MST record; physical properties data interpretation is therefore limited. Initial investigation suggests that the laminated beds below 250 mbsf are derived from the diamicts, or the same material source. Interestingly, this source differs from that at Site 1097, also on the shelf.

## Palmer Deep Sites (1098 and 1099)

Sites 1098 and 1099 (Figs. **F2, F19**) lie in the inner-shelf basins of Palmer Deep, south of Anvers Island, where an expanded, mainly biogenic sediment record has accumulated since the retreat of the ice sheet. The prime site, 1098, was in the small, narrow Basin I, at a water

F19. Bathymetry and location of site-survey seismic reflection profiles on Palmer Deep, **p. 46.**

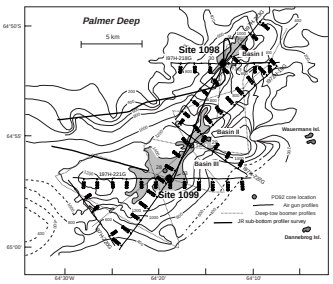

depth of 1012 m. Site 1099 was in Basin III, a larger basin in a water depth of 1425 m. Seismic profiles had shown that sediments in Basin I were thinner than in Basin III (Fig. **F20**), but short piston cores showed that the sediment record in Basin I was less prone to deposition of locally derived turbidites. Drilling was expected to provide an ultra-high-resolution paleoclimatic record of the Holocene that might show short-term (200 yr) and longer term (2500 yr) cyclic variation (Leventer et al., 1996) most probably related to global climate variation. Paleoclimatic and paleoenvironmental information from such a record would be compared with records from drilling in the Cariaco Basin, Santa Barbara Basin, and Saanich Inlet and with the record from ice cores.

Three APC holes extended to basement at 47 mbsf at Site 1098, and at Site 1099 a single section was recovered to 108 m (Figs. **F21, F22**). At Site 1098 we recovered diatom ooze to diatom-bearing mud. Deposition was by pelagic settling of diatom blooms and by gravity flow from the steep margins of the basin. Three prominent silt or sand turbidites occur between 23 and 40 mbsf. The uppermost is nearly 4 m thick, graded from diatom-bearing sandy mud to ooze, and shows a magnetic susceptibility high produced by the terrigenous component. Slumped and inclined diamict and thin-graded fine sand-silt beds were seen at the base of the holes, but most of the sequence at Site 1098 is horizontally bedded and finely laminated.

Laminae are diatom oozes of different species composition. Microfossil preservation is excellent, and this site will provide an unparalleled record of Antarctic Holocene paleoproductivity. Variation in magnetic susceptibility may show millenial and decadal cyclicity in broad intervals of high susceptibility from 0 to 8 mbsf and 30 to 38 mbsf. Cores provide an extremely high-resolution record of variation in geomagnetic field direction. GRAPE densities identify turbidite sequences between 24 and 30 mbsf, superimposed on a general trend of increasing density with depth. The approach to basement is marked by a greater increase in density coincident with the lithologic change to terrigenous silt and sand at around 42 mbsf. Natural gamma levels show some cyclicity on the order of 10 m while generally increasing downhole. Sampling for interstitial water at unusually high resolution (one per section) resulted in puzzling profiles of interstitial water chemistry at Site 1098. The sulfate reduction zone lies between 20 and 30 mbsf. Organic matter decay has surprisingly little effect on interstitial water chemistry above the sulfate reduction zone. Despite relatively high organic carbon content (1.0–1.2 wt%) and extremely rapid sedimentation, alkalinity, ammonium, and phosphate, direct by-products of organic matter decay, increase only slightly with depth in the upper 20 m. We speculate that the tightly encased *Chaetoceros* spores, the majority of diatoms in Palmer Deep, render organic material unavailable for bacterial consumption until dissolution breaches the external casing.

Site 1099 recovered a diatom ooze section like that of Site 1098 but greatly expanded by biogenic turbidites (Figs. **F21, F22**). The lowest 20 m contained black, organic-rich, laminated diatom ooze. The major diatom species at Sites 1098 and 1099 reveal a downward trend of decreasing open-ocean influence and increasing sea-ice and basin restriction. Other microfossils show similar trends: radiolarians are common and well preserved in the upper 28 mbsf of Site 1098 with relatively diverse assemblages, but diversity and abundance gradually decrease to zero at the bottom of the hole. At Site 1099 the pattern of decreasing abundance and diversity downcore is similar, but it occurs over 108 m (the record was expanded because of increased terrigenous

F20. GI air gun seismic profile I97H-228G across Palmer Deep sites, Basins I and III, **p. 47.**

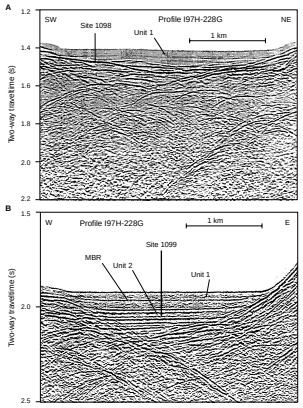


F21. Lithostratigraphic columns for Site 1098, **p. 48.**

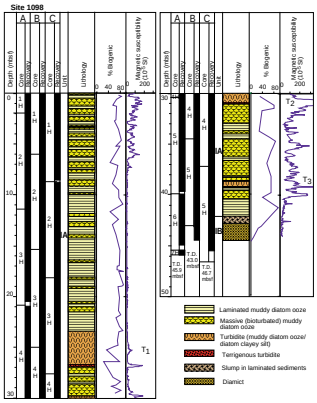


F22. Lithostratigraphic columns for Site 1099, **p. 49.**

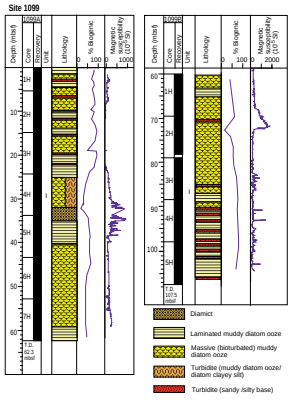

supply). Benthic foraminifers are well preserved and abundant in the upper 87 m of Hole 1099A. They appear similar to previously reported benthic foraminiferal fauna of the Bellingshausen Sea, fluctuating between open-ocean (Circumpolar Deep Water [CDW]) and shelf-water conditions and tied to 200-yr productivity cycles. However, beneath 87 mbsf in Hole 1099B, the depth of the highest black interval, the microfossil assemblages suggest more restricted oceanographic conditions (decreased CDW influence and colder shelf waters). Samples at the bottom of the hole contain large amounts of pyrite and a few foraminifers.

The sulfate reduction zone at Site 1099 lies between the seafloor and 10 mbsf, shallower than at Site 1098, and is accompanied by a steady downward increase in alkalinity and ammonium. The unusual interstitial water chemistry profiles of Site 1098 are not found at Site 1099, but organic carbon contents are comparable. Overall, at Palmer Deep sites, organic carbon content was 1.0–1.5 wt%, and the effects of organic matter decay were an order of magnitude greater than at the continental rise Sites 1095, 1096, and 1101.

MST data for the three holes at Site 1098 allow good correlation between holes to the full depth and match previous measurements on shallow cores in their upper part. The two broad intervals of high magnetic susceptibility at 0–8 and 30–38 mbsf are also marked in gamma-ray attenuation density. Deep-tow boomer records around Site 1098 show an upper stratified seismic unit and a lower, more transparent unit. The base of the stratified unit corresponds at Site 1098 to the change from mainly bioturbated to mainly laminated sediments. At Site 1099, using a synthetic seismogram derived from MST data, eight distinct reflectors in the deep-tow boomer section correlate exactly with distinct turbidite horizons. A widespread, strong mid-basin reflector beneath them coincides with a sand and pebble layer at 33 mbsf.

## Conclusions

Nine sites on the Pacific margin of the Antarctic Peninsula were drilled during Leg 178 in three depositional environments. Four (1097, 1100, 1102, and 1103) were on the glacial, overdeepened outer continental shelf to investigate sediments deposited by grounded ice over the past 10 m.y. Three (1095, 1096, and 1101) were on sediment drifts on the continental rise to examine the fine-grained component of glacial shelf sediments. These sediments, moved there by turbidity and bottom currents, contain a more complete, higher resolution, more easily recovered and dated glacial record. The two remaining sites (1098 and 1099) were drilled in Palmer Deep, an isolated basin of the inner shelf that contains an ultrahigh-resolution record of Holocene paleoenvironmental change.

The outer continental shelf sites and the rise sites are complementary: the more direct but less complete record on the shelf helps interpretation of the record on the rise. Together they provide insights useful in attempts to recover the much longer but possibly less accessible record of East Antarctic glaciation. The inner-shelf basin record was assumed to represent regional paleoclimate and will be compared with records from similar environments drilled by ODP (Cariaco Basin, Santa Barbara Basin, and Saanich Inlet) and with ice-core records.

Sites 1095, 1096, and 1101 on the continental rise sediment drifts provided virtually continuous cores, back to about 10 Ma at Site 1095, 4.7 Ma at Site 1096, and 3.1 Ma at Site 1101 (Figs. **F2, F3, F8, F11, F13**). The depositional environments at the sites were different, ranging from

a dominantly hemipelagic mode on the rise crest and center to a dominantly turbiditic mode at the distal site. However, none of the sites was an end-member environment: the distal site received mainly fine-grained distal turbidites but with a substantial hemipelagic/pelagic component, and the rise-crest sites were not isolated from deposition of fine-grained graded beds within a dominantly hemipelagic environment. All sites revealed a cyclicity in sedimentation that, whatever the dominant depositional mode at the site, was considered to reflect the cyclic provision of glacial sediments to the uppermost continental slope. Concerning the value of drilling at this margin as a guide to drilling at other Antarctic margins, this mixed depositional environment was an advantage: few of the other drifts around Antarctica are as isolated from distal turbidite deposition as Drift 7 (Site 1096). It is therefore reassuring to know that a signal of cyclic glacial loading of the upper slope is provided also, within even a dominantly turbiditic environment such as Site 1095.

Sedimentation rates were highest on the drift crest (Site 1096 [Fig. F11]) and lowest on the distal flank (Site 1095 [Fig. F8]) as expected. At all three sites, the rates decreased through the Pliocene and into the Pleistocene. The high rates make possible a detailed study of cyclicity in deposition. No such investigation has progressed far as yet, but it is reassuring to know that several parameters show a variability with a period similar to the Milankovic cyclicity seen in lower latitudes (notably 40 k.y. within the Pliocene). This includes lithologic alternations (turbidite abundance, bioturbation, possibly ice-rafted debris, and color), magnetic susceptibility, and density (cores and logs). Clay mineralogy appears to have glacial–interglacial variability (Fig. F23) and could become a useful additional proxy. We even recovered calcareous nannofossils and foraminifers through part of the Pliocene–Pleistocene, an unexpected bonus. It would seem clear that the continental rise is sensitive to variations in the glacial state of the continent and that these reflect the orbital variation in insolation through much of the period examined. A downward change at Site 1095 that sees no cyclicity before about 9 Ma may mark a change in the level or nature of glaciation on the shelf, if not its initiation.

The objectives of drilling on the continental shelf were to test the pre-existing depositional model, to date major changes in depositional geometry (so these could be compared with changes in continental rise deposition), and to improve understanding of shelf sedimentation ahead of similar proposed drilling elsewhere around Antarctica. We drilled three sites on a dip transect of a depositional lobe (1102, 1100, and 1103, in landward order [Fig. F17]), and Site 1097 was drilled in an interlobe area farther south (Fig. F15). Drilling was severely hindered by swell, and recovery was made difficult (as expected) by the unsorted nature of unconsolidated subglacial tills and related diamicts. In drilling we were largely limited to the basic RCB technique, and recovery was very poor until the fine-grained matrix of a diamict became hard enough to support the large clasts that were inevitably encountered. Recovery then improved (e.g., to an average 34% below 250 m at Site 1103).

The glacial nature of the youngest sequence group (S1) was amply confirmed, and much of it could be given a Pleistocene or latest Pliocene age, but recovery was poor everywhere (the outermost shelf was particularly unfriendly). The most information on S1 is likely to come from the broad suite of logs obtained at Site 1103 (Fig. F24). Sequence Group S2 was sampled only at Site 1097, where it is thin; its

F23. Relative abundances of chlorite, illite, and mixed-layer clays from Sites 1095, 1096, 1097, and 1101, p. 50.

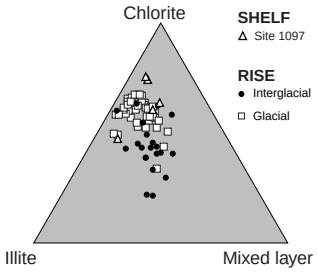


F24. Downhole logs from Hole 1103A with core measurements, p. 51.

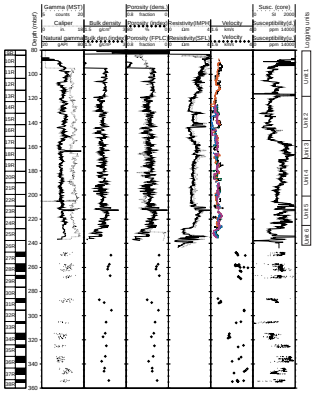

older part is early Pliocene in age (Fig. F25). Sequence S3, whose age and origin were in doubt before drilling, was sampled at Sites 1097 and 1103. This sequence is continuous and similar in seismic expression (Fig. F17) along the West Antarctic margin to at least 105°W, and it lacks the focus into depositional lobes of the overlying S2 and S1. It was clearly established as a mostly glacial sequence, although probably reflecting a greater range of environments than S2 and S1 (from subglacial to glaciomarine) and a lesser level of glaciation. The conformity of its top with the base of S2, deduced from seismic profiles in the region of Site 1097, was essentially confirmed by the age range for the boundary (between 4.5 and 4.6 Ma) established by drilling. Seismic data suggest that the part of S3 sampled at Site 1103 is older than at Site 1097. The inferred depositional environment at Site 1097, near the paleoshelf edge, was perhaps more open marine than that at Site 1103, although the depositional environment was of lower energy. It is uncertain whether this reflects a time change in climate or in depositional environment. Dating of the lower part of S3 is uncertain as yet but should be improved by a range of shore-lab studies. It seems unlikely that the recovered sediments range back to 9 Ma, the time of a change in shelf environment inferred at Site 1095 on the rise.

Preliminary results of drilling in Palmer Deep accorded with expectations based on piston cores. Basin I, the narrowest basin with the thinner sediment fill, is less affected by turbiditic sedimentation than Basin III. The 45-m-thick sediment fill of Basin I (Site 1098) contains mainly laminated and massive muddy diatom ooze, with laminae probably reflecting changes in surface productivity (Figs. F21, F22). In Basin III (Site 1099), the alternation of laminated and massive muddy diatom oozes is interrupted more frequently by turbidites with a terrigenous graded base. The highly reflective lower seismic unit (Fig. F20B) is an alternation of thin turbidites and laminated diatom ooze, with a strong impedance contrast with the upper semitransparent unit. At this stage, we cannot say how the sedimentary records of the two basins correlate. The downhole change of diatom and foraminifer assemblages indicating more restricted oceanographic conditions at the base of Basin I and in the lower part of Hole 1099B suggests that the two recovered sections underwent a similar evolution and may therefore be approximately coeval.

Shipboard analysis of Palmer Deep cores was limited, with sampling mainly postponed to the Bremen Core Repository. It is worth noting, however, that the only high-resolution shipboard study (of pore-water composition) revealed anomalous and still-puzzling chemical gradients. Despite the inferred rapid but steady accumulation of sediment, pore waters in the upper 20 m at Site 1098 reveal a homogeneous composition that suggests almost complete mixing. The explanation of these gradients will come from postcruise studies of the relationships between pelagic settling of organic-rich material, turbiditic sedimentation, and bioturbation.

Several additional opportunities offered by Leg 178 drilling are being exploited by the shipboard party. The continuous, high-resolution, partly terrigenous record of the continental rise drift sites—and the high southern latitudes of this leg—provide excellent magnetostratigraphic data (e.g., Fig. F26). They also present opportunities for a wide range of studies, including field paleointensity, rock magnetism, detailed examination of particular reversals, and the nature of certain cryptochrons. The Palmer Deep sediments should also provide high-resolution paleointensity and secular variation data. The existence of a

F25. Biostratigraphic summary of shelf sites with seismic correlation, p. 52.

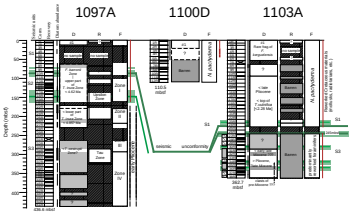


F26. Magnetostratigraphic summary for continental rise sites, p. 53.

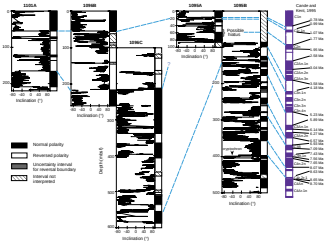

detailed high-latitude magnetostratigraphy and the location of the rise sites in a low-energy environment securely within the Antarctic water masses provide further opportunities to check and refine high-latitude biostratigraphy. These will be further enhanced if an orbital chronology can be established.

Pore-water geochemistry is of interest at several sites, notably Palmer Deep, where it seems capable of informing the wide range of high-resolution investigations currently planned. The logging effort, though curtailed by hole conditions in places, also shows promise. In general terms, we have a wide range of physical properties and log data from a cluster of generically related environments that will repay closer study. This leg has seen the first-ever FMS examination of subglacial tills (at Site 1103), and the comparison between high-quality core magnetostratigraphy and the GHMT record at Site 1095 is likely also to be productive. VSP and sonic logs will aid correlation between the hole and the seismic record and allow the results of drilling to feed back into the exceptionally large regional seismic reflection data set.

An additional opportunity, not considered within either proposal or discussed in the leg prospectus, was to detect at the continental rise sites the late Pliocene Eltanin asteroid impact. The renewed interest was generated by Gersonde et al. (1997). The Leg 178 sites lay 1300 km distant from the likely impact area. The rise drifts, being at their crest perhaps only three-quarters of the water depth of the direct path, seemed areas where a sedimentological event might be detectable, helping to guide us to geochemical and paleontological anomalies that would otherwise be difficult to find. At present, until stratigraphic control has improved, the impact is not clearly identified within the sediments. Each rise site, however, shows a single anomalous depositional or erosional event that may be associated with it.

## REFERENCES

Alley, R.B., Blankenship, D.D., Rooney, S.T., and Bentley, C.R., 1989. Sedimentation beneath ice shelves—the view from Ice Stream B. *Mar. Geol.,* 85:101–120.

Anderson, J.B., Pope, P.G., and Thomas, M.A., 1990. Evolution and hydrocarbon potential of the Antarctic Peninsula continental shelf. *In* St. John, B. (Ed.), *Antarctica as an Exploration Frontier: Hydrocarbon Potential, Geology and Hazards*. AAPG Stud. Geol., 31:1–12.

Barker, P.F., 1982. The Cenozoic subduction history of the Pacific margin of the Antarctic Peninsula: ridge crest-trench interactions. *J. Geol. Soc. London,* 139:787–801.

————, 1992. The sedimentary record of Antarctic climate change. *Philos. Trans. R. Soc. London B,* 338:259–267.

Barker, P.F., 1995. The proximal marine sediment record of Antarctic climate since the late Miocene. *In* Cooper, A.K., Barker, P.F., and Brancolini G. (Eds.), *Geology and Seismic Stratigraphy of the Antarctic Margin.* Am. Geophys. Union, Antarct. Res. Ser., 68:25–57.

Barker, P.F., and Cooper, A.K., 1997. *Geology and Seismic Stratigraphy of the Antarctic Margin* (Pt. 2). Am. Geophys. Union, Antarctic Res. Ser., 71.

Barron, J., Larsen, B., et al., 1989. *Proc. ODP, Init. Repts.,* 119: College Station, TX (Ocean Drilling Program).

Bart, P.F., and Anderson, J.B., 1995. Seismic record of glacial events affecting the Pacific margin of the Northwestern Antarctic Peninsula. *In* Cooper, A.K., Barker, P.F., and Brancolini, G. (Eds.), *Geology and Seismic Stratigraphy of the Antarctic Margin.* Am. Geophys. Union, Antarct. Res. Ser., 68:75–96.

Bartek, L.R., Vail, P.R., Anderson, J.B., Emmet, P.A., and Wu, S., 1991. Effect of Cenozoic ice sheet fluctuations in Antarctica on the stratigraphic signature of the Neogene. *J. Geophys. Res.,* 96:6753–6778.

Birkenmajer, K., 1992. Evolution of the Bransfield basin and rift, West Antarctica. *In* Yoshida, Y., Kaminuma, K., and Shiraishi, K. (Eds.), *Recent Progress in Antarctic Earth Science:* Tokyo (Terra Sci. Publ.), 405–410.

Camerlenghi, A., Rebesco, M., and Pudsey, C.J., 1997. High resolution terrigenous sedimentary record of the sediment drifts on the Antarctic Peninsula Pacific margin. *In* Ricci, C.A. (Ed.), *The Antarctic Region: Geological Evolution and Processes*. Init. Results, SEDANO Progr., *Terra Antarct.,* 705–710.

Cooper, A.K., Barker, P.F., and Brancolini, G., 1995. *Geology and Seismic Stratigraphy of the Antarctic Margin*. Am. Geophys. Union, Antarct. Res. Ser., 68. (Atlas, CD-ROM).

Cooper, A.K., Barker, P.F., Webb, P.-N., and Brancolini, G., 1994. The Antarctic continental margin—the Cenozoic record of glaciation, paleoenvironments and sea-level change. *Terra Antarct.,* 1/2:236–480.

Cooper, A.K., Barrett, P.F., Hinz, K., Traube, V., Leitchenkov, G., and Stagg, H.M.J., 1991. Cenozoic prograding sequences of the Antarctic continental margin: a record of glacio-eustatic and tectonic events. *Mar. Geol.,* 102:175–213.

Cunningham, A.P., Vanneste, L.E., and the ANTOSTRAT Antarctic Peninsula Regional Working Group, 1995. The ANTOSTRAT Antarctic Peninsula Regional Working Group Digital Navigation Compilation. *In* Cooper, A.K., Barker, P.F., and Brancolini, G. (Eds.), *Geology and Seismic Stratigraphy of the Antarctic Margin*. Am. Geophys. Union, Antarct. Res. Ser., 68:A297–A301.

Denton, G.H., Sugden, D.E., Marchant, D.R., Hall, B.L., and Wilch, T.I., 1993. East Antarctic ice sheet sensitivity to Pliocene climate change from a Dry Valleys perspective. *Geograf. Ann.,* 75A:155–204.

Domack, E.W., and McClennen, C.E., 1996. Accumulation of glacial marine sediments in fjords of the Antarctic Peninsula and their use as late Holocene paleoenvironmental indicators. *Am. Geophys. Union, Antarct. Res. Ser.,* 70:135–154.

Drewry, D.J., and Morris, E.M., 1992. The response of large ice sheets to climate change. *Philos. Trans. R. Soc. London B.,* 338:235–242.

Gersonde, R., Kyte, F.T., Bleil, U., Diekmann, B., Flores, J.A., Gohl, K., Grahl, G., Hagen, R., Kuhn, G., Sierro, F.J., Voelker, D., Abelmann, A., and Bostwick, J. A., 1997. Geological record and reconstruction of the late Pliocene impact of the Eltanin asteroid in the Southern Ocean. *Nature,* 390:357–363.

Haq, B.U., Hardenbol, J., and Vail, P.R., 1987. Chronology of fluctuating sea levels since the Triassic. *Science,* 235:1156–1167.

Hayes, D.E., Frakes, L.A., et al., 1975. *Init. Repts. DSDP,* 28: Washington (U.S. Govt. Printing Office).

Huybrechts, P., 1993. Glaciological modelling of the Late Cenozoic East Antarctic ice sheet: stability or dynamism. *Geograf. Ann.,* 75A:221–238.

Kuvaas, B., and Kristoffersen, Y., 1991. The Crary Fan: a trough-mouth fan on the Weddell Sea continental margin, Antarctica. *Mar. Geol.,* 97:345–362.

Kuvaas, B., and Leitchenkov, G., 1992. Glaciomarine turbidite and current-controlled deposits in Prydz Bay, Antarctica. *Mar. Geol.,* 108:365–381.

Larter, R.D., and Barker, P.F., 1989. Seismic stratigraphy of the Antarctic Peninsula Pacific margin: a record of Pliocene-Pleistocene ice volume and paleoclimate. *Geology,* 17:731–734.

————, 1991a. Effects of ridge-crest trench interaction on Antarctic-Phoenix spreading: Forces on a young subducting plate. *J. Geophys. Res.,* 96:19583–19607.

————, 1991b. Neogene interaction of tectonic and glacial processes at the Pacific margin of the Antarctic Peninsula. *In* Macdonald, D.I.M. (Ed.), *Sedimentation, Tectonics and Eustasy.* Spec. Publ. Int. Assoc. Sedimentol., 12:165–186.

Larter, R.D., and Cunningham, A.P., 1993. The depositional pattern and distribution of glacial-interglacial sequences on the Antarctic Peninsula Pacific Margin. *Mar. Geol.,* 109:203–219.

Larter, R.D., Rebesco, M., Vanneste, L.E., Gamboa, L.A.P., and Barker, P.F., 1997. Cenozoic tectonic, sedimentary and glacial history of the continental shelf west of Graham Land, Antarctic Peninsula. *In* Barker, P.F., and Cooper, A.K. (Eds.), *Geology and Seismic Stratigraphy of the Antarctic Margin* (Pt. 2). Am. Geophys. Union, Antarct. Res. Ser., 71:1–27.

Leventer, A., Domack, E.W., Ishman, E., Brachfeld, S., McClennen, C.E., and Manley, P., 1996. Productivity cycles of 200–300 years in the Antarctic Peninsula region: understanding linkages among the sun, atmosphere, oceans, sea ice, and biota. *Geol. Soc. Am. Bull.,* 108:1626–1644.

McGinnis, J.P., and Hayes, D.E., 1995. The roles of downslope and along-slope depositional processes: southern Antarctic Peninsula continental rise. *In* Cooper, A.K., Barker, P.F., and Brancolini, G. (Eds.), *Geology and Seismic Stratigraphy of the Antarctic Margin.* Am. Geophys. Union, Antarct. Res. Ser., 68:141–156.

Miller, K.G., Fairbanks, R.G., and Mountain, G.S., 1987. Tertiary oxygen isotope synthesis, sea-level history, and continental margin erosion. *Paleoceanography,* 2:1–19.

Pope, P.G., and Anderson, J.B., 1992. Late Quaternary glacial history of the northern Antarctic Peninsula's western continental shelf: evidence from the marine record. *Am. Geophys. Union, Antarct. Res. Ser.,* 57:63–91.

Pudsey, C.J., Barker, P.F., and Larter, R.D., 1994. Ice sheet retreat from the Antarctic Peninsula shelf. *Continental Shelf Res.,* 14:1647–1675.

Rebesco, M., Camerlenghi, A., DeSantis, L., Domack, E.W., and Kirby, M.E., 1998. Seismic stratigraphy of Palmer Deep: a fault-bounded Late Quaternary sediment trap on the inner continental shelf, Antarctic Peninsula Pacific margin. *Mar. Geol.,* 151:89-110.

Rebesco, M., Camerlenghi, A., and Zanolla, C., in press. Bathymetry and morphogenesis of the continental margin west of the Antarctic Peninsula. *Terra Antarct.*

Rebesco, M., Larter, R.D., Barker, P.F., Camerlenghi, A., and Vanneste, L.E., 1997. The history of sedimentation on the continental rise west of the Antarctic Peninsula. *In* Barker, P.F., and Cooper, A.K. (Eds.), *Geology and Seismic Stratigraphy of the Antarctic Margin* (Pt. 2). Am. Geophys. Union, Antarctic Res. Ser., 71:29–50.

Rebesco, M., Larter, R.D., Camerlenghi, A., and Barker, P.F., 1996. Giant sediment drifts on the continental rise of the Antarctic Peninsula. *Geo-Mar. Lett.,* 16:65–75.

Sahagian, D.L., and Watts, A.B., 1991. Introduction to the Special Section on measurement, causes and consequences of long-term sea level changes. *J. Geophys. Res.,* 96:6585–6589.

Shackleton, N.J., Hall, M.A., and Pate, D., 1995. Pliocene stable isotope stratigraphy of Site 846. *In* Pisias, N.G., Mayer, L.A., Janecek, T.R., Palmer-Julson, A., and van Andel, T.H. (Eds.), *Proc. ODP, Sci. Results,* 138: College Station, TX (Ocean Drilling Program), 337–355.

Tiedemann, R., Sarnthein, M., and Shackleton, N.J., 1994. Astronomic timescale for the Pliocene Atlantic $\delta^{18}O$ and dust flux records of Ocean Drilling Program Site 659. *Paleoceanography,* 9:619–638.

Tomlinson, J.S., Pudsey, C.J., Livermore, R.A., Larter, R.D., and Barker, P.F., 1992. GLORIA survey of the Pacific margin of the Antarctic Peninsula: tectonic fabric and sedimentary processes. *In* Yoshida, Y., Kaminuma, K., and Shiraishi, K. (Eds.), *Recent Progress in Antarctic Earth Science:* Tokyo (Terra Sci. Publ.), 423–429.

Vanneste, L.E., and Larter, R.D., 1995. Deep-tow boomer survey on the Antarctic Peninsula Pacific margin: an investigation of the morphology and acoustic characteristics of Late Quaternary sedimentary deposits on the outer continental shelf and upper slope. *In* Cooper, A.K., Barker, P.F., and Brancolini, G. (Eds.), *Geology and Seismic Stratigraphy of the Antarctic Margin.* Am. Geophys. Union, Antarct. Res. Ser., 68:97–121.

Webb, P.-N., and Harwood, D.M., 1991. Late Cenozoic glacial history of the Ross Embayment, Antarctica. *Quat. Sci. Rev.,* 10:215–223.

# APPENDIX

## Descriptive Notes of Site-Survey Seismic Profiles[3]

Acquisition parameters for the profiles displayed in Figure AF1 (an oversized figure that accompanies this volume) and others used for Ocean Drilling Program Leg 178 site locations are given in Tables T9, p. 65, and T10, p. 66, both in the "Explanatory Notes" chapter. Figure F10, p. 38, in Barker and Camerlenghi (Chap. 2, this volume), is a track chart of all the seismic profiles available in the ANTOSTRAT Antarctic Peninsula Regional Working Group database (see also Cunningham et al., 1995), including those displayed in Figure AF1. The profiles in Figure AF1 are located with respect to seafloor morphology in the two maps in the lower right corner of Figure AF1, side 1. All times referred to are two-way traveltime (TWT).

AF1. Seismic reflection profiles crossing sites drilled during Leg 178, p. 59.

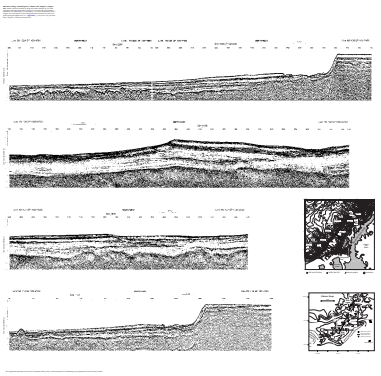

### Profiles I95-135, I95-135A, I95-137, and I95-130

The Programma Nazionale di Ricerche in Antartide (Italy) (PNRA) profiles on Drift 7 (Sites 1095 and 1096) are 60-fold stacks of common depth point (CDP) gathers spaced 12.5 m apart. Traces have been deconvolved before stack with a 160-ms operator and 4-ms predictive interval. Velocity analyses were performed every 4 km. The display sections were produced with time-variant three-trace lateral mix, time-variant band-pass filter, and trace equalization using a variable window.

These profiles illustrate the three-dimensional structure of Drift 7: profile I95-135 is a dip section from the continental shelf to the lower continental rise along the axis of elongation of Drift 7. The drift is separated from the steep (up to 20°) continental slope by an area highly incised by gullies and incipient deep-sea channels. The sediments rest on oceanic basement and thin from the drift crest seaward. The limited energy provided by the two Generator Injector guns prevents unequivocal detection of oceanic basement below the thicker and rougher sediment section at the base of the slope, although the main shallow sedimentary reflectors can be traced from the continental rise into the slope. Note the transition from a basin-fill geometry, for sediments directly overlying oceanic basement, to a drape geometry in overlying units. This transition is considered to represent a change from turbiditic sedimentation, on young basaltic seafloor approaching the paleosubduction zone, to mainly pelagic, alternating with contouritic and distal turbiditic deposition during the drift growth and maintenance stages of Rebesco et al. (1996, 1997).

Profile I95-130A is a proximal strike section through the drift crossing Site 1096. The drift is asymmetric, with a steep side and a gentle side, and is bounded to the northeast and southwest by large deep-sea channel systems, each displaying local and asymmetric levee deposits. Drift growth is identified by reflector divergence below the present-day steep side of the drift and by progressive migration of the paleodrift crest to the northeast. The bottom-simulating reflector at ~700 ms below seafloor, particularly evident under the steep side of the drift, is believed to be a silica diagenetic front (see also "Physical Properties," p. 21, in the "Site 1096" chapter). Profile I95-137 is a distal strike section through Drift 7, crossing Site 1095. Note that the relief of the drift is considerably reduced with respect to the proximal drift. This allows more silt turbidite deposition on the drift, which inverts its sense of asymmetry: its steeper side is to the northeast, and it assumes the char-

[3]Signal processing was performed as follows: PNRA profiles by Claudio Pelos and Lorenzo Sormani, Osservatorio Geofisico Sperimentale, Trieste, Italy; AMG profile by Alex P. Cunningham, BAS, Cambridge, United Kingdom; and AISM profile by Emilia L. Gulmezova and J. Maldonado, Universidad de Granada, Spain. Signal acquisition and recording of NSF-USAP deep-tow boomer profiles were done by Michael Belliveau, Geoforce Consultants Ltd., Dartmouth NS, Canada.

acter of an overbank deposit of the channel system to the northeast. The loss of seismic energy below this channel system, evident on profile I95-130A, is the result of the presence of coarse sediments of irregular geometry within the channels. The two cross sections show that the channel systems are long-lived features that have never migrated through the position of the present-day sediment drift.

## Profile IT92-114

Profile IT92-114A (Site 1101) is a 30-fold stack of CDP gathers spaced 25 m apart. Although this line was acquired with a streamer configuration similar to that of the lines collected in 1995 (above), the shot spacing was wider (50 m), reducing coverage. Compared to the 1995 profiles, profile IT92-114A has less vertical and horizontal resolution (4-ms sampling and 25-m CDP spacing) but larger total source volume (72 L) and thus greater penetration. Traces were deconvolved before stack with a 160-ms operator and 16-ms predictive interval. Velocity analyses were every 5 km. The display section was produced with time-variant three-trace lateral mix, time-variant band-pass filter, and trace equalization using a 300-ms window.

Profile IT92-114A is a dip section from the continental shelf to the lower continental rise along the axis of elongation of Drift 4 across Site 1101. Note the similar morphological and stratigraphic elements on this profile and profile I95-135 (the slope angle is 16.5°). The oceanic basement reflector can be followed here to the base of slope, where it is affected by velocity pull-up. The deep, discontinuous subhorizontal reflector at ~7.5 s TWT is the Mohorovicic Discontinuity (Moho). A strong reflector can be traced from the drift to the continental shelf that correlates with the uplift unconformity of Larter and Barker (1991b) and Larter et al. (1997).

## Profile AMG 845-08

British Antarctic Survey (BAS) profile AMG 845-08 (shelf transect, Sites 1100, 1102, and 1103) is a 24-fold stack of CDP gathers spaced 25 m apart with 4-ms sampling. Traces were deconvolved before stack with a 300-ms operator and 24-ms predictive interval. Velocity analyses were every 3 km. The display section was produced with three-trace lateral mix, time-variant band-pass filter, and trace equalization using a 500-ms window. No attempt was made to remove the seafloor multiple for this display.

Part of profile AMG 845-08 lies along the same track as profile I95-152, which was obtained to improve vertical resolution. The two profiles are complementary. Profile AMG 845-08 extends from the continental rise to the mid-shelf basin. On the rise, it crosses from the small Drift 2 to the lower continental slope via the channel-dissected uppermost continental rise (this area has GLORIA coverage; see Rebesco et al., 1996). Oceanic crust here is aged ~11 Ma (see also Fig. **F7,** p. 35, in Barker and Camerlenghi (Chap. 2, this volume), and, beneath the rise, reflections from the Moho are seen at 7–7.5 s. Sediments overlying the ocean floor can be traced beneath the slope. The uppermost 2 s of the shelf section of the profile may be compared with the expanded and higher resolution profile I95-152. Below 2 s, Sequence Group S2 and Sequence S3 may be seen downlapping onto a strong reflector considered to be the top of the precollision accretionary prism. This strong reflector is common along the margin and forms part of the S4/S3

"uplift unconformity" of Larter et al. (1997). Its equivalent in an older collision segment farther to the southwest continues seaward to the hiatus in terrigenous sedimentation discovered at Deep Sea Drilling Project Site 325 and considered by Larter and Barker (1991a) to have been caused by collision-related uplift at that segment of the margin.

## Profile I95-152

PNRA profile I95-152 (shelf transect, Sites 1100, 1102, and 1102) is a 30-fold stack of CDP gathers spaced 6.26 m apart with 2-ms sampling. Traces were deconvolved before stack with an 80-ms operator and 4-ms predictive interval. Velocity analyses were every 2 km. The seafloor multiple reflection was attenuated by the application of a median filter to CDP gathers corrected for multiple velocity. The display section was produced with time-variant three-trace lateral mix, deconvolution in the frequency domain, time-variant band-pass filter, and trace equalization using a variable window.

Profile I95-152 provides a high-resolution image of the geometry of the glacial prograding wedge and of the "preglacial" structure of the continental shelf, complementary to that of profile AMG 845-08, which follows the same track. Figure **F2,** p. 30, in the "Shelf Transect" chapter, shows the boundaries of the major seismic Sequence Groups S1 through S4 of Larter and Barker (1991b), Larter and Cunningham (1993), and Larter et al. (1997). A distinctive feature of this profile and of AMG 845-08 (above) is the comparative strength of topset reflectors within Sequence Group S1, considered to result from ice loading and related shear, which is greatly reduced in related foresets beyond the paleoshelf edge. The low-profile near-surface wedge of sediment landward of shotpoint (S.P.) 950 (sampled at Site 1100) was interpreted by Vanneste and Larter (1995) as a prograding till body emplaced during the last glaciation but not reaching the continental shelf edge at that location (see also Fig. **F3,** p. 31, in the "Shelf Transect" chapter).

## Profile AISM-06

Most of Programa Nacional de Investigación en la Antártida (Spain) profile AISM-06 (Site 1097) is a 48-fold stack of CDP gathers 12.5 m apart from shots at 25-m intervals with 2-ms sampling (resampled to 4 ms), obtained from the *Hesperide* in December 1997. Traces were deconvolved before stack with a 250-ms operator and 8-ms predictive interval. Velocity analyses were every 6 km. The display section was produced with time-variant band-pass filter and trace equalization. The continental slope section of AISM-06 (S.P. >5480) was shot at 50-m intervals with 24-fold cover.

Profile AISM-06 was obtained along virtually the same track as the PD-88 profile used to locate Site 1097 (see Fig. **F1,** p. 23, in the "Site 1097" chapter). It crosses an interlobe region where the progradational Sequence Groups S1 and S2 thin to ~150 ms (at Site 1097), and access to Sequence S3 is therefore easier. Previously published analyses of shelf sedimentation (Larter and Barker, 1989, 1991b; Larter et al., 1997) have interpreted Sequence S3 as having an upper boundary (with S2) that was climate-related and thus essentially synchronous along the margin. Its lower boundary (with S4) was associated with ridge-crest subduction and therefore diachronous along the margin. Sequence S3 shows little variation in thickness or geometry along the margin, in contrast to the

overlying Sequence Groups S2 and S1, which are focused into progradational lobes.

## Profile I97H-221G

Single-channel line I97H-221G was obtained by stacking eight traces of a 10-hydrophone ministreamer. Shot spacing was 12.5 m, and the sampling interval was 1 ms (high-cut filter 308 Hz). Traces were deconvolved with a 60-ms operator and 1-ms predictive interval. The display sections were produced with three-trace time-variant lateral mix, time-variant band-pass filter, and trace equalization using a variable window.

PNRA profile I97H-221G (Site 1099) shows the structural setting of Palmer Deep Basin III. The sediment fill is as much as 300 ms thick. It displays high-amplitude reflectors, with many hyperbolae produced by diffractions from both the seafloor and deeper lithologic or structural discontinuities. A reflector of unknown origin is seen between 1 and 1.5 s TWT below the seafloor. A prominent reflector with eastward apparent dip below the depocenter of Basin III has been interpreted by Rebesco et al. (1998) as the master fault of a half-graben structure producing the inferred active subsidence of the basin floor. Other, weaker reflectors on the footwall side of the master fault have been judged to be conjugate faults. Profile I97H-221G also shows a twofold division of the sedimentary fill: a low-reflectivity subunit above and a high-reflectivity subunit below. The boundary between the two, at 76 meters below seafloor (mbsf) at Site 1099, has been identified by drilling as a downward transition from massive, bioturbated clayey silts to thinly spaced alternations of massive diatom ooze and fine-grained graded turbidites.

## Profiles LMG 98-2

National Science Foundation–United States Antarctic Program (NSF-USAP) profiles LMG 98-2 (Palmer Deep, Sites 1098 and 1099) were acquired from the *L. M. Gould* in Palmer Deep during drilling of Leg 178 and were used to refine the positions of the two sites. The Huntec deep-tow boomer was towed ~100 m below the sea surface; the firing interval was either 1000 or 750 ms, depending on water depth, and the record length was 250 ms. The displays were obtained with automatic gain control, with band-pass filters of 1.4–5.0 kHz (Basin I) and 2.0–4.0 kHz (Basin III).

The profile across Basin I shows the drape geometry of the thin sedimentary fill in the southwest corner of Basin I, where Site 1098 is located. The strong hyperbolic basal reflectors are hard rock, hit by the hydraulic piston corer at 46 mbsf at Hole 1098A but not sampled. The profile across Basin III shows only the upper part of the sediment fill. Acoustic basement of this profile is the high-amplitude mid-basin reflector, which corresponds to a clast-poor diamict layer within a mixed pelagic and turbiditic upper unit at 34 mbsf at Site 1099. (See also **"Background and Scientific Objectives,"** p. 1, and **"Seismic Stratigraphy,"** p. 22, in the "Palmer Deep" chapter, and Rebesco et al. [1998]).

**Figure F1.** General map of Leg 178 ship track with drill sites starred.

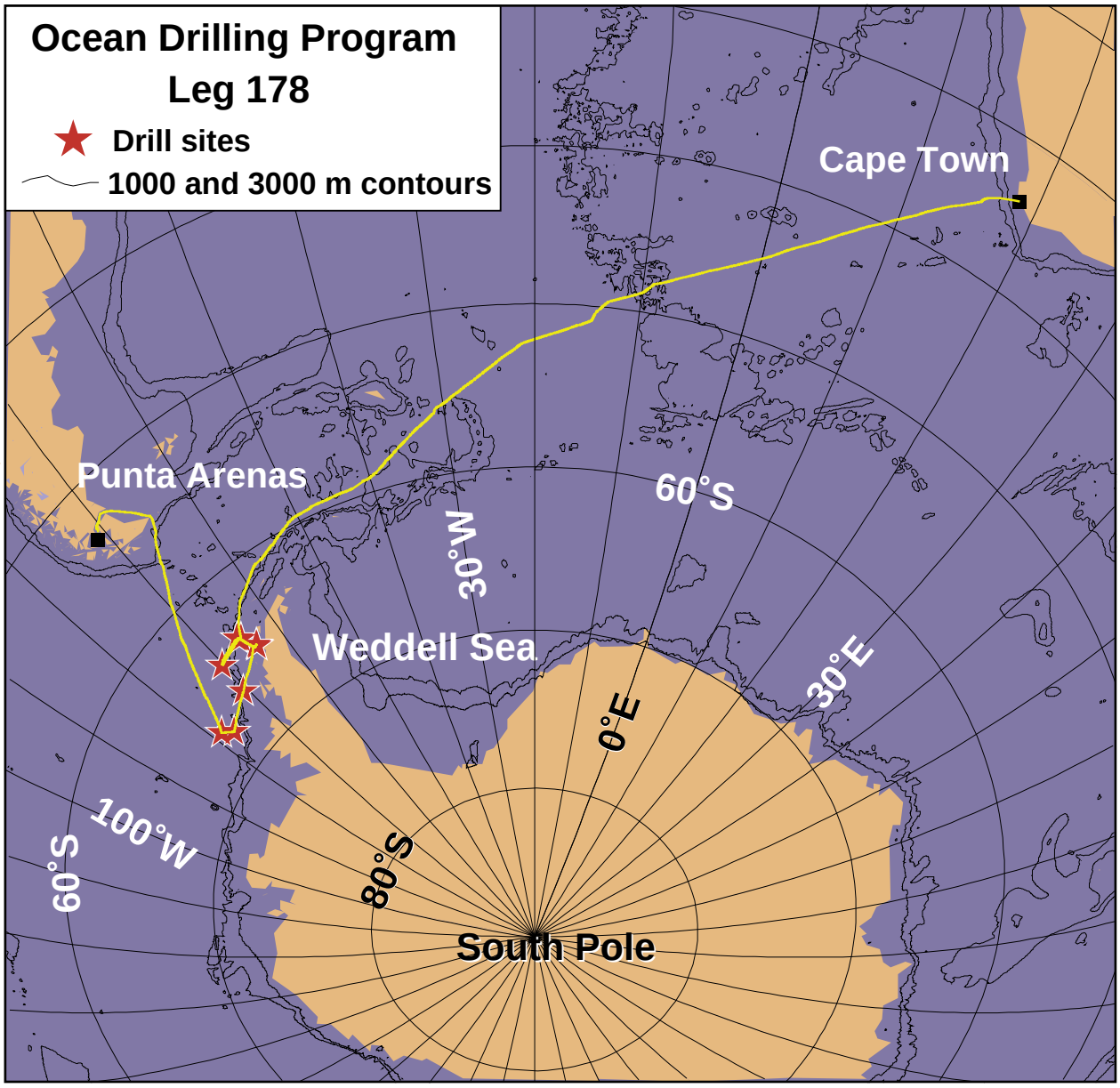

**Figure F2.** Bathymetric chart of the Antarctic Peninsula Pacific margin (after Rebesco et al., in press) with Leg 178 sites marked (bathymetry in meters). SM = seamount.

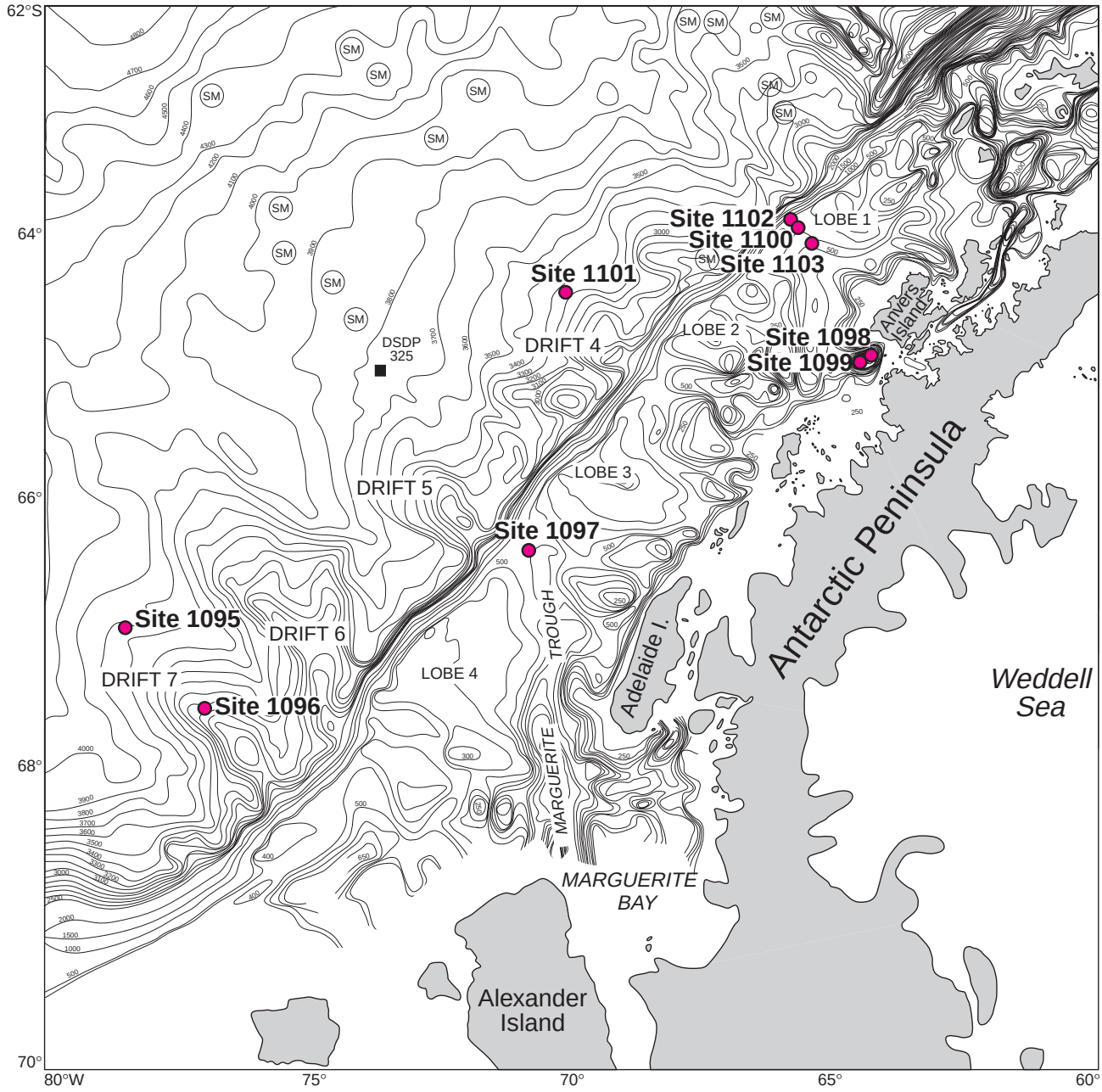

**Figure F3.** Schematic figure of tectonic and glacial elements of the Antarctic Peninsula margin and sites drilled during Leg 178 (revised from Barker, 1995).

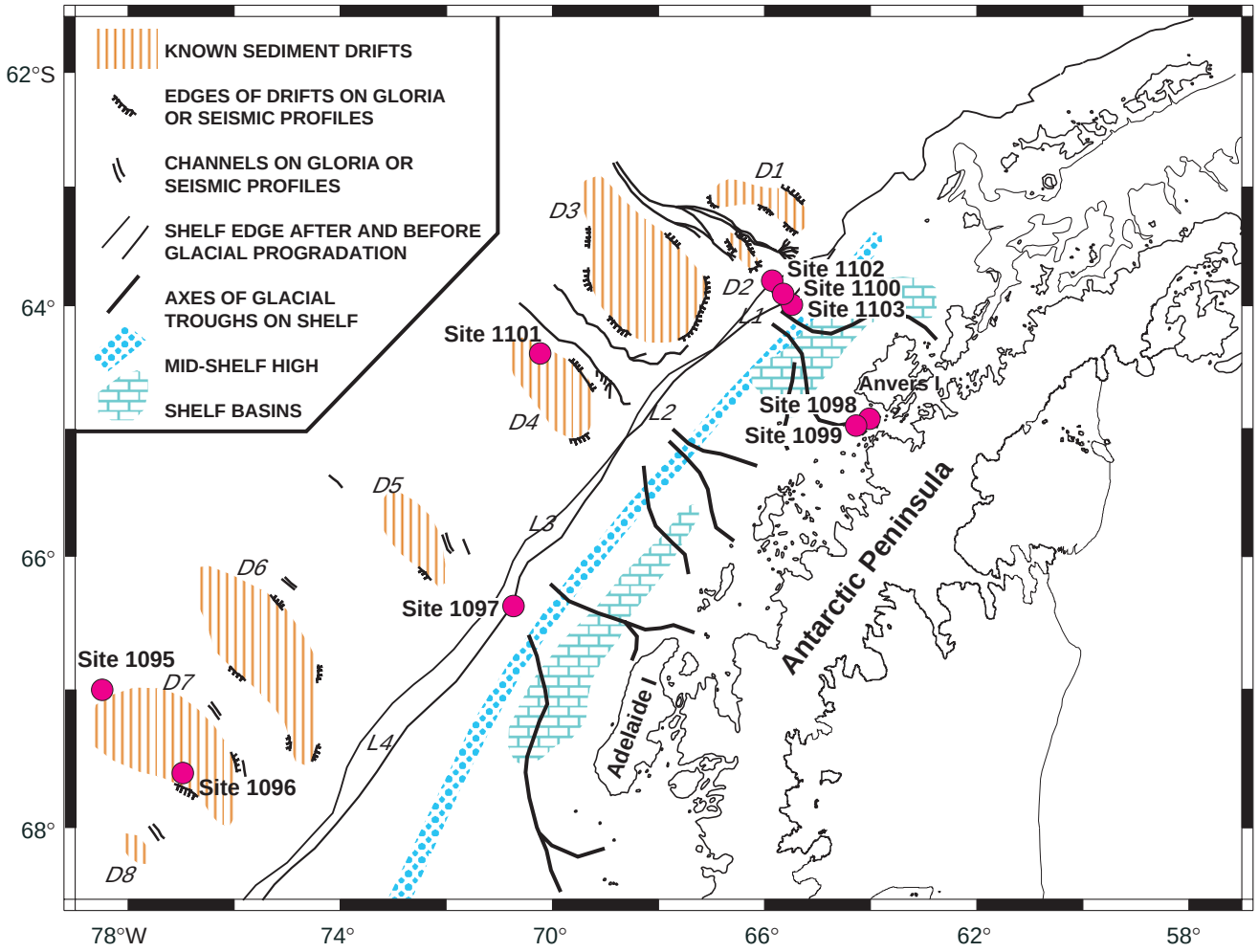

**Figure F4.** Graph and maps of ice-sheet size and location at mean sea-level temperatures 5, 9, 10, 15, 19, and 20 Kelvin (K) above present. The maps indicate where margin sedimentation might be sensitive to particular stages of ice-sheet growth. Antarctic Peninsula glaciation appears to have developed during the last 5–9 K of cooling (from Huybrechts, 1993).

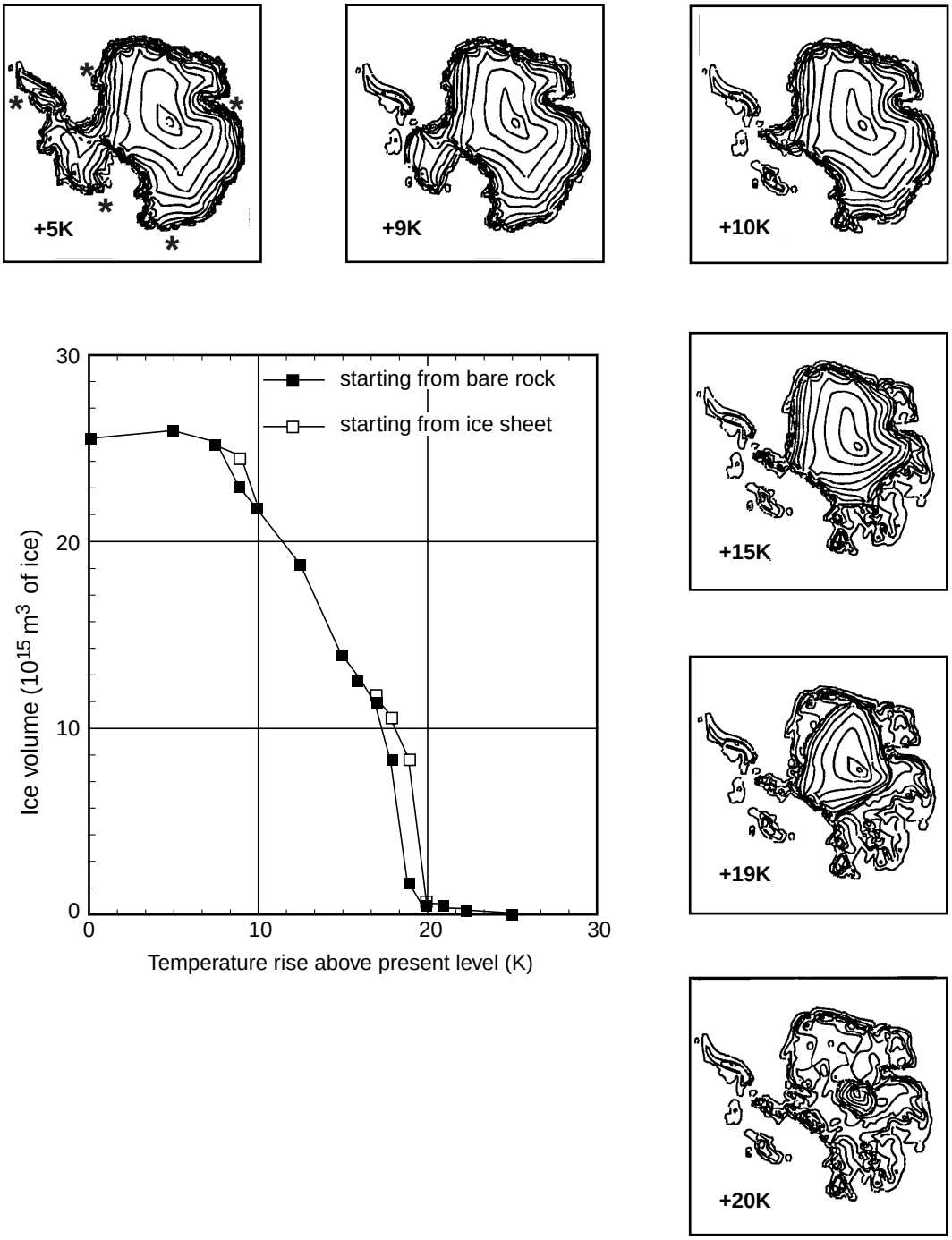

**Figure F5.** Sequence model of deposition on shelf and slope through a glacial cycle (adapted from Larter and Barker, 1989, 1991b). Unsorted till is deposited on the slope (foresets) during glacial maxima and on the shelf (topsets) during retreat. Pelagic or hemipelagic sediment is deposited on the slope and rise during interglacials. With re-advance, some or all shelf topsets may be eroded.

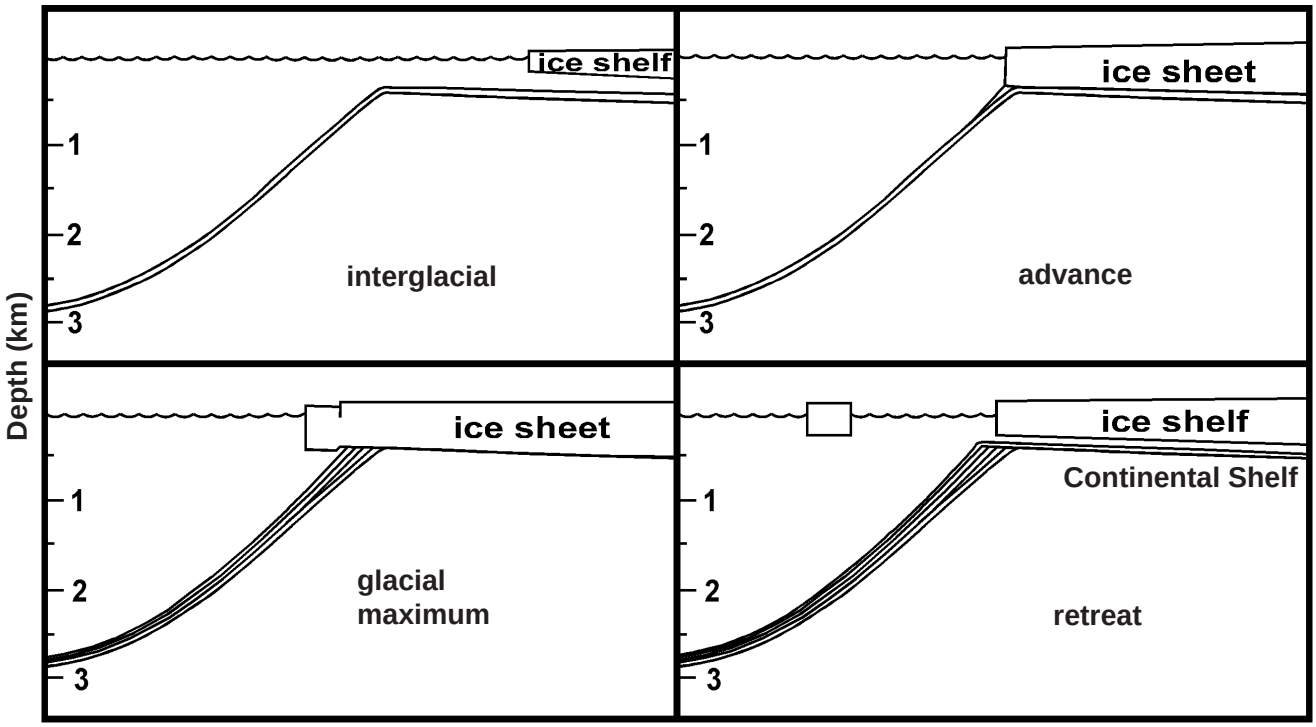

**Figure F6.** Schematic drawing of the processes active during glacial half-cycles, leading to the development of hemipelagic sediment drifts on the continental rise (adapted from Rebesco et al., 1997). The unstable component of unsorted upper-slope deposits forms first debris flows, then turbidity currents. The fine fraction is suspended and entrained in ambient bottom currents to be deposited downcurrent. Drifts are built above the level of the turbidity current channels because (in the case of the Antarctic Peninsula margin and perhaps elsewhere) subsequent turbidity currents erode the deposited sediment everywhere *except* upon the drifts and maintain the steeper drift slopes at the limit of stability.

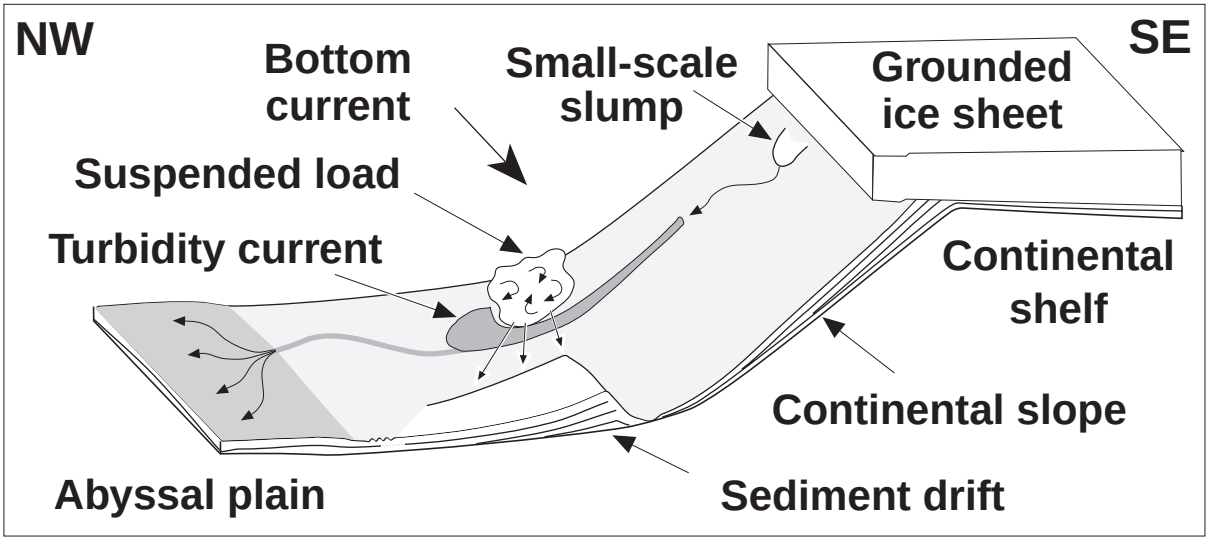

**Figure F7.** Part of MCS reflection profile I95-137 across Site 1095. S.P. = shotpoint.

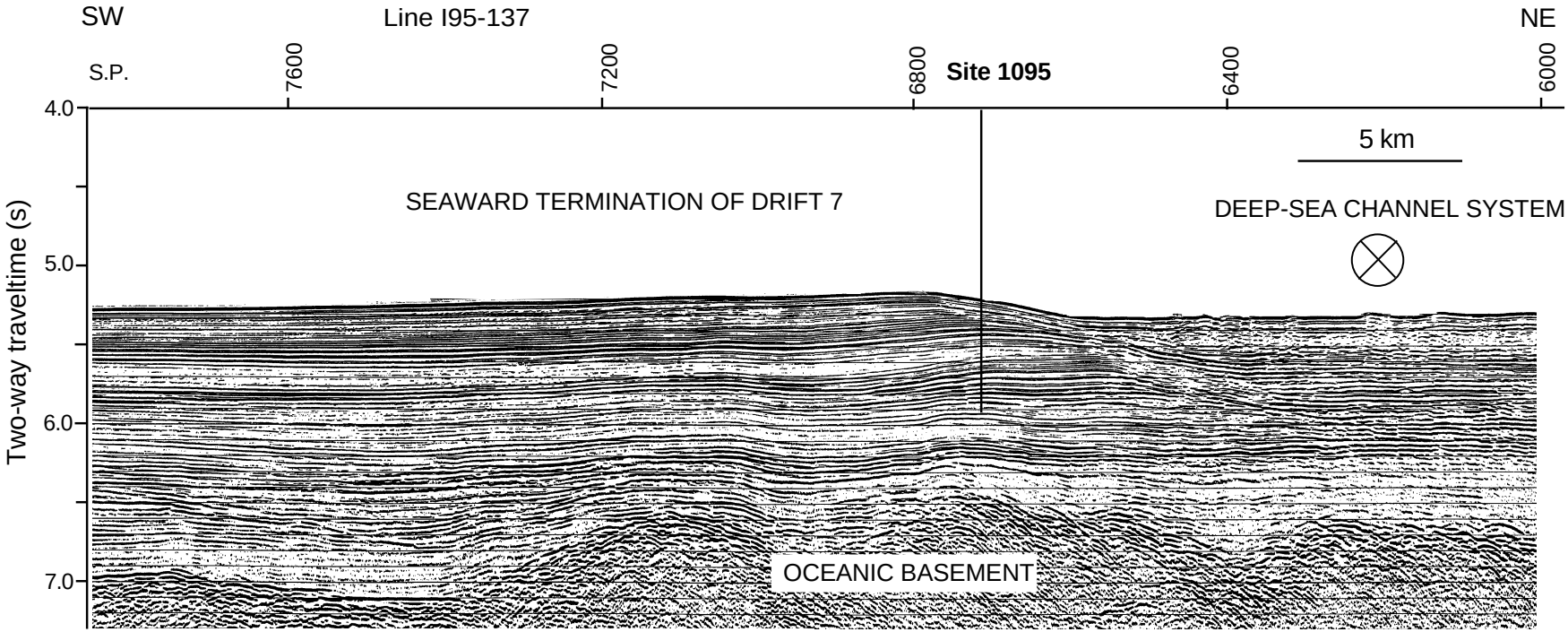

**Figure F8.** Depth-age profile determined from geomagnetic reversals and diatom and radiolarian datums at Site 1095. Paleomagnetic data were drawn from analysis of split-core (X's) and GHMT logging data (diamonds). Separate curves for split-core (thin line) and GHMT magnetic data (heavy broken line) are interpolations that pass through all data points within each data set and match the slopes at those points. Diatom and radiolarian datum intervals are marked with a circle (radiolarian) and with a dark bar (diatom). B = base first occurrence, T = top last occurrence, TC = top of common occurrence/last common occurrence. *P. sulcata* abundance is shown with gray shaded bars. The hole is barren of microfossils below ~520 mbsf. Mean sedimentation rates (underlined) determined for the three intervals show an uphole decrease.

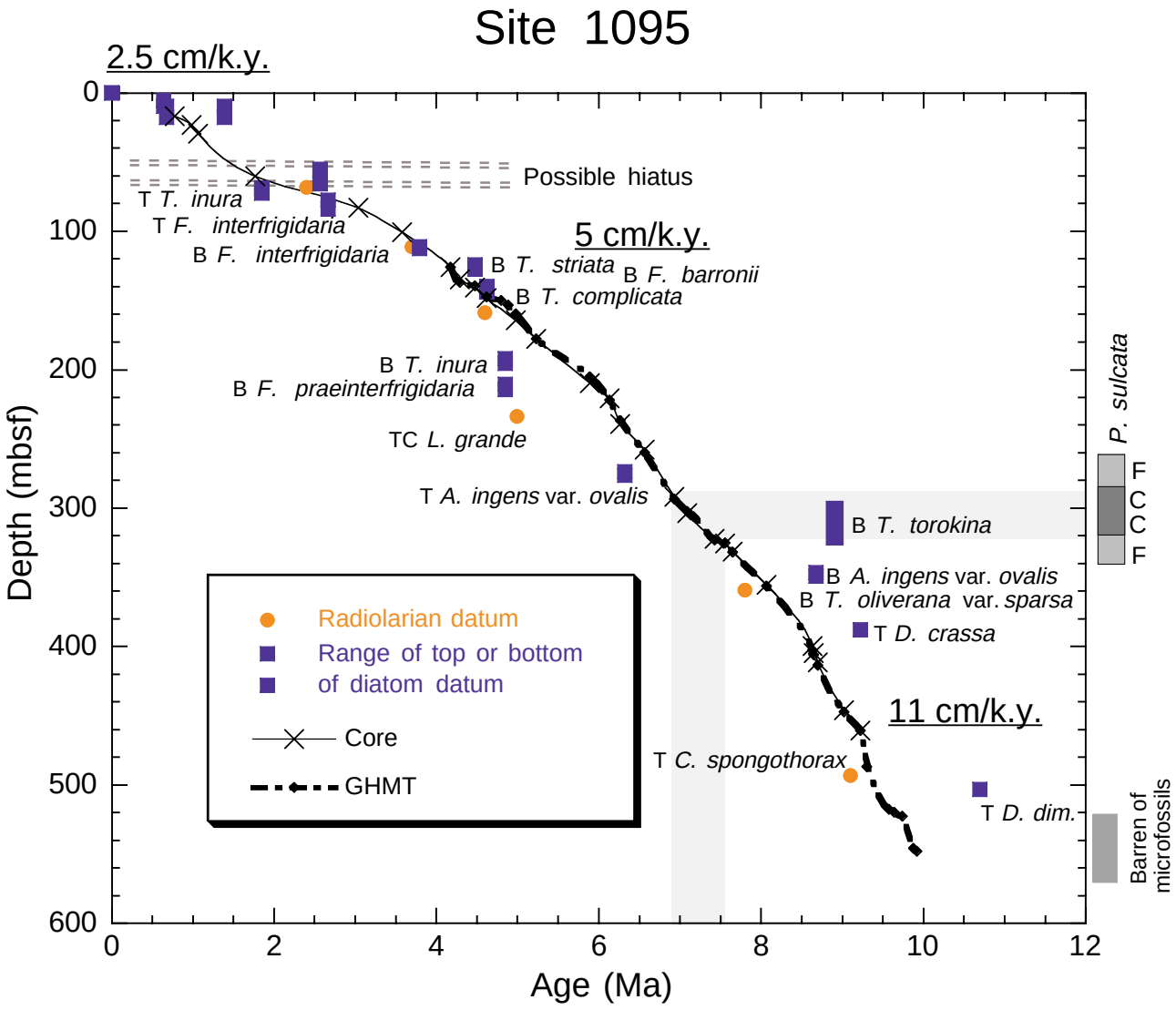

**Figure F9.** Summary of lithostratigraphic, magnetostratigraphic, and biostratigraphic findings in Leg 178 sediment drift sites. The record of magnetic susceptibility and natural gamma-ray attenuation is shown for comparison.

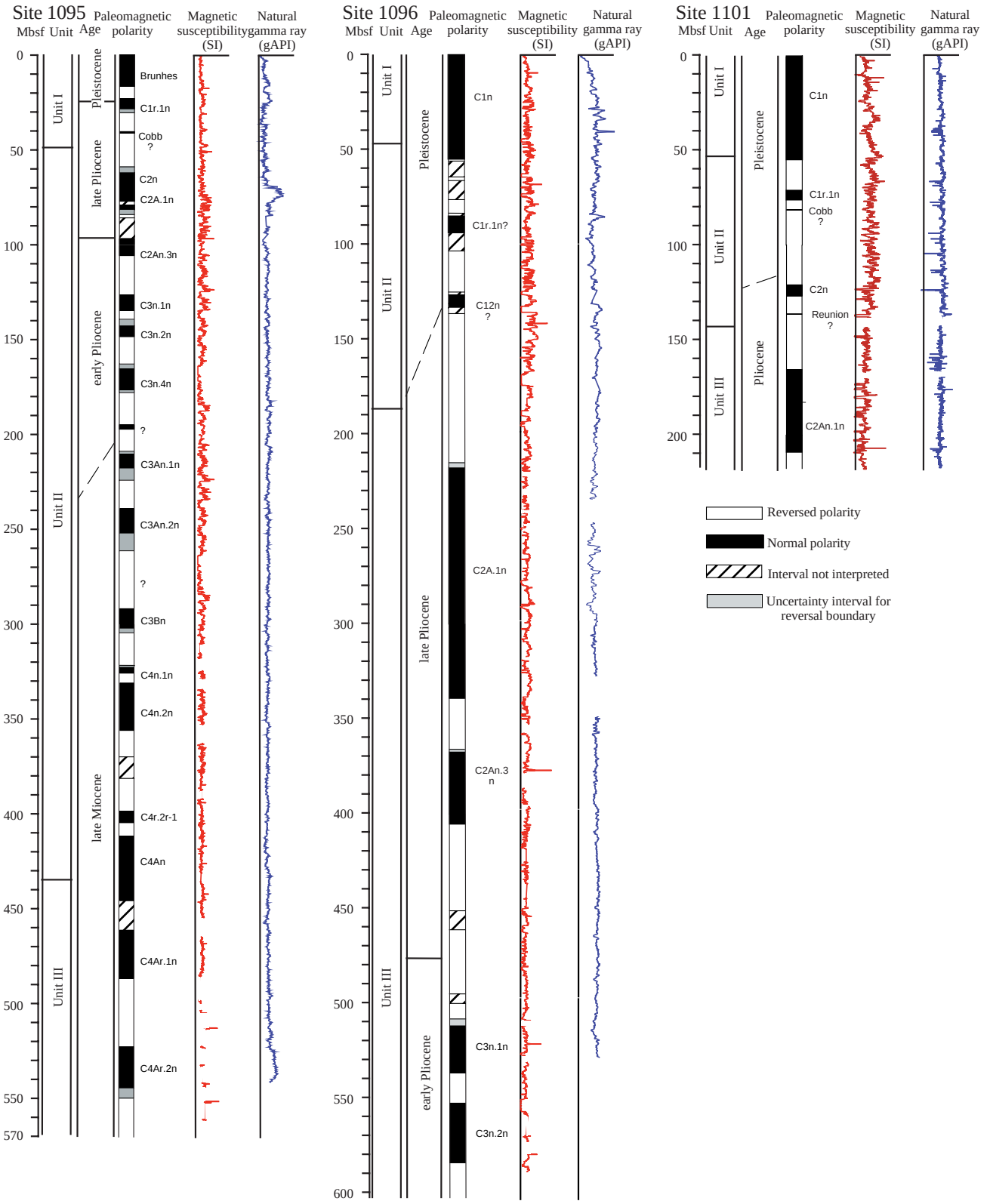

**Figure F10.** Part of MCS reflection profile I95-130A across Site 1096 (see location in Fig. F1, p. 38, in the "Site 1096" chapter). Note the BSR at ~700 ms two-way traveltime below the seafloor, interpreted as the opal-A to opal-CT transition. S.P. = shotpoint.

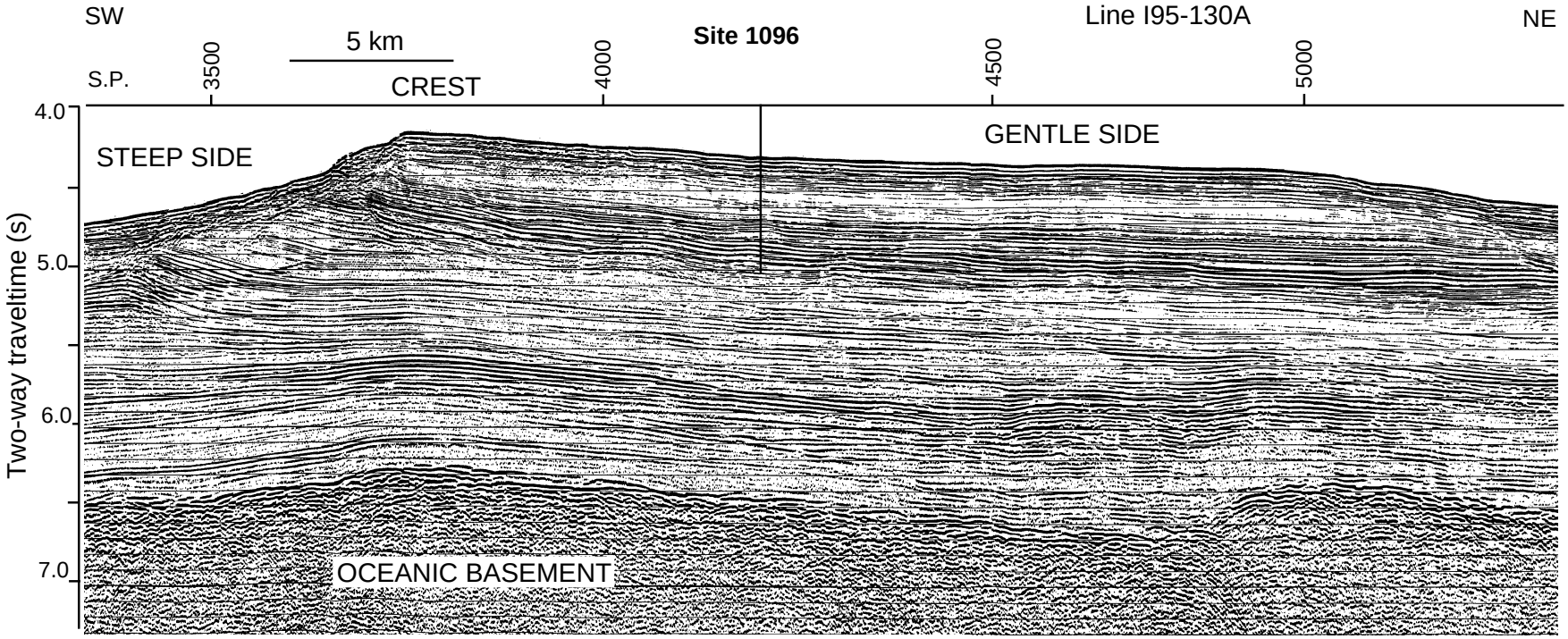

**Figure F11.** Depth-age relationship for Site 1096 based on geomagnetic reversals (X) and diatom (dark bars) and radiolarian (circles) datums. Paleomagnetic data were drawn from shipboard analysis of cores. Diatom and radiolarian datum intervals are marked with a circle (radiolarian) and with a dark bar (diatom). In labels indicating species identity, B = base/first occurrence and T = top/last occurrence. Sedimentation rates (underlined) for selected intervals are adjacent to the corresponding curve. Vertical solid arrows indicate dominant age-diagnostic fossil type (biosiliceous vs. calcareous) for respective intervals of this site. The dashed vertical line below B *Fragilariopsis interfrigidaria* datum interval indicates range of published depths for this datum.

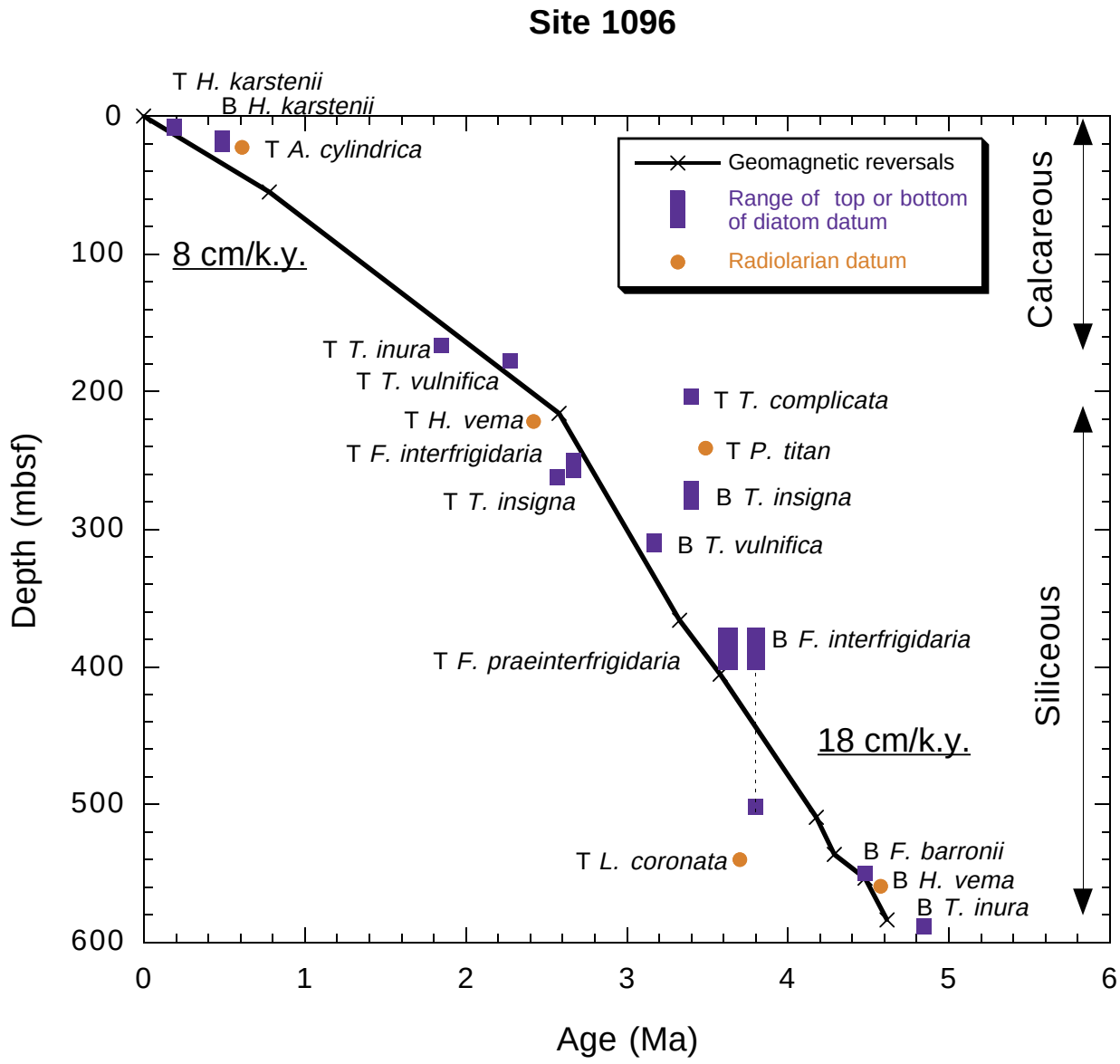

**Figure F12. A.** Part of MCS reflection profile IT92-114 across Site 1101 (see location in Fig. **F1B,** p. 26, in the "Site 1101" chapter). **B.** Seismic stratigraphic record at location of proposed site APRIS-05A (proximal site on Drift 4). **C.** Seismic stratigraphic record at location of proposed site APRIS-06A (distal site on Drift 4). Units M1–M4 are from Rebesco et al. (1997). S.P. = shotpoint.

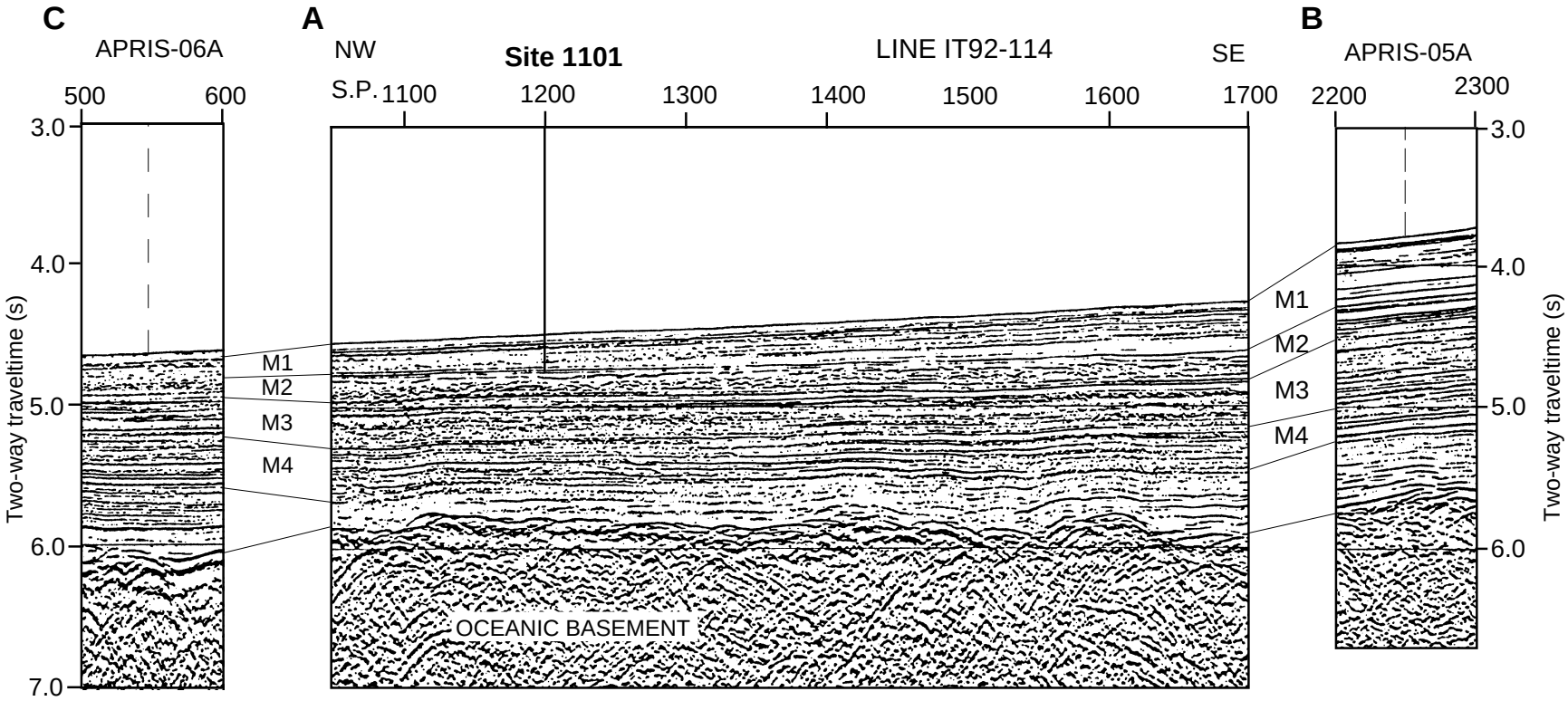

**Figure F13.** Depth-age profile determined from geomagnetic reversals and diatom and calcareous nannofossil datums at Site 1101. The curve fit to the paleomagnetic data is an interpolation that passes through all data points within the data set and matches the slope at those points. Diatom and calcareous nannofossil datum intervals are marked with a dark bar (diatom) and a light bar (calcareous nannofossil). B = base first occurrence, T = top last occurrence.

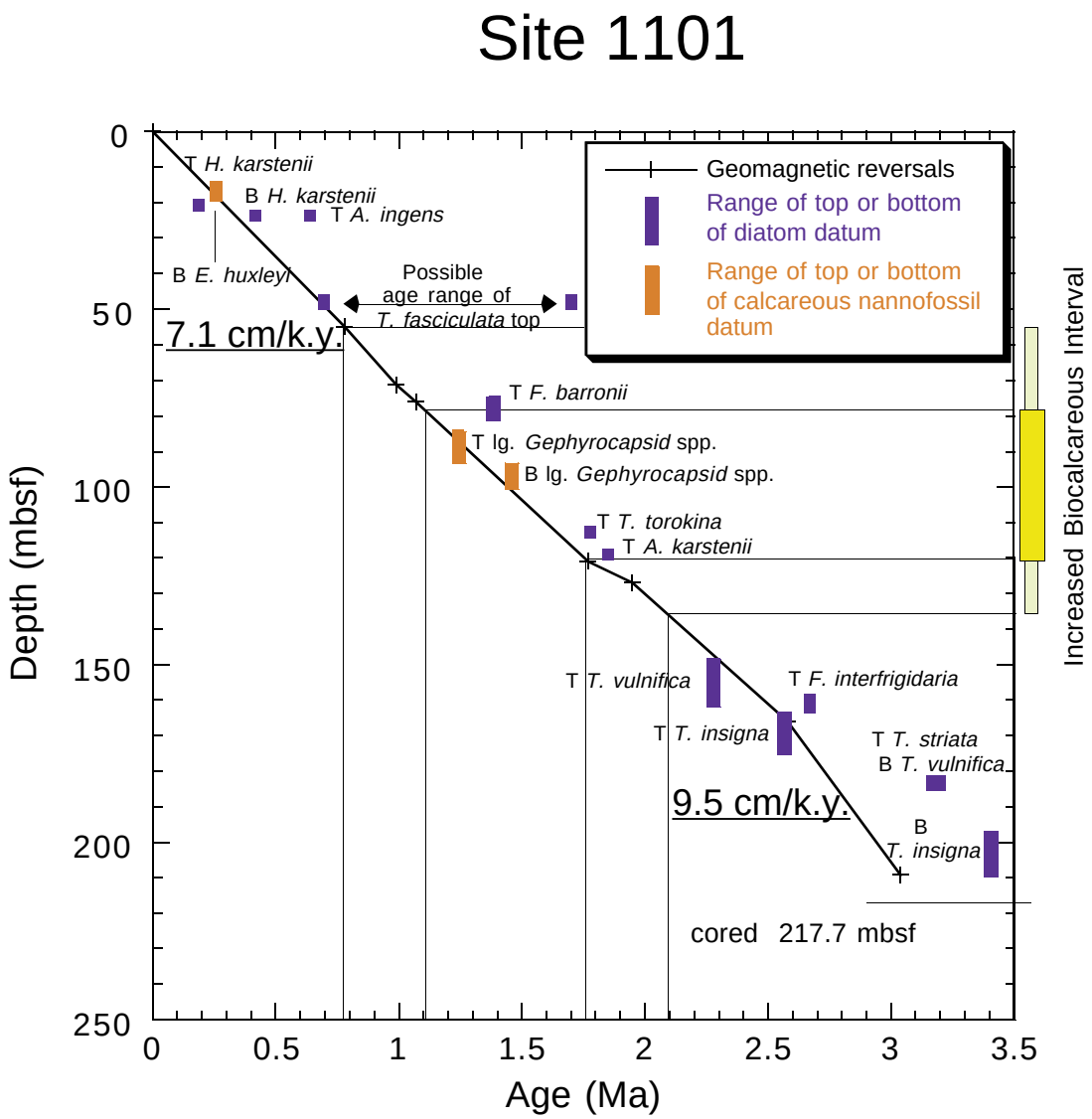

**Figure F14.** Summary of biostratigraphic findings and correlation in Leg 178 continental rise sites.

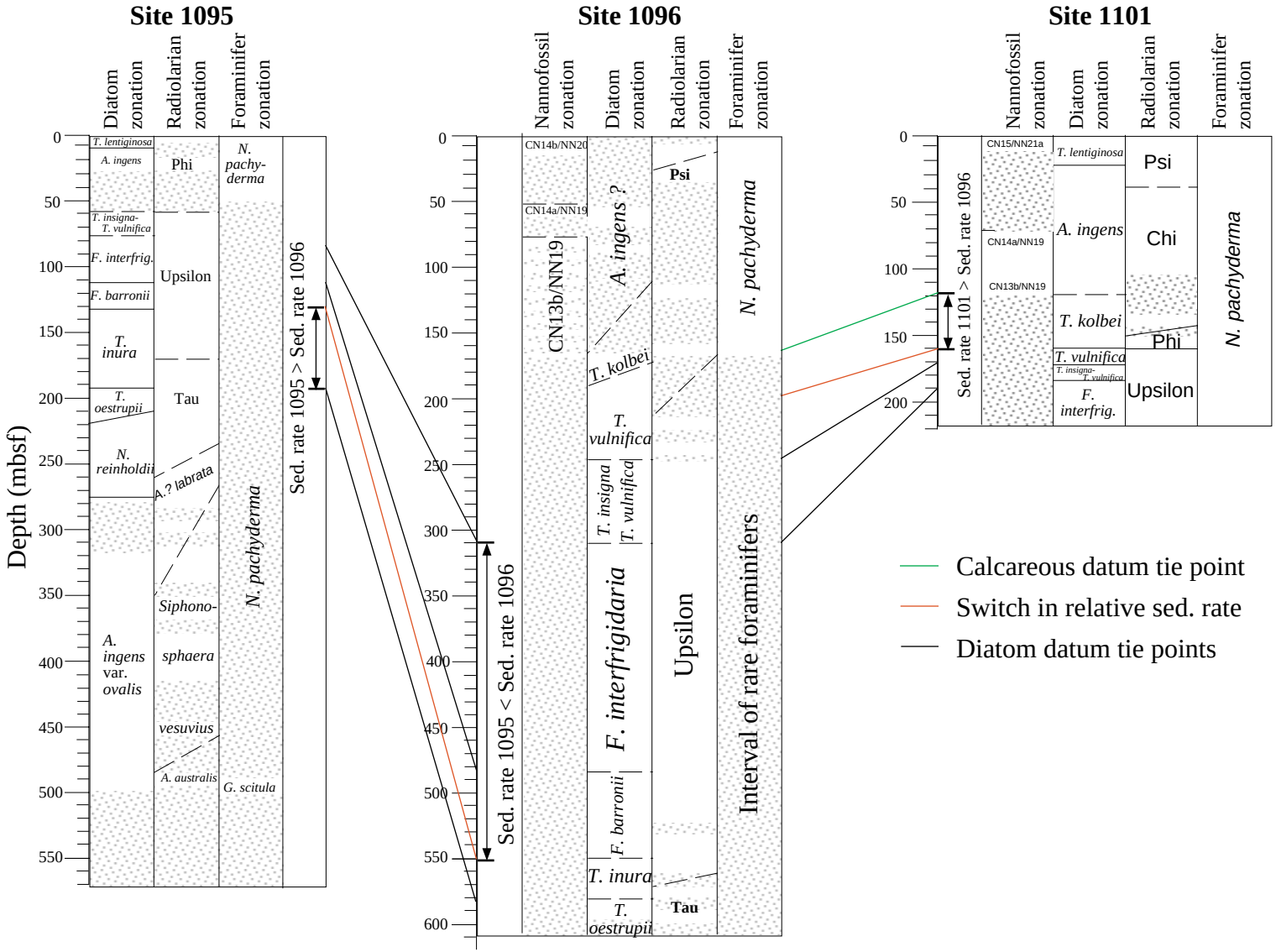

**Figure F15.** Location of Site 1097 on single-channel seismic reflection profile PD88-04 (Bart and Anderson, 1995) across the continental shelf seaward of Adelaide Island, Antarctic Peninsula.

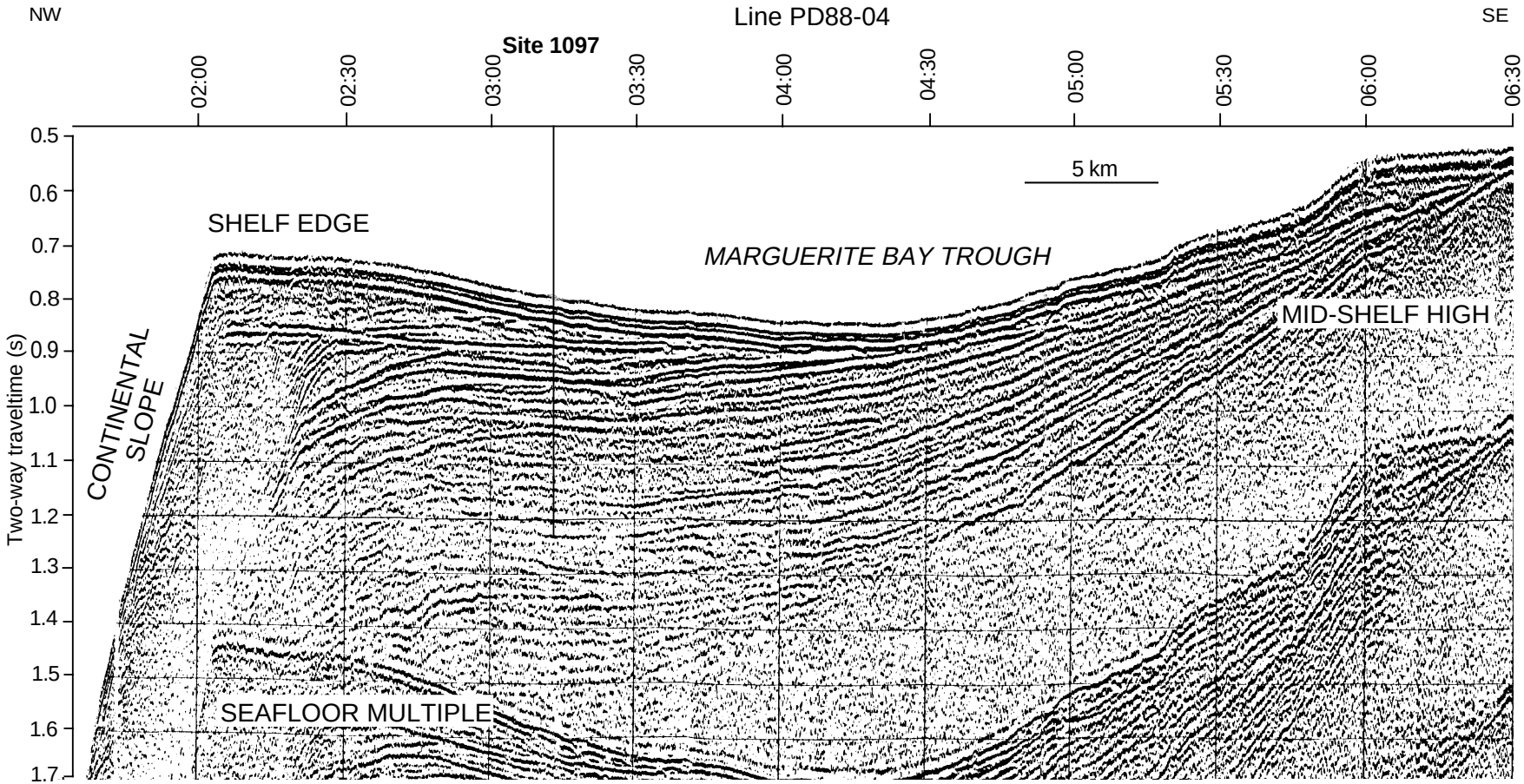

**Figure F16.** Summary of facies recovered at Site 1097, associated biofacies, and environmental interpretation. Representative cores are identified at top.

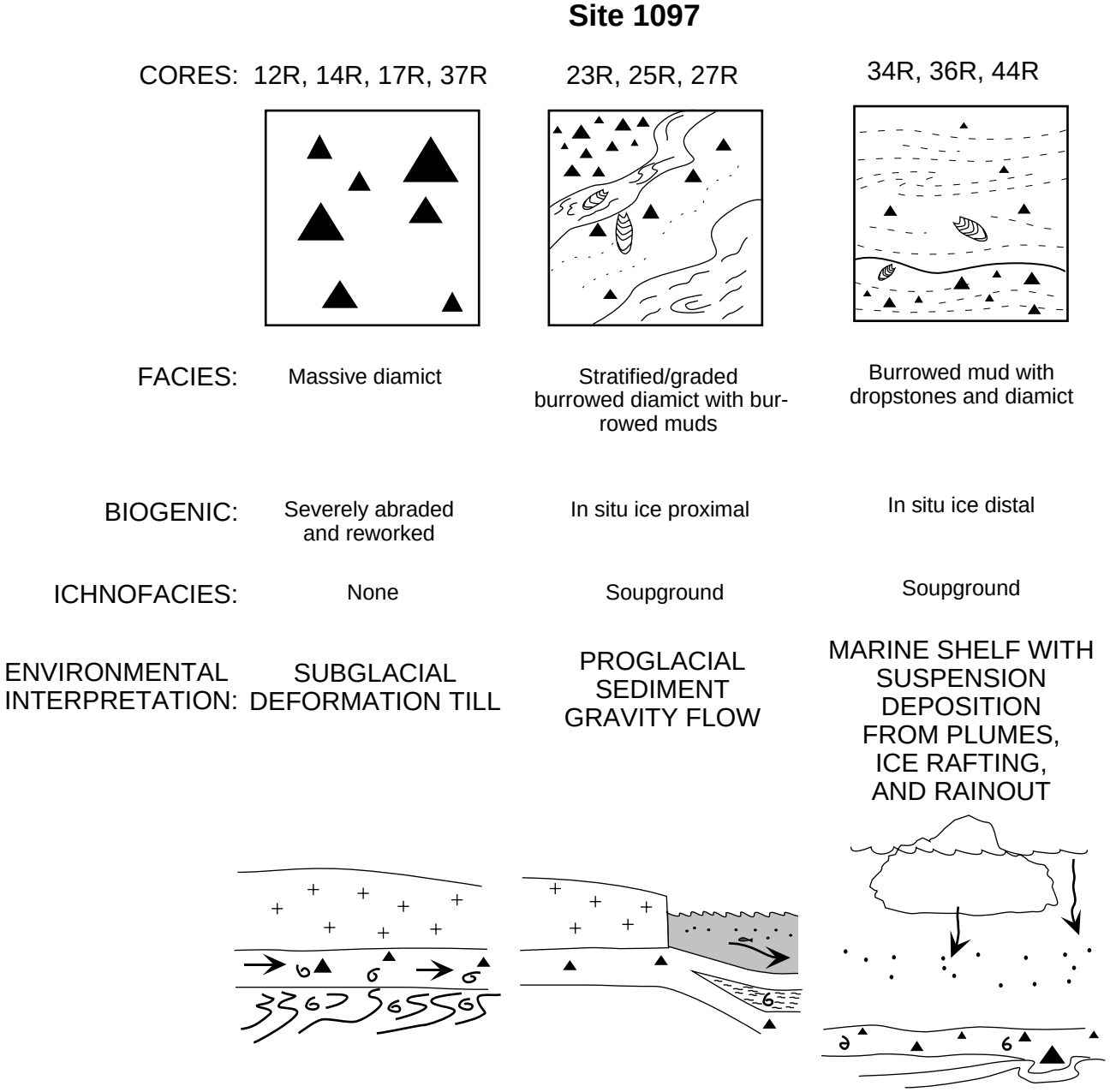

**Figure F17.** Continental shelf transect. Location of Sites 1100, 1102, and 1103 on MCS reflection profile I95-152 across the continental shelf seaward of Adelaide Island, Antarctic Peninsula. S.P. = shotpoint.

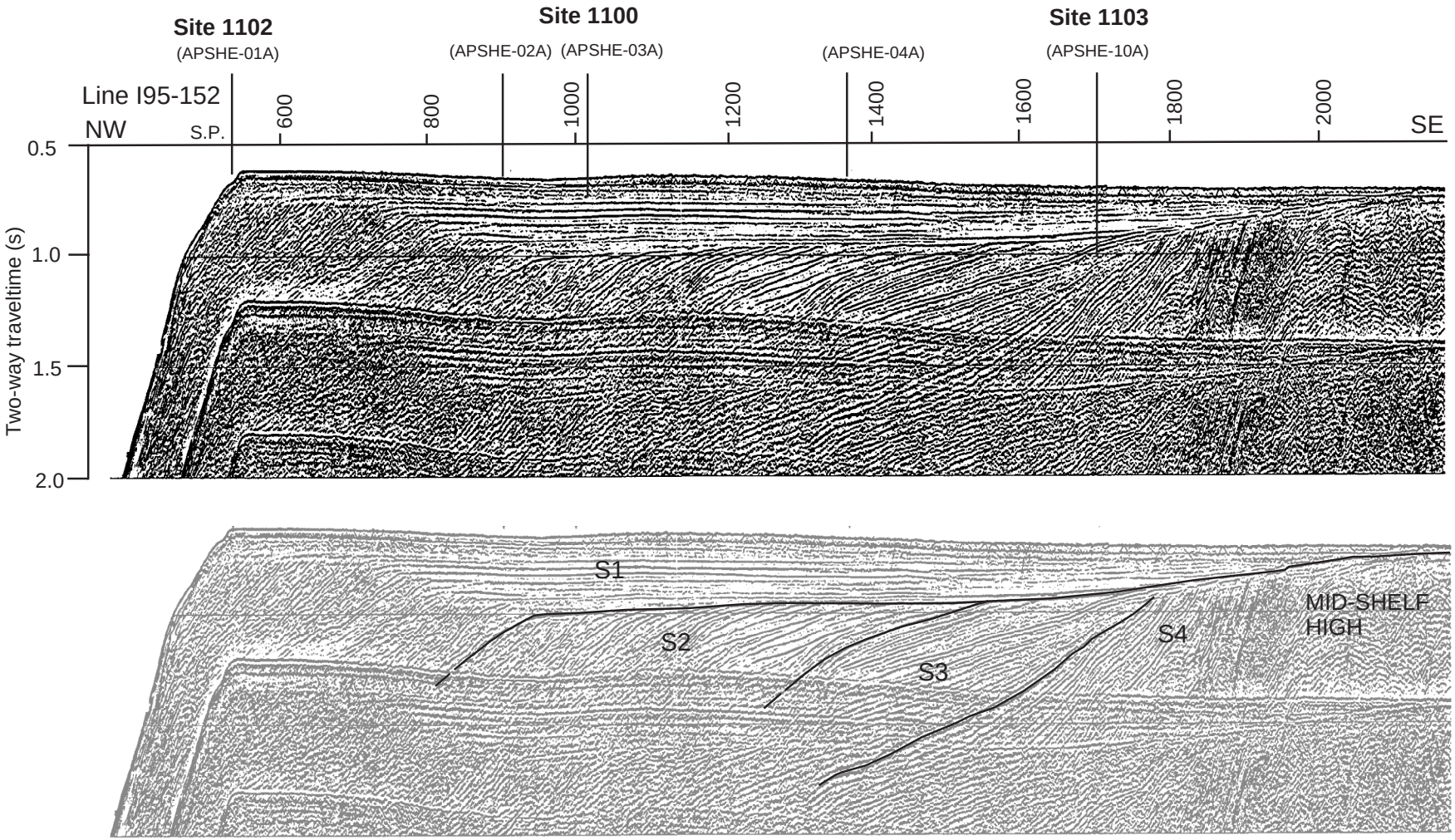

**Figure F18.** Simplified lithostratigraphy at Site 1103 showing lithofacies.

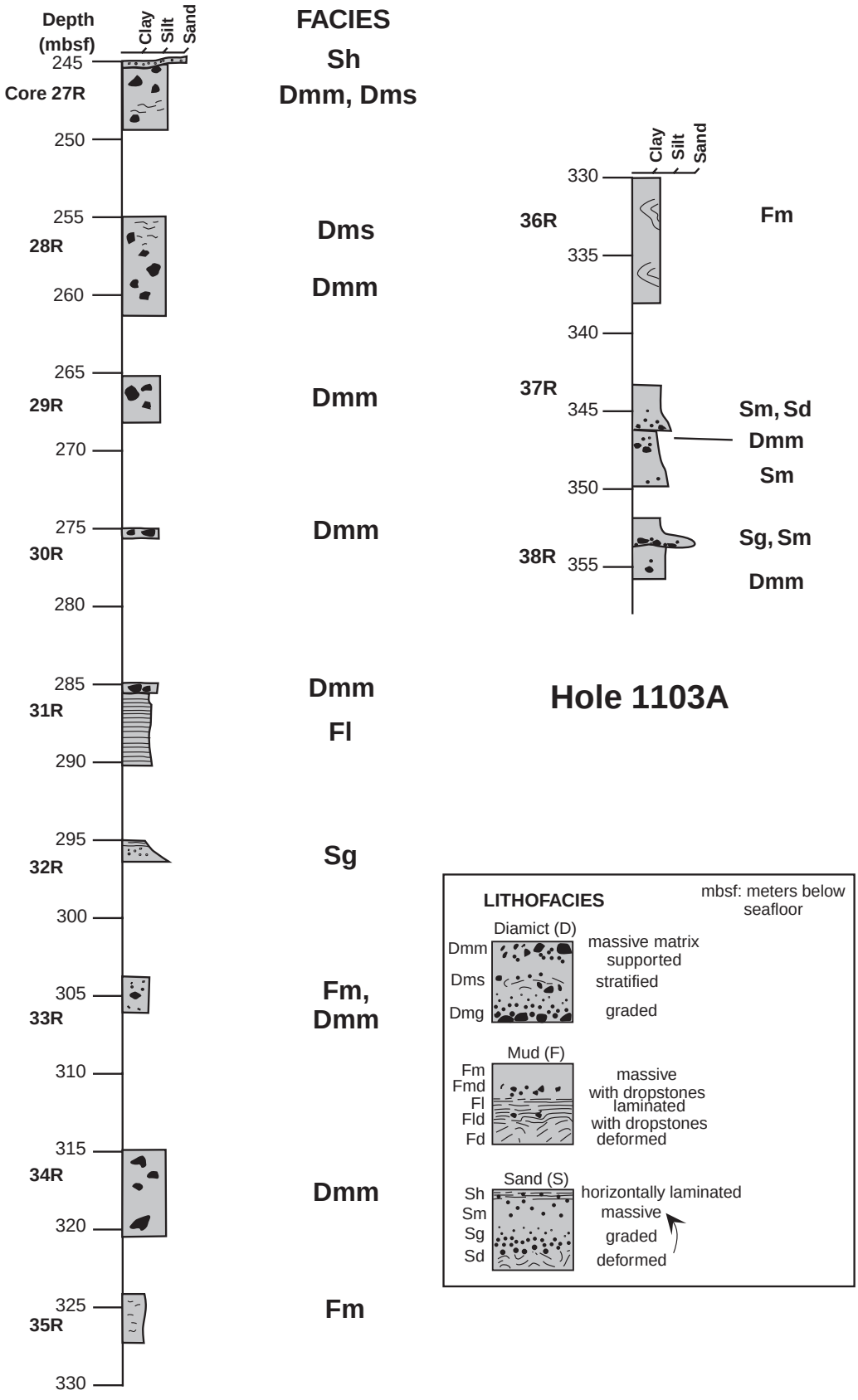

**Figure F19.** Bathymetry and location of site-survey seismic reflection profiles on Palmer Deep. Tracks of the 3.5-kHz sub-bottom profiles obtained by the *JOIDES Resolution* (*JR*) are indicated by the thickest bold line. Floor of basins is shaded.

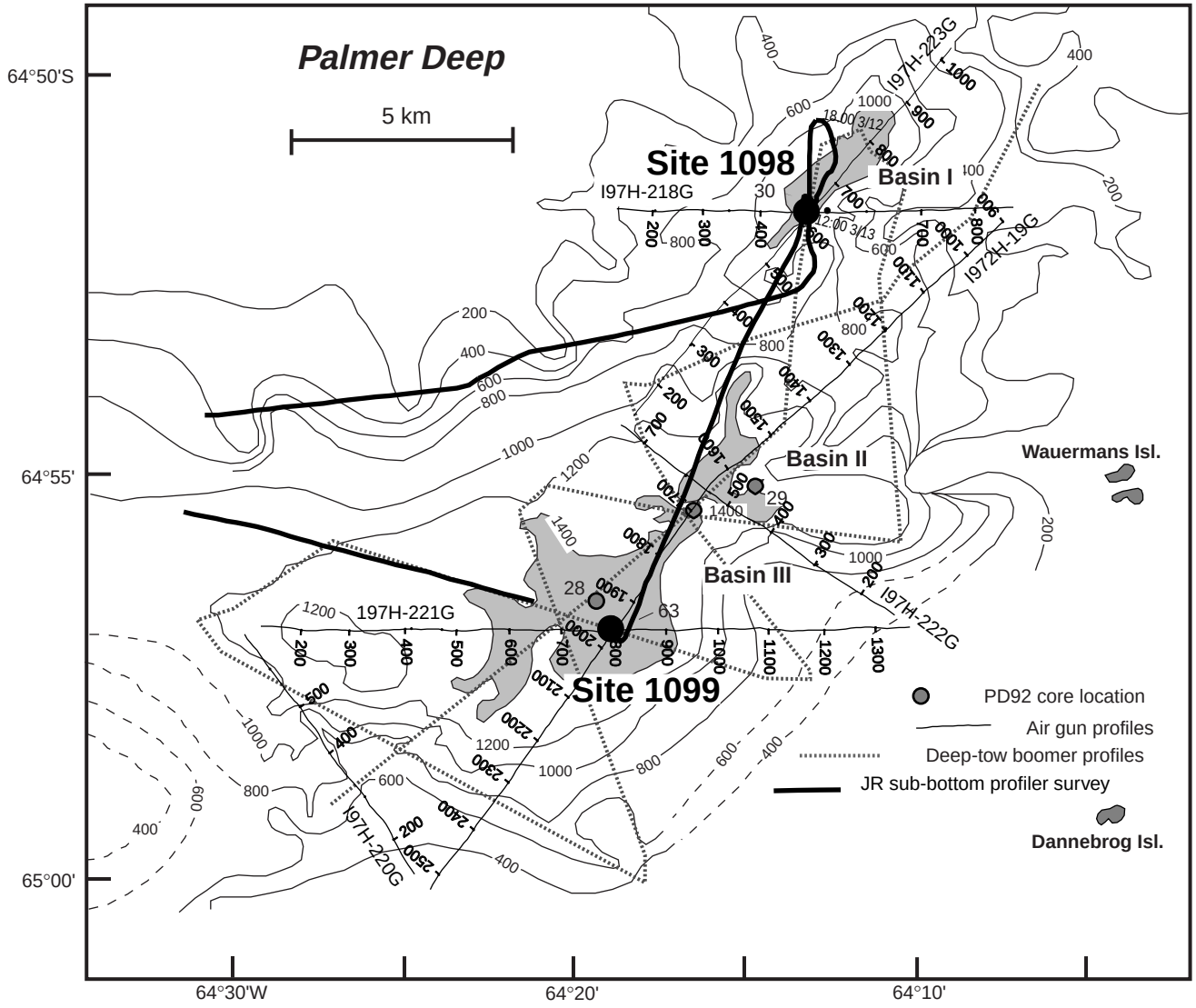

**Figure F20.** Generator Injector (GI) air gun seismic profile I97H-228G **(A)** across Palmer Deep Site 1098, Basin I, and **(B)** across Palmer Deep Site 1099, Basin III (modified from Rebesco et al., 1998).

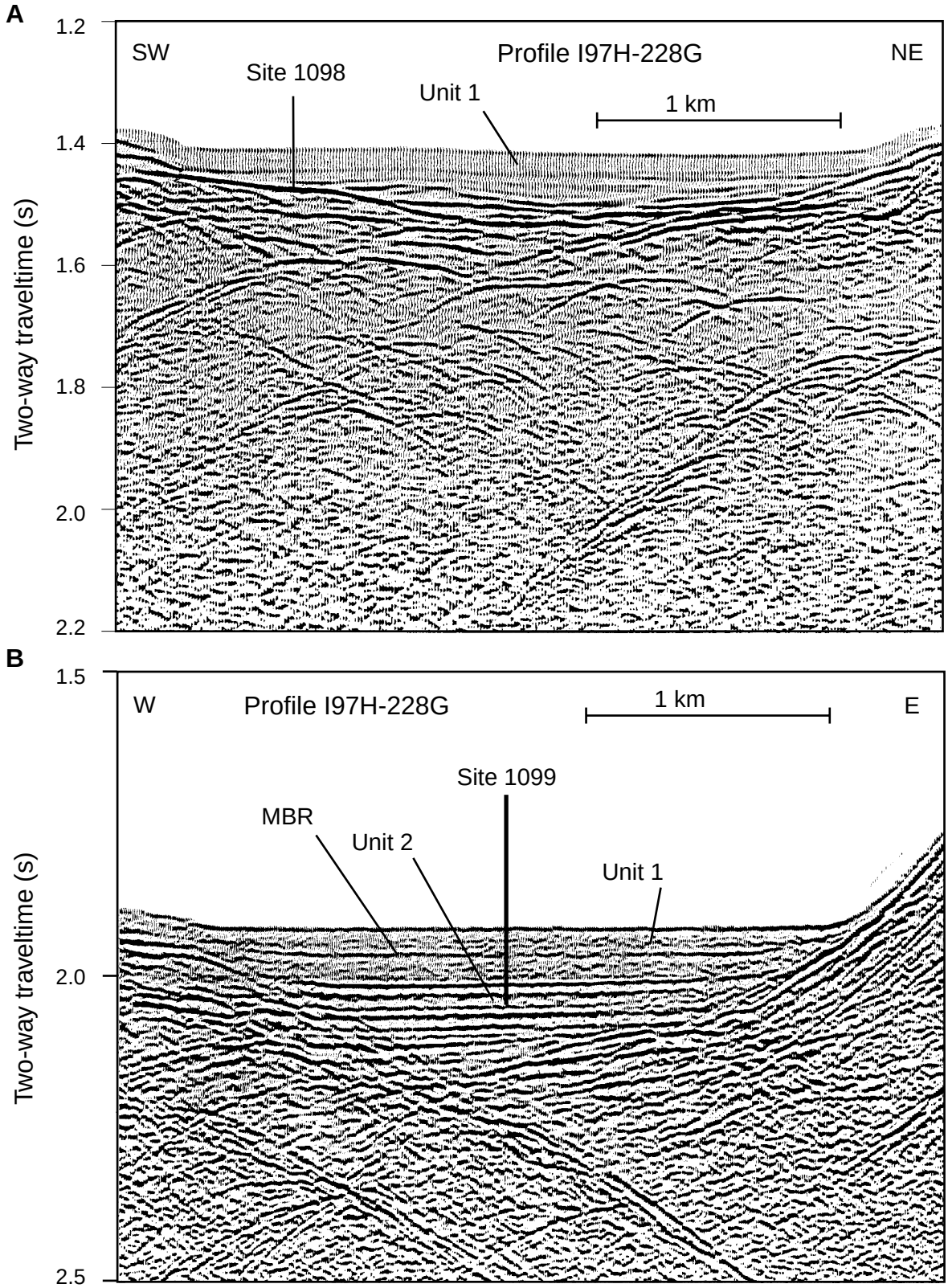

**Figure F21.** Lithostratigraphic columns for Site 1098. T.D. = total depth.

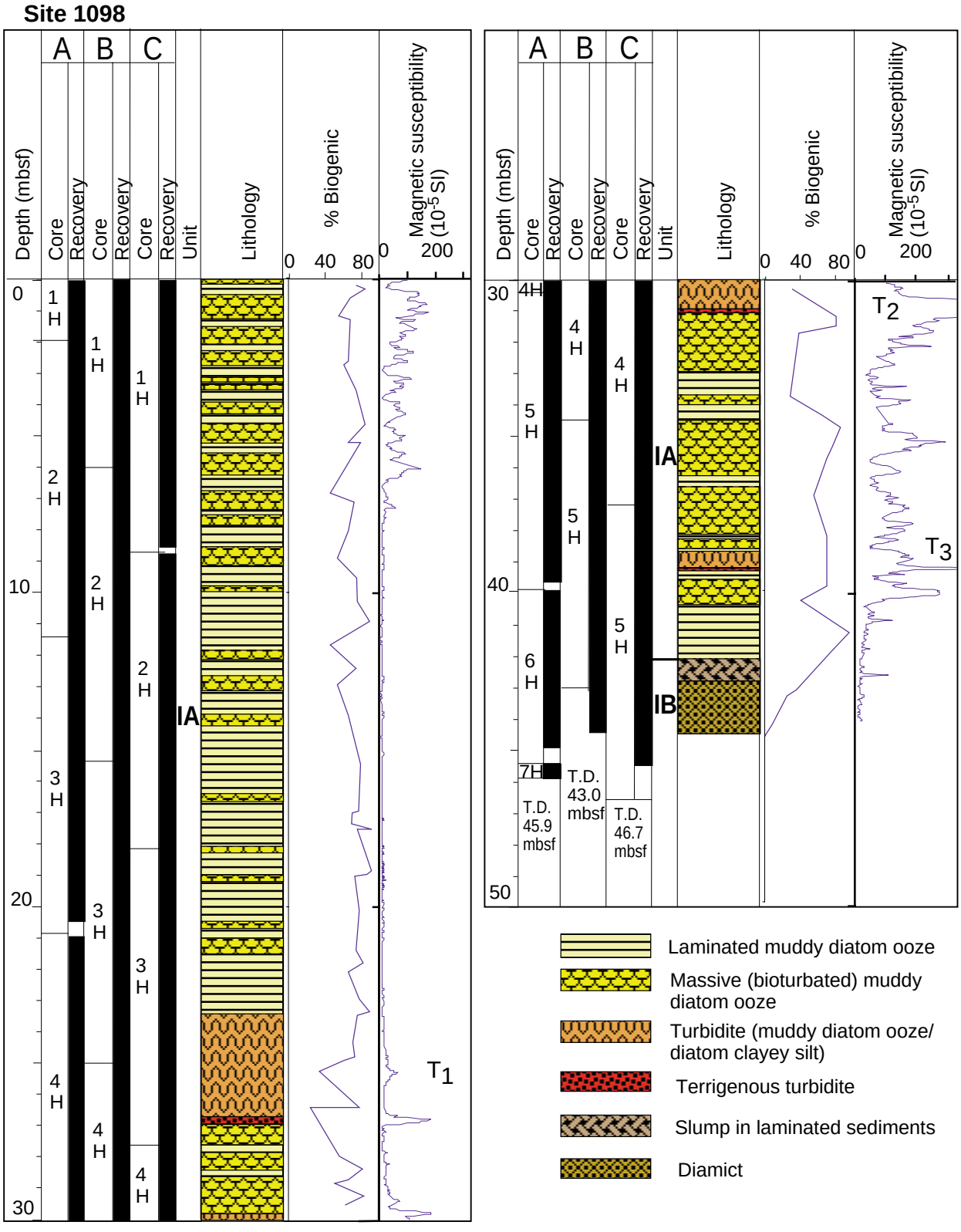

**Figure F22.** Lithostratigraphic columns for Site 1099. T.D. = total depth.

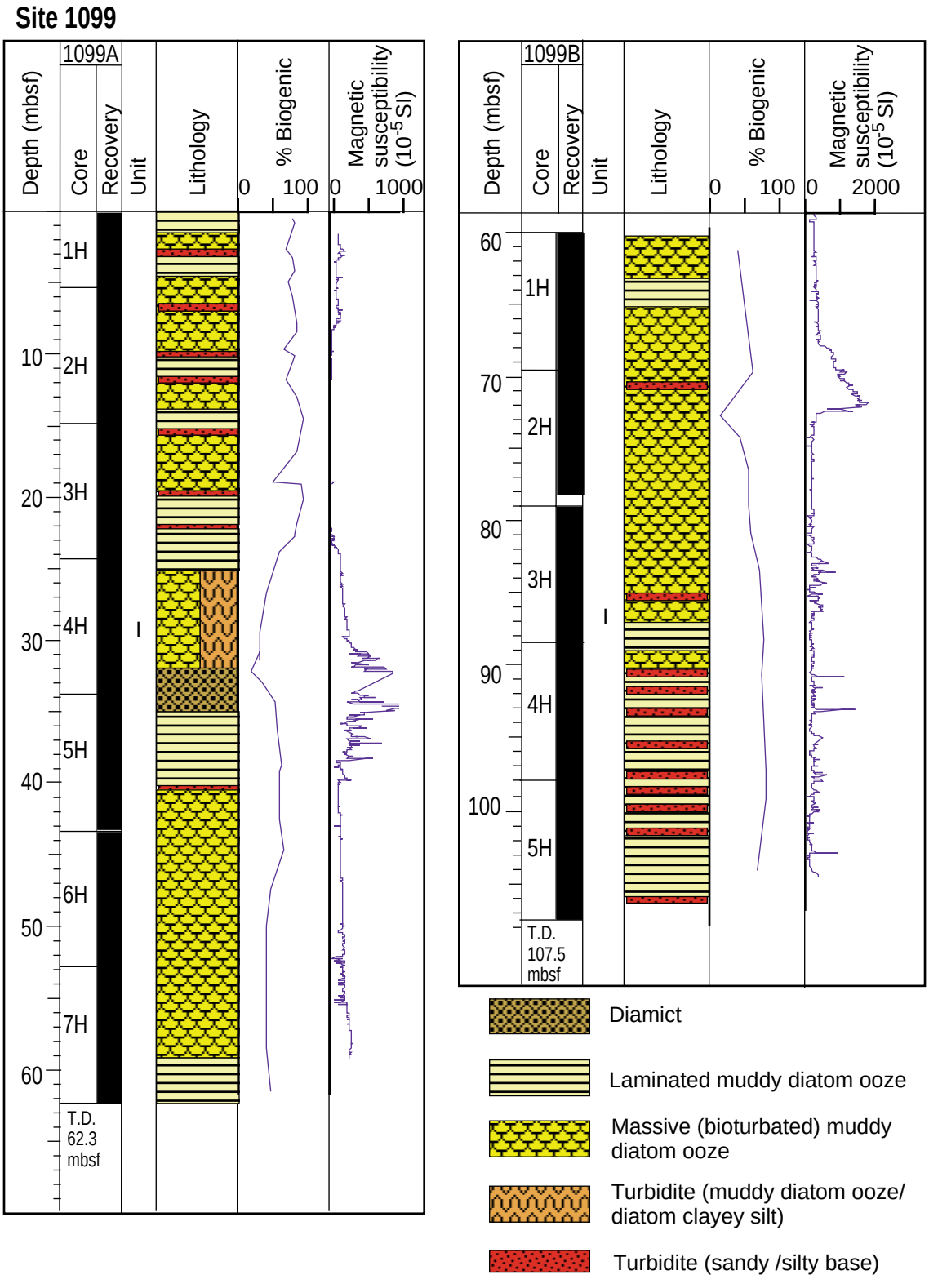

**Figure F23.** Relative abundances of chlorite, illite, and mixed-layer clays in sediments from the continental shelf (Site 1097) and rise (Sites 1095, 1096, and 1101) analyzed during Leg 178.

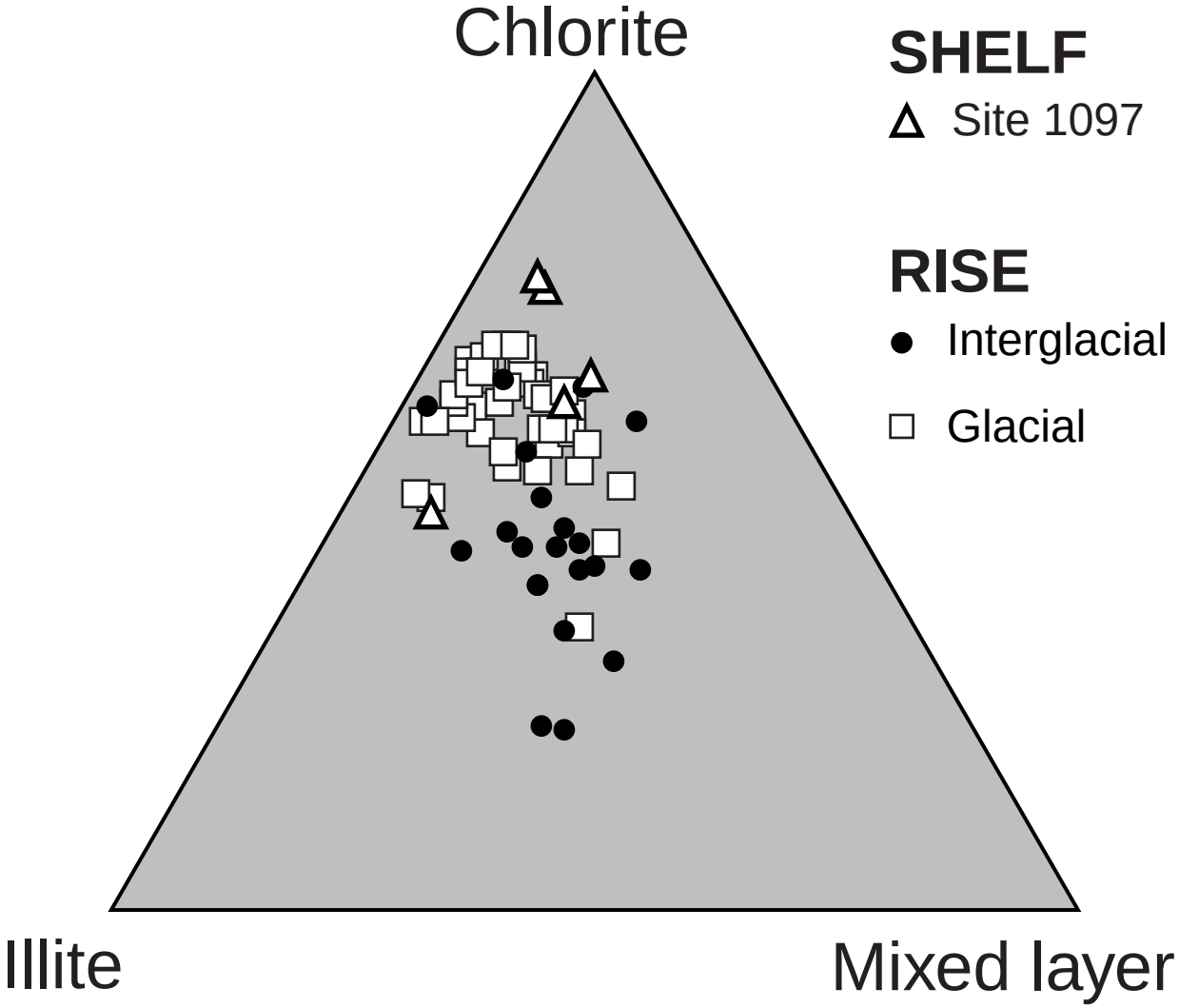

**Figure F24.** Downhole logs of hole diameter, total natural gamma, bulk density, porosity, resistivity, sonic velocity, and magnetic susceptibility from Hole 1103A, with core measurements of natural gamma, bulk density, porosity, sonic velocity, and magnetic susceptibility.

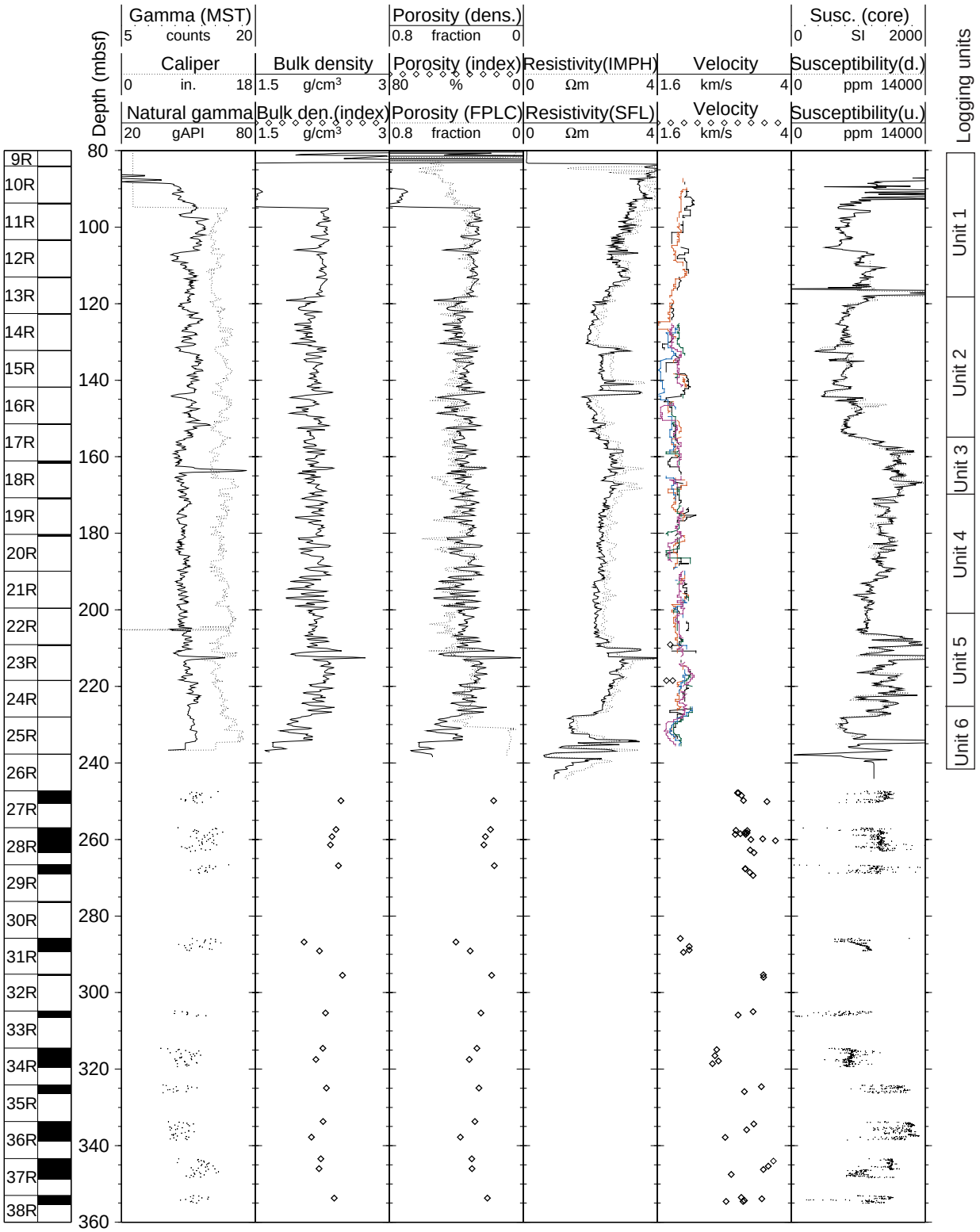

**Figure F25.** Biostratigraphic summary of shelf sites (Holes 1097A, 1100D, and 1103A), based on shipboard observation, with seismic correlation. Light gray horizons show materials of very rare diatom occurrence. Dark gray horizons show intervals barren of microfossils. Age assignment of S3 at Hole 1097A is based on benthic foraminifers, diatoms, and radiolarian biostratigraphy. The depths of seismic reflectors at Hole 1103A are refined with logging information.

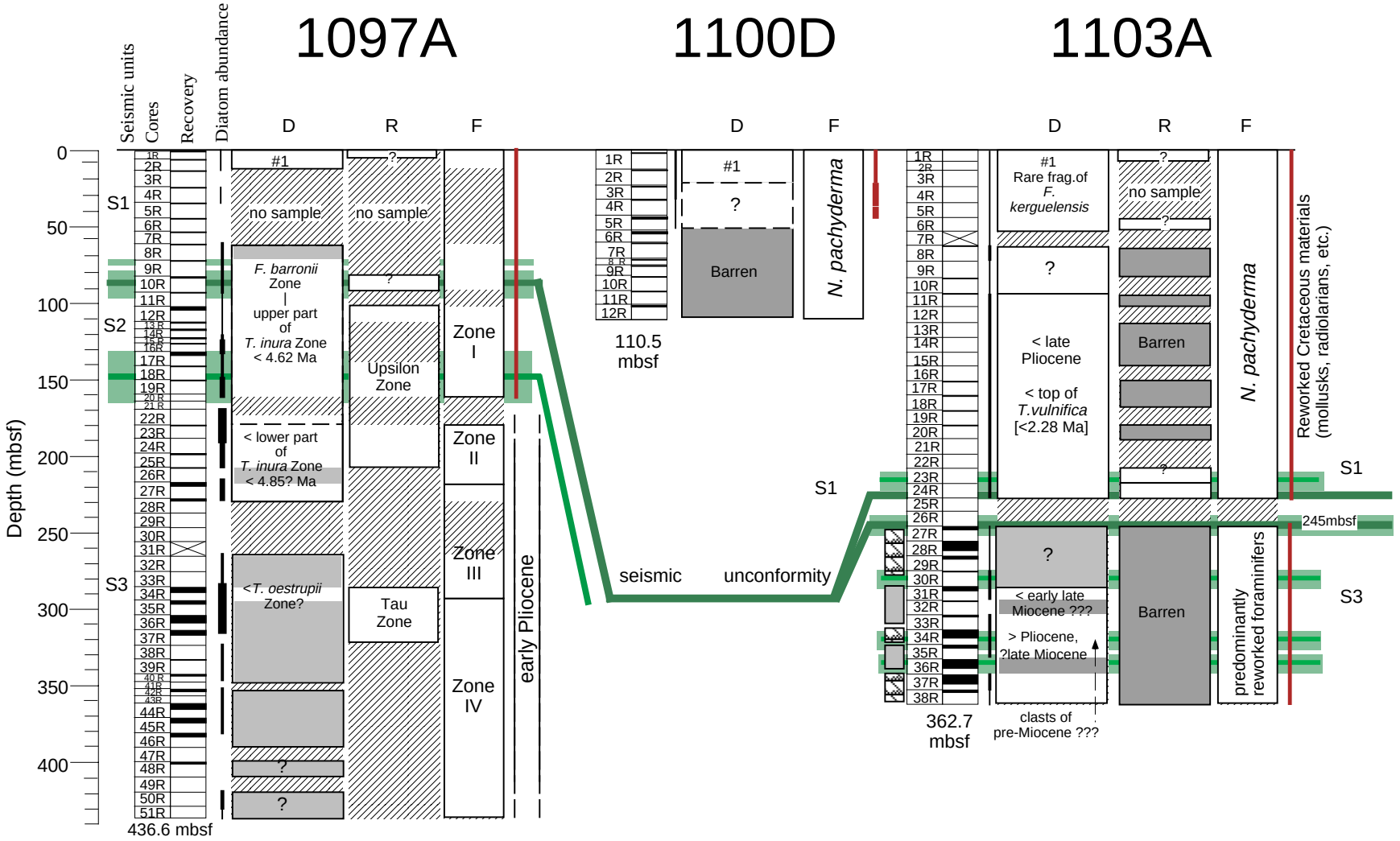

**Figure F26.** Magnetostratigraphic summary for Leg 178 continental rise sites.

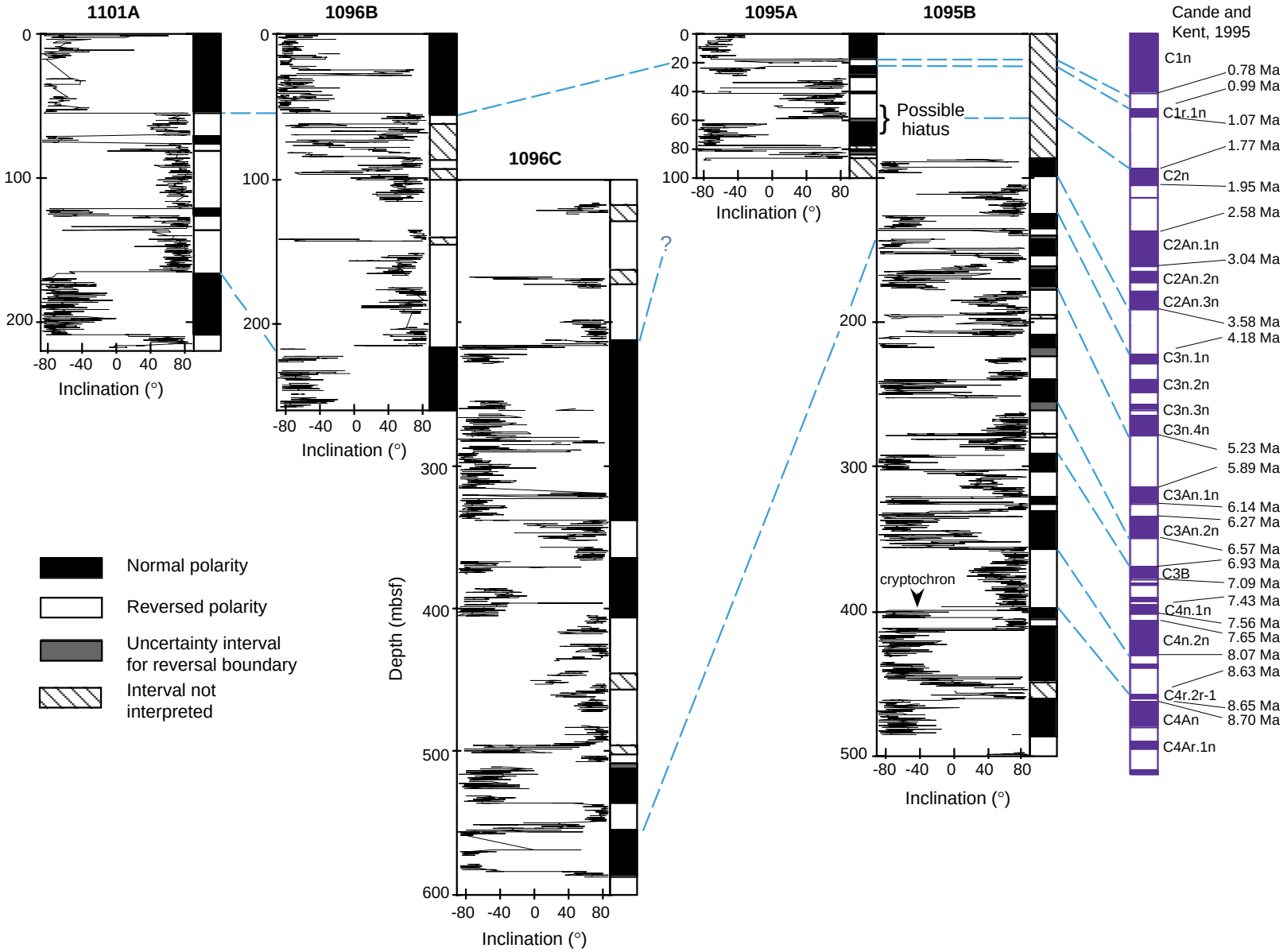

**Table T1.** Leg 178 coring summary. (Continued on next four pages.)

| | Hole | Statistics |
|---|---|---|
| Continental Rise Drift Sites | 1095A | **Position:** 66°59.1266′S, 78°29.2387′W<br>**Start hole:** 1615 hr, 17 February 1998<br>**End hole:** 1930 hr, 18 February 1998<br>**Seafloor (drill-pipe measurement from rig floor, mbrf):** 3852.6<br>**Distance between rig floor and sea level (m):** 11.0<br>**Water depth (drill-pipe measurement from sea level, m):** 3841.6<br>**Total depth (from rig floor, mbrf):** 3939.90<br>**Total penetration (mbsf):** 87.30<br>**Total number of cores:** 10<br>**Total length of cored section (m):** 87.30<br>**Total core recovered (m):** 86.48<br>**Core recovery (%):** 99.06<br>**Oldest formation cored:** upper Pliocene silty clay |
| | 1095B | **Position:** 66°59.1266′S, 78°29.2699′W<br>**Start hole:** 1930 hr, 18 February 1998<br>**End hole:** 0045 hr, 24 February 1998<br>**Seafloor (drill-pipe measurement from rig floor, mbrf):** 3852.6<br>**Distance between rig floor and sea level (m):** 11.0<br>**Water depth (drill-pipe measurement from sea level, m):** 3841.6<br>**Total depth (drill-pipe measurement from rig floor, mbrf):** 4422.80<br>**Penetration (mbsf):** 570.20<br>**Total number of cores:** 52<br>**Total length of cored section (m):** 487.20<br>**Total core recovered (m):** 385.75<br>**Core recovery (%):** 79.18<br>**Oldest formation cored:** upper Miocene clayey siltstone |
| | 1095C | **Position:** 66°59.1216′S, 78°29.2950′W<br>**Start hole:** 0045 hr, 24 February 1998<br>**End hole:** 0215 hr, 24 February 1998<br>**Seafloor (drill-pipe measurement from rig floor, mbrf):** 3852.6<br>**Distance between rig floor and sea level (m):** 11.0<br>**Water depth (drill-pipe measurement from sea level, m):** 3841.6<br>**Total depth (drill-pipe measurement from rig floor, mbrf):** 3855.50<br>**Penetration (mbsf):** 2.90<br>**Total number of cores:** 1<br>**Total length of cored section (m):** 2.90<br>**Total core recovered (m):** 2.87<br>**Core recovery (%)** 98.97<br>**Oldest formation cored:** Pleistocene sandy silty clay |
| | 1095D | **Position:** 66°59.1211′S, 78°29.2854′W<br>**Start hole:** 0215 hr, 24 February 1998<br>**End hole:** 1930 hr, 24 February 1998<br>**Seafloor (drill-pipe measurement from rig floor, mbrf):** 3851.9<br>**Distance between rig floor and sea level (m):** 11.0<br>**Water depth (drill-pipe measurement from sea level, m):** 3840.9<br>**Total depth (drill-pipe measurement from rig floor, mbrf):** 3936.50<br>**Penetration (mbsf):** 84.60<br>**Total number of cores:** 9<br>**Total length of cored section (m):** 84.60<br>**Total core recovered (m):** 78.96<br>**Core recovery (%):** 93.33<br>**Oldest formation cored:** upper Pliocene silty clay |
| | 1096A | **Position:** 67°34.0086′S, 76° 57.7936′W<br>**Start hole:** 0300 hr, 25 February 1998<br>**End hole:** 0145 hr, 26 February 1998<br>**Seafloor (drill-pipe measurement from rig floor, mbrf):** 3163.2<br>**Distance between rig floor and sea level (m):** 11.2<br>**Water depth (drill-pipe measurement from sea level, m):** 3152.0<br>**Total depth (drill-pipe measurement from rig floor, mbrf):** 3303.90<br>**Penetration (mbsf):** 140.70<br>**Total number of cores:** 15<br>**Total length of cored section (m):** 140.70<br>**Total core recovered (m):** 118.52<br>**Core recovery (%):** 84.24<br>**Oldest formation cored:** lower Pleistocene silty clay |

Table T1 (continued).

| | Hole | Statistics |
|---|---|---|
| | 1096B | **Position:** 67°34.0091′S, 76°57.8119′W<br>**Start hole:** 0145 hr, 26 February 1998<br>**End hole:** 1030 hr, 28 February 1998<br>**Seafloor (drill-pipe measurement from rig floor, mbrf):** 3163.7<br>**Distance between rig floor and sea level (m):** 11.2<br>**Water depth (drill-pipe measurement from sea level, m):** 3152.5<br>**Total depth (drill-pipe measurement from rig floor, mbrf):** 3424.30<br>**Penetration (mbsf):** 260.60<br>**Total number of cores:** 32<br>**Total length of cored section (m):** 260.60<br>**Total core recovered (m):** 209.77<br>**Core recovery (%):** 80.50<br>**Oldest formation cored:** upper Pliocene silty clay |
| | 1096C | **Position:** 67°34.0091′S, 76°57.8261′W<br>**Start hole:** 1030 hr, 28 February 1998<br>**End hole:** 1530 hr, 5 March 1998<br>**Seafloor (drill-pipe measurement from rig floor, mbrf):** 3163.7<br>**Distance between rig floor and sea level (m):** 11.2<br>**Water depth (drill-pipe measurement from sea level, m):** 3152.5<br>**Total depth (drill-pipe measurement from rig floor, mbrf):** 3771.40<br>**Penetration (mbsf):** 607.70<br>**Total number of cores:** 43<br>**Total length of cored section (m):** 409.90<br>**Total core recovered (m):** 344.98<br>**Core recovery (%):** 84.16<br>**Oldest formation cored:** lower Pliocene diatomite and claystone |
| | 1101A | **Position:** 64°22.3315′S, 70°15.6706′W<br>**Start hole:** 1030 hr, 18 March 1998<br>**End hole:** 0145 hr, 20 March 1998<br>**Seafloor (drill-pipe measurement from rig floor, mbrf):** 3291.2<br>**Distance between rig floor and sea level (m):** 11.5<br>**Water depth (drill-pipe measurement from sea level, m):** 3279.7<br>**Total depth (drill-pipe measurement from rig floor, mbrf):** 3508.90<br>**Penetration (mbsf):** 217.70<br>**Total number of cores:** 24<br>**Total length of cored section (m):** 217.70<br>**Total core recovered (m):** 215.75<br>**Core recovery (%):** 99.10<br>**Oldest formation cored:** upper Pliocene diatom-bearing silty clay |
| Continental Shelf Sites | 1097A | **Position:** 66°23.5680′S, 70°45.3841′W<br>**Start hole:** 0630 hr, 6 March 1998<br>**End hole:** 2100 hr, 11 March 1998<br>**Seafloor (drill-pipe measurement from rig floor, mbrf):** 563.0<br>**Distance between rig floor and sea level (m):** 11.3<br>**Water depth (drill-pipe measurement from sea level, m):** 551.7<br>**Total depth (drill-pipe measurement from rig floor, mbrf):** 999.60<br>**Penetration (mbsf):** 436.60<br>**Total number of cores:** 51<br>**Total length of cored section (m):** 436.60<br>**Total core recovered (m):** 59.30<br>**Core recovery (%):** 13.58<br>**Oldest formation cored:** lower Pliocene(?) diamict |
| | 1100A | **Position:** 63°53.0010′S, 65°42.3390′W<br>**Start hole:** 1445 hr, 14 March 1998<br>**End hole:** 0115 hr, 15 March 1998<br>**Seafloor (drill-pipe measurement from rig floor, mbrf):** 470.0<br>**Distance between rig floor and sea level (m):** 11.4<br>**Water depth (drill-pipe measurement from sea level, m):** 458.6<br>**Total depth (drill-pipe measurement from rig floor, mbrf):** 503.80<br>**Penetration (mbsf):** 33.80<br>**Total number of cores:** 4<br>**Total length of cored section (m):** 33.80<br>**Total core recovered (m):** 0.00<br>**Core recovery (%):** 0.00<br>**Oldest formation cored:** No recovery |

Table T1 (continued).

| Hole | Statistics |
|---|---|
| 1100B | **Position:** 63°53.0100′S, 65°42.3486′W<br>**Start hole:** 0115 hr, 15 March 1998<br>**End hole:** 1315 hr, 15 March 1998<br>**Seafloor (drill-pipe measurement from rig floor, mbrf):** 470.0<br>**Distance between rig floor and sea level (m):** 11.4<br>**Water depth (drill-pipe measurement from sea level, m):** 458.6<br>**Total depth (drill-pipe measurement from rig floor, mbrf):** 505.90<br>**Penetration (mbsf):** 35.90<br>**Total number of cores:** 1<br>**Total length of cored section (m):** 2.00<br>**Total core recovered (m):** 0.15<br>**Core recovery (%):** 7.50<br>**Oldest formation cored:** rocks from a Pleistocene(?) diamict |
| 1100C | **Position:** 63°52.9985′S, 65°42.3637′W<br>**Start hole:** 1315 hr, 15 March 1998<br>**End hole:** 0800 hr, 16 March 1998<br>**Seafloor (drill-pipe measurement from rig floor, mbrf):** 470.0<br>**Distance between rig floor and sea level (m):** 11.4<br>**Water depth (drill-pipe measurement from sea level, m):** 458.6<br>**Total depth (drill-pipe measurement from rig floor, mbrf):** 475.00<br>**Penetration (mbsf):** 5.00<br>**Total number of cores:** 1<br>**Total length of cored section (m):** 5.00<br>**Total core recovered (m):** 4.05<br>**Core recovery (%):** 81.00<br>**Oldest formation cored:** Pleistocene(?) diamict |
| 1100D | **Position:** 63°53.0051′S, 65°42.3523′W<br>**Start hole:** 0800 hr, 16 March 1998<br>**End hole:** 2030 hr, 17 March 1998<br>**Return to Hole:** 1315 hr, 20 March 1998<br>**End hole:** 0515 hr, 21 March 1998<br>**Seafloor (drill-pipe measurement from rig floor, mbrf):** 470.0<br>**Distance between rig floor and sea level (m):** 11.4<br>**Water depth (drill-pipe measurement from sea level, m):** 458.6<br>**Total depth (drill-pipe measurement from rig floor, mbrf):** 580.50<br>**Penetration (mbsf):** 110.50<br>**Total number of cores:** 12<br>**Total length of cored section (m):** 110.50<br>**Total core recovered (m):** 5.28<br>**Core recovery (%):** 4.78<br>**Oldest formation cored:** upper Pliocene(?) or Pleistocene diamict |
| 1102A | **Position:** 63°48.1709′S, 65°51.4934′W<br>**Start hole:** 0645 hr, 21 March 1998<br>**End hole:** 1130 hr, 21 March 1998<br>**Seafloor (drill-pipe measurement from rig floor, mbrf):** 442.0<br>**Distance between rig floor and sea level (m):** 11.5<br>**Water depth (drill-pipe measurement from sea level, m):** 430.5<br>**Total depth (drill-pipe measurement from rig floor, mbrf):** 449.90<br>**Penetration (mbsf):** 7.90<br>**Total number of cores:** 1<br>**Total length of cored section (m):** 7.90<br>**Total core recovered (m):** 0.42<br>**Core recovery (%):** 5.32<br>**Oldest formation cored:** rocks from a Pleistocene(?) diamict |
| 1102B | **Position:** 63°48.1675′S, 65°51.4728′W<br>**Start hole:** 1130 hr, 21 March 1998<br>**End hole:** 1600 hr, 21 March 1998<br>**Seafloor (drill-pipe measurement from rig floor, mbrf):** 442.0<br>**Distance between rig floor and sea level (m):** 11.5<br>**Water depth (drill-pipe measurement from sea level, m):** 430.5<br>**Total depth (drill-pipe measurement from rig floor, mbrf):** 449.50<br>**Penetration (mbsf):** 7.50<br>**Total number of cores:** 1<br>**Total length of cored section (m):** 7.50<br>**Total core recovered (m):** 0.39<br>**Core recovery (%):** 5.20<br>**Oldest formation cored:** rocks from a Pleistocene(?) diamict |

Table T1 (continued).

| | Hole | Statistics |
|---|---|---|
| | 1102C | **Position:** 63°48.1405′S, 65°51.4920′W<br>**Start hole:** 1600 hr, 21 March 1998<br>**End hole:** 0315 hr, 22 March 1998<br>**Seafloor (drill-pipe measurement from rig floor, mbrf):** 442.0<br>**Distance between rig floor and sea level (m):** 11.5<br>**Water depth (drill-pipe measurement from sea level, m):** 430.5<br>**Total depth (drill-pipe measurement from rig floor, mbrf):** 448.50<br>**Penetration (mbsf):** 6.50<br>**Total number of cores:** 2<br>**Total length of cored section (m):** 6.50<br>**Total core recovered (m):** 0.01<br>**Core recovery (%):** 0.15<br>**Oldest formation cored:** Pleistocene(?) diamict |
| | 1102D | **Position:** 63°48.0714′S, 65°51.3872′W<br>**Start hole:** 0315 hr, 22 March 1998<br>**End hole:** 1730 hr, 22 March 1998<br>**Seafloor (drill-pipe measurement from rig floor, mbrf):** 442.0<br>**Distance between rig floor and sea level (m):** 11.5<br>**Water depth (drill-pipe measurement from sea level, m):** 430.5<br>**Total depth (drill-pipe measurement from rig floor, mbrf):** 456.90<br>**Penetration (mbsf):** 14.90<br>**Total number of cores:** 1<br>**Total length of cored section (m):** 14.90<br>**Total core recovered (m):** 0.85<br>**Core recovery (%):** 5.70<br>**Oldest formation cored:** rocks from a Pleistocene(?) diamict |
| | 1103A | **Position:** 63°59.9700′S, 65°27.9190′W<br>**Start hole:** 2000 hr, 22 March 1998<br>**End hole:** 1130 hr, 26 March 1998<br>**Seafloor (drill-pipe measurement from rig floor, mbrf):** 505.0<br>**Distance between rig floor and sea level (m):** 11.5<br>**Water depth (drill-pipe measurement from sea level, m):** 493.5<br>**Total depth (drill-pipe measurement from rig floor, mbrf):** 867.70<br>**Penetration (mbsf):** 362.70<br>**Total number of cores:** 38<br>**Total length of cored section (m):** 362.70<br>**Total core recovered (m):** 44.54<br>**Core recovery (%):** 12.28<br>**Oldest formation cored:** late Miocene(?) diamictite |
| Palmer Deep Sites | 1098A | **Position:** 64°51.7236′S, 64°12.4709′W<br>**Start hole:** 0615 hr, 12 March 1998<br>**End hole:** 2315 hr, 12 March 1998<br>**Seafloor (drill-pipe measurement from rig floor, mbrf):** 1022.6<br>**Distance between rig floor and sea level (m):** 10.6<br>**Water depth (drill-pipe measurement from sea level, m):** 1012.0<br>**Total depth (drill-pipe measurement from rig floor, mbrf):** 1068.50<br>**Penetration (mbsf):** 45.90<br>**Total number of cores:** 7<br>**Total length of cored section (m):** 45.90<br>**Total core recovered (m):** 45.78<br>**Core recovery (%):** 99.74<br>**Oldest formation cored:** Holocene diatom clayey silt |
| | 1098B | **Position:** 64°51.7163′ S, 64°12.4796′W<br>**Start hole:** 2315 hr, 12 March 1998<br>**End hole:** 0355 hr, 13 March 1998<br>**Seafloor (drill-pipe measurement from rig floor, mbrf):** 1022.0<br>**Distance between rig floor and sea level (m):** 11.4<br>**Water depth (drill-pipe measurement from sea level, m):** 1010.6<br>**Total depth (drill-pipe measurement from rig floor, mbrf):** 1065.00<br>**Penetration (mbsf):** 43.00<br>**Total number of cores:** 5<br>**Total length of cored section (m):** 43.00<br>**Total core recovered (m):** 44.66<br>**Core recovery (%):** 103.86<br>**Oldest formation cored:** Holocene mud-bearing diatom ooze and muddy diatom ooze |

Table T1 (continued).

| Hole | Statistics |
|---|---|
| 1098C | **Position:** 64°51.7104′S, 64°12.4690′W<br>**Start hole:** 0355 hr, 13 March 1998<br>**End hole:** 0930 hr, 13 March 1998<br>**Seafloor (drill-pipe measurement from rig floor, mbrf):** 1021.8<br>**Distance between rig floor and sea level (m):** 11.4<br>**Water depth (drill-pipe measurement from sea level, m):** 1010.4<br>**Total depth (drill-pipe measurement from rig floor, mbrf):** 1068.50<br>**Penetration (mbsf):** 46.70<br>**Total number of cores:** 5<br>**Total length of cored section (m):** 46.70<br>**Total core recovered (m):** 46.30<br>**Core recovery (%):** 99.14<br>**Oldest formation cored:** Holocene muddy diatom ooze and silty clay |
| 1099A | **Position:** 64°56.7078′S, 64°18.9175′W<br>**Start hole:** 1030 hr, 13 March 1998<br>**End hole:** 1900 hr, 13 March 1998<br>**Seafloor (drill-pipe measurement from rig floor, mbrf):** 1411.2<br>**Distance between rig floor and sea level (m):** 11.4<br>**Water depth (drill-pipe measurement from sea level, m):** 1399.8<br>**Total depth (drill-pipe measurement from rig floor, mbrf):** 1473.50<br>**Penetration (mbsf):** 62.30<br>**Total number of cores:** 7<br>**Total length of cored section (m):** 62.30<br>**Total core recovered (m):** 63.74<br>**Core recovery (%):** 102.31<br>**Oldest formation cored:** Holocene diatom clayey silt |
| 1099B | **Position:** 64°56.7073′S, 64°18.9157′W<br>**Start hole:** 1900 hr, 13 March 1998<br>**End hole:** 0455 hr, 14 March 1998<br>**Seafloor (drill-pipe measurement from rig floor, mbrf):** 1411.2<br>**Distance between rig floor and sea level (m):** 11.4<br>**Water depth (drill-pipe measurement from sea level, m):** 1399.8<br>**Total depth (drill-pipe measurement from rig floor, mbrf):** 1518.70<br>**Penetration (mbsf):** 107.50<br>**Total number of cores:** 5<br>**Total length of cored section (m):** 47.50<br>**Total core recovered (m):** 48.34<br>**Core recovery (%):** 101.77<br>**Oldest formation cored:** Holocene mud-bearing diatom ooze and muddy diatom ooze |

**Figure AF1.** (An **oversized figure** accompanies this volume.) Seismic reflection profiles crossing sites drilled during Leg 178, with schematic maps showing profile locations. For a description of acquisition parameters, see Tables **T9,** p. 65, and **T10,** p. 66, in the "Explanatory Notes" chapter. For a description of processing parameters and brief accounts of regional geological significance, see **"Appendix,"** p. 24, in the "Leg 178 Summary" chapter. (Continued on next page.)

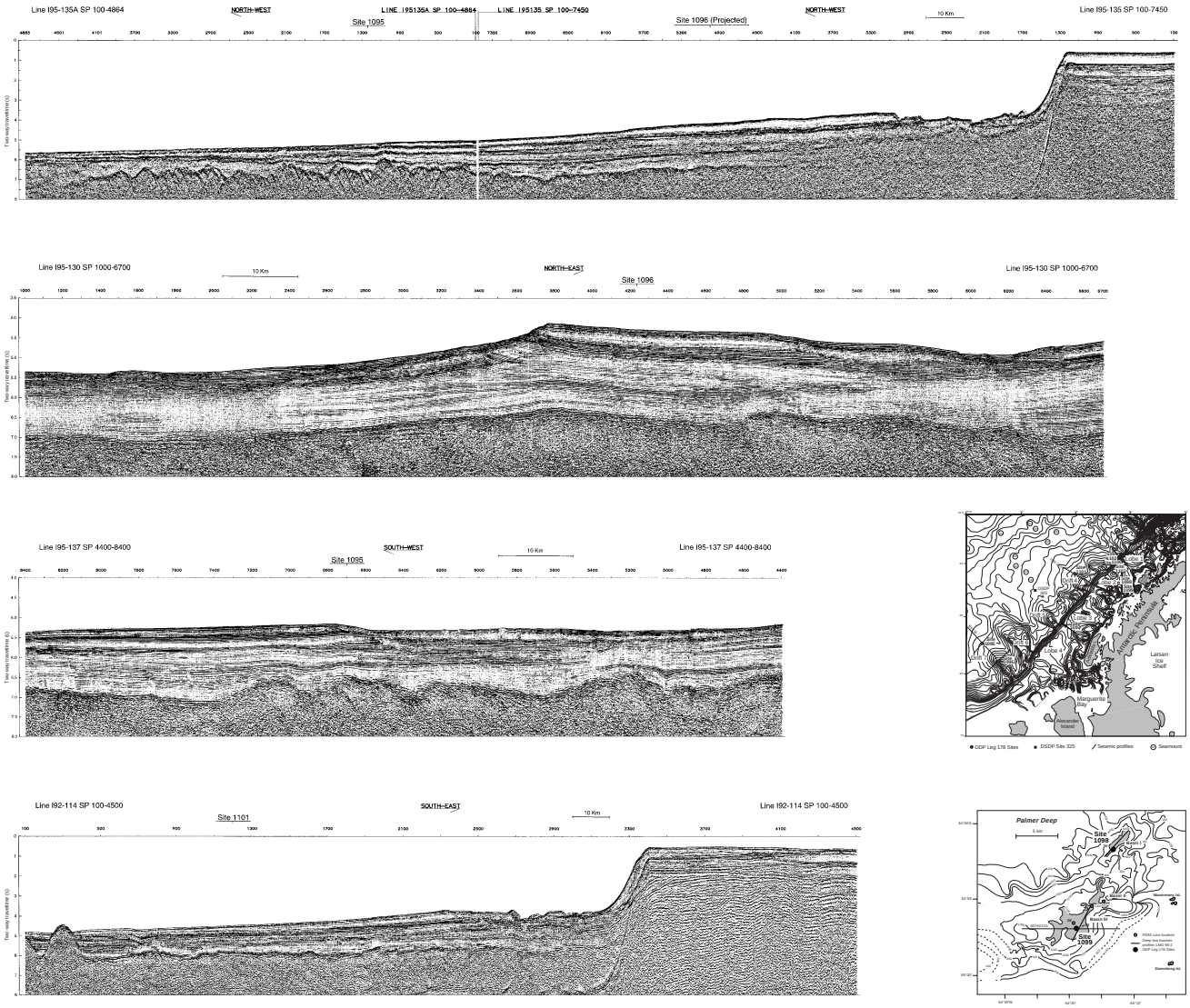


The Programma Nazionale di Ricerche in Antartide (PNRA), Italy, is acknowledged for contributing to the publication of these seismic profiles.

Figure AF1 (continued).